Doctoral Thesis

Anomalous Hall effect on a vortex of supercurrent in type-II superconductors

(第二種超伝導体の超伝導渦電流に対する異常Hall効果)

Marie OHUCHI

Department of Physics, Graduate School of Science, Hokkaido University

March, 2021

Contents

Acknowledgements

I would like to express my sincere appreciation to my supervisor, Professor Takafumi Kita, for his continuous support and constructive suggestions. Under his guidance, I have acquired most of my knowledge of physics, and have also learnt how to formulate my ideas and perform analytical calculations, and I could spend valuable time.

I would like to acknowledge Professor Migaku Oda, Professor Kenji Kondo, and Professor Takashi Uchihashi who were sub-chief examiners for many valuable comments and suggestions in the review process of this thesis.

I am indebted to thank Professor Jun Goryo for giving me the opportunity to talk about my study and discuss it at Hirosaki University.

I would like to thank past and present members of Statistical Physics Laboratory. In particular, I am deeply grateful to Dr. Hikaru Ueki for everything his help as a collaborator and many discussions of the vortex physics in superconductors. Special thanks also to Dr. Joshua Ezekiel Sambo for fruitful discussion and carefully proofreading the manuscripts.

I would like also to thank Dr. Robert C. Regan at Northwestern University for helpful discussions and comments on the manuscript.

I would like to appreciate my parents for supporting me all my life.

The computations in this work were carried out using the facilities of the Supercomputer Center, the Institute for Solid State Physics, the University of Tokyo.

1 Introduction

Vortices in type-II superconductors have not only a single magnetic flux quantum and circulating supercurrents, but also accumulated charge. This *vortex-core charging* has attracted the interest of numerous researchers. The earliest phenomenological studies on the vortex-core charging were carried out by London and Khomskii *et al.* [1, 2]. London proposed the phenomenological equations of superconductivity with the Lorentz force acting on supercurrents, and showed that supercurrents in the magnetic field induce the Hall electric field. When we consider the vortex state in type-II superconductors, we can also show the existence of the vortex-core charge due to the Lorentz force acting on circulating supercurrents [1, 3]. Khomskii and Freimuth considered a simplified model, with the pair potential in the form of the step function, and calculated the vortex-core charge due to the chemical potential difference between the vortex-core in the normal state and its surrounding region in the superconducting state [2, 4]. Goryo studied the vortex-core charging in a chiral p-wave superconductor based on the Ginzburg–Landau (GL) Lagrangian with the Chern–Simons term [5]. After these phenomenological studies, more microscopic calculations of the vortex-core charge were performed. Matsumoto and Heeb calculated the vortex-core charge in chiral p-wave superconductors by solving the Bogoliubov–de Gennes (BdG) equations with Maxwell's equations self-consistently [6]. Although the standard Eilenberger equations [7] (i.e., the quasiclassical equations of superconductivity) cannot describe the static vortex-core charging [3, 8, 9], the dynamical dipole charge in the vortex core in type-II superconductors under an AC electromagnetic field was calculated based on the standard Eilenberger equations in the Keldysh formalism by Eschrig *et al.* [10, 11]. In this thesis, we study the vortex-core charge as a function of temperature, magnetic field, and a material parameter such as the quasiclassical parameter [12] based on the two different approaches, namely; the quasiclassical theory and the BdG theory.

1.1 Quasiclassical theory

Although it is well-known that the standard Eilenberger equations are a powerful tool for studying inhomogeneous superconductors in the presence of magnetic fields, the force terms which are necessary for transparently describing electric charging in equilibrium superconductors were missing from the standard formalism [7, 13–15]. Recently, the augmented quasiclassical (AQC) equations of superconductivity with the three force terms as seen in Fig. 1.1, namely; (i) the Lorentz force that acts on supercurrents [1, 16, 17], (ii) pair-potential gradient (PPG) force [8, 9, 12, 18], and (iii) the pressure difference of the chemical potential arising from the slope in the density of states (SDOS) [2, 4, 9], were derived and used to study the vortex-core charging in type-II superconductors. The main part of this AQC equations were derived by incorporating the next-to-leading-order contributions in the expansion of the Gor'kov equations [19, 20] in terms of the quasiclas-

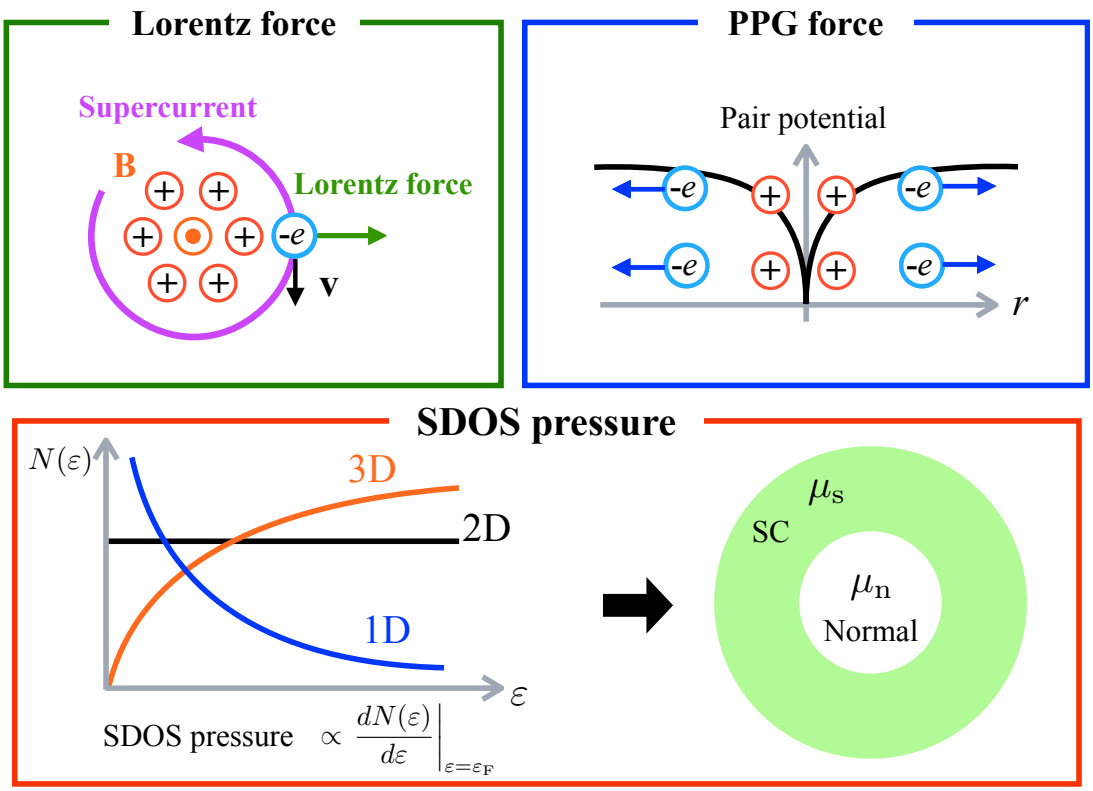

Figure 1.1: Schematic representation of the Lorentz force, PPG force and SDOS pressure which lead to vortex-core charging. $N(\varepsilon)$ is a normal density of states, $\mu_{\rm s}$ and $\mu_{\rm n}$ are the chemical potentials in the superconducting and normal states, respectively.

sical parameter $\delta \equiv 1/k_{\rm F}\xi_0$ [9]. Here $k_{\rm F}$ is the amplitude of the Fermi wavenumber and $\xi_0 \equiv \hbar v_{\rm F}/\Delta_0$ is the coherence length, where Δ_0 is the energy gap at zero magnetic field and zero temperature, and $v_{\rm F}$ is the amplitude of the Fermi velocity.

The vortex-core charge near the lower critical field, was calculated in an isolated vortex of s-wave superconductors with a cylindrical Fermi surface [8] and a spherical Fermi surface [9], based on the AQC equations with the three force terms. The temperature and magnetic-penetration-depth dependence of the vortex-core charge in an isolated vortex of s-wave superconductors with a spherical Fermi surface was plotted in Ref. [9] as seen in Fig. 1.2. It is shown that the vortex-core charging is dominated by the PPG force near zero temperature and by the SDOS pressure near the superconducting transition temperature when the magnetic penetration depth is larger than the coherence length, and the PPG force also gives dominant contribution at low temperatures even if the magnetic penetration depth is almost the same as the coherence length [9]. Thus, the vortex-core charge in s-wave superconductors with an isolated vortex is dominated by the PPG force in a wide parameter range. We also studied the spread of charge around the vortex core estimating the charge Q accumulated below radius r of s-wave superconductors with a cylindrical Fermi surface as seen in Fig. 1.3 [8]. As the result, we found that the

charge accumulation by the PPG force is concentrated in the core region. On the other hand, that by the Lorentz force is smaller at the core center but extends far outside the core over the magnetic penetration depth.

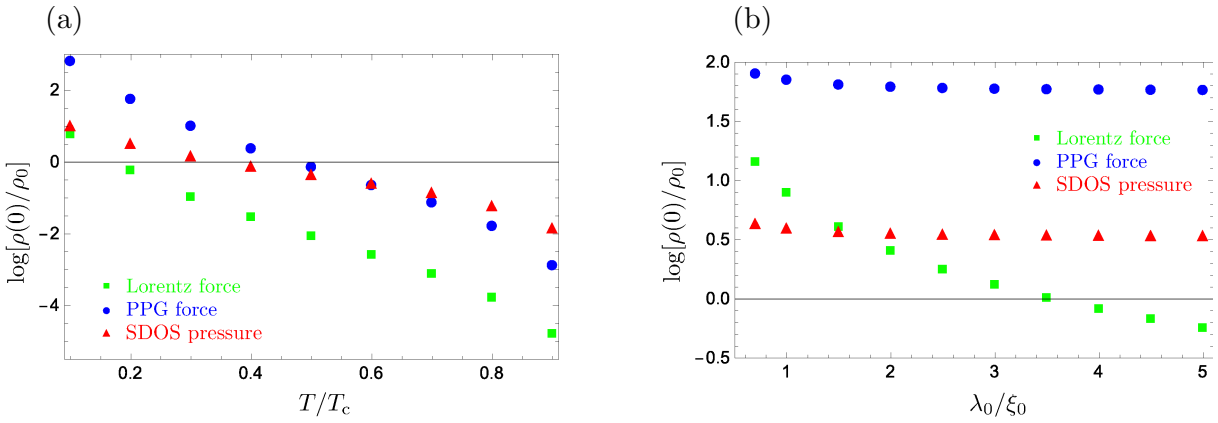

Figure 1.2: Charge density at the vortex core $\rho(\mathbf{0})$ in units of $\rho_0 \equiv \Delta_0\epsilon_0/|e|\xi_0^2$ due to the Lorentz force (green square points), PPG force (blue circular points), and SDOS pressure (red triangular points) in an s-wave superconductor with a spherical Fermi surface as a function of (a) temperature and (b) magnetic penetration depth [9].

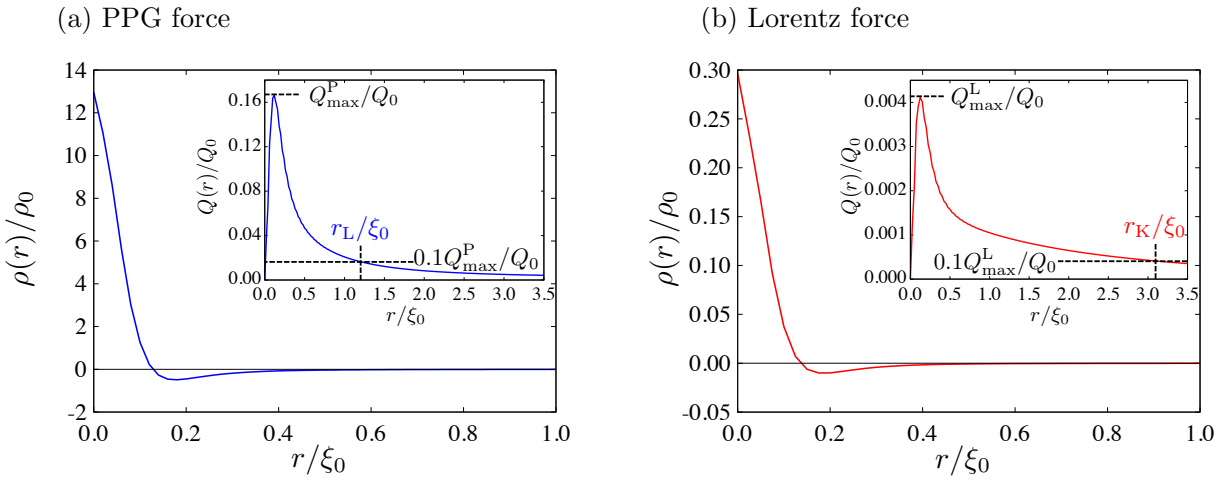

Figure 1.3: Charge redistribution $\rho(r)$ due to the PPG force (a), and the Lorentz force (b) in units of $\rho_0 \equiv \Delta_0\epsilon_0/|e|\xi_0^2$ over $r \le \xi_0$ at $T = 0.2T_c$, and accumulated charge $Q(r)$ below the radius r in units of $Q_0 \equiv \Delta_0\epsilon_0/|e|$ within $r \le 3.5\xi_0$ [8].

The vortex-core charging was studied in s- and chiral p-wave superconductors with an isolated vortex using the AQC equations with the Lorentz and PPG forces by Masaki [21]. The PPG force terms are divided into three parts, namely; the radial parts, which are the radial derivatives of the cylindrical coordinates around the vortex center, the angular parts, which are the angular derivatives, and the vector potential terms originating from the gauge invariance of the AQC equations. He pointed out that the vortex-core charging

is dominated by the angular parts arising from the phase of the pair potential in the PPG force terms. Therefore, since the phase coming from the chirality and vorticity cancels each out if they are antiparallel, i.e. $L_z = 0$, the vortex-core charge is very small. Here L_z denotes the total angular momentum. The vortex-core charge chiral p-wave superconductors with the parallel chirality and vorticity, i.e. $L_z = 2$ is also more enhanced than that in s- and antiparallel chiral p-wave superconductors with $L_z = 1$ and $L_z = 0$, respectively. These results are consistent with those obtained from the BdG equations proposed by Matsumoto *et al.* [6]. However, despite these efforts, we have not yet fully understood the vortex-core charging due to the PPG force. On the other hand, it is well known that the vortex-core charging due to the Lorentz force arises from the magnetic Hall effect due to the Lorentz force acting on a vortex of supercurrent, and we also see roughly that the vortex-core charging due to the SDOS pressure comes from the (effective) chemical potential difference between the core and its surrounding region by assuming a roughly normal metal at the core [9]. One may think about what the difference between the charging due to the PPG force and the SDOS pressure is, since the chemical potential difference between the normal and superconducting states of the homogeneous system is exactly equal zero when taking into account only the PPG force [9]. This issue is discussed by using the recent results [8, 9, 21] and the calculation in this thesis.

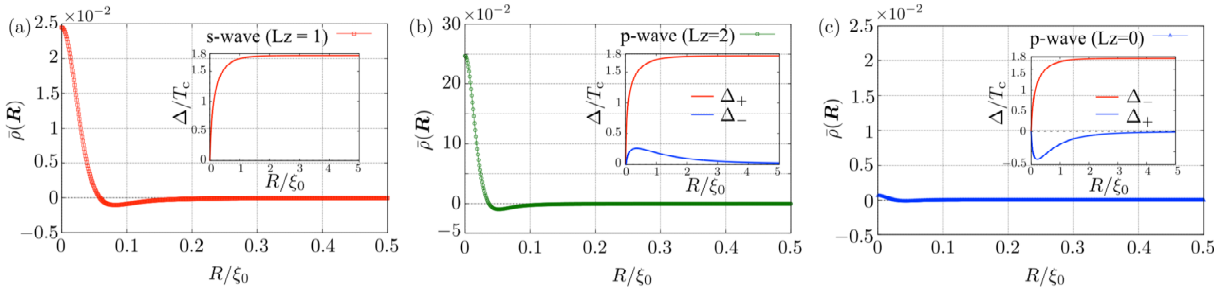

Figure 1.4: Charge density in units of $\rho_0 \equiv 2|e|N(0)T_c$ for (a) the s-wave superconductor ($L_z = 1$) and the chiral p-wave superconductors with (b) the parallel vortex ($L_z = 2$) and (c) the antiparallel vortex ($L_z = 0$). The inset of each panel shows the radial profile of the pair potential [21].

Kohno *et al.* calculated the vortex-core charge as a function of the magnetic field in the vortex lattice [23] of s-wave superconductors with a cylindrical Fermi surface [22] as shown in Fig. 1.5 and d-wave superconductors with anisotropic Fermi surfaces used for cuprates [24] using the AQC equations with only the Lorentz force. They showed that the charge density at the vortex center has a large peak as a function of the magnetic field. Therefore, one may expect that the vortex-core charge due to the Lorentz force may be larger than that due to the PPG force at strong magnetic fields.

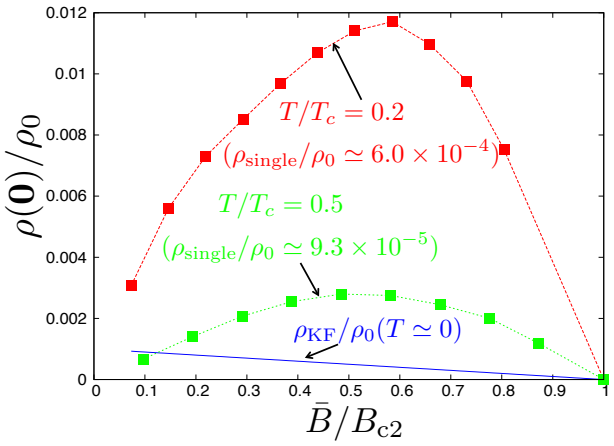

Figure 1.5: Charge density at the vortex center $\rho(\mathbf{0})$ in units of $\rho_0 \equiv \Delta_0\epsilon_0/|e|\xi_0^2$ as a function of magnetic field calculated for $T = 0.2T_{\rm c}$ (red line) and $T = 0.5T_{\rm c}$ (green line) [22].

1.2 Bogoliubov–de Gennes theory

Type-II superconductors magnetic field host quasiparticle states in their vortex core, with discrete energies which are below the bulk superconducting gap. This discretized energy levels are called the Caroli–de Gennes–Matricon (CdGM) modes [25], and the energy intervals are given by $\Delta_0/2k_{\rm F}\xi_0$ or $\Delta_0^2/\varepsilon_{\rm F}$, where $\varepsilon_{\rm F}$ is the Fermi energy. The energy interval of the CdGM modes is very small in conventional superconductors as $\Delta_0/\varepsilon_{\rm F} \sim 10^{-3}$ and the discretization cannot be found in experimental data of $NbSe_2$ [26]. On the other hand, in cuprate and heavy fermion superconductors, the coherence length is smaller and the quasiclassical parameter, $\delta \equiv (k_{\rm F}\xi_0)^{-1}$, is larger than that in conventional superconductors. Therefore, it is expected that the discretized energy levels of the vortex states in these anisotropic superconductors are observed experimentally. Hayashi *et al.* calculated the local density of states (LDOS) around the vortex core in type-II superconductors near the quantum limit of $\delta = 1$ based on the BdG equations [27], and showed in the LDOS as seen in Fig. 1.6 that the spectra are discretized below the gap energy and consist of several isolated peaks, each of which corresponds to the energy levels of the vortex states, the particle-hole asymmetry appears even if the normal-state density of states is symmetric, and the spatial variation also exhibits the Friedel-like oscillation [28]. Recently, the discretization of the energy levels was observed in the LDOS of YNi_2B_2C using scanning tunneling spectroscopy with high energy resolution [14]. More recently, the parameter δ of the layered iron-based superconductor FeSe has also been reported to reach about the quantum limit $\delta \sim 1$ [29]. Thus, the vortex states of conventional and unconventional superconductors are very different in this regard.

As mentioned above, since the standard Eilenberger equations [7] are obtained from the Gor'kov equations [19, 20] by taking the limit $\delta = 0$, the calculated LDOS has continuous and particle-hole symmetric spectra [30], and the charging and Hall effect cannot be

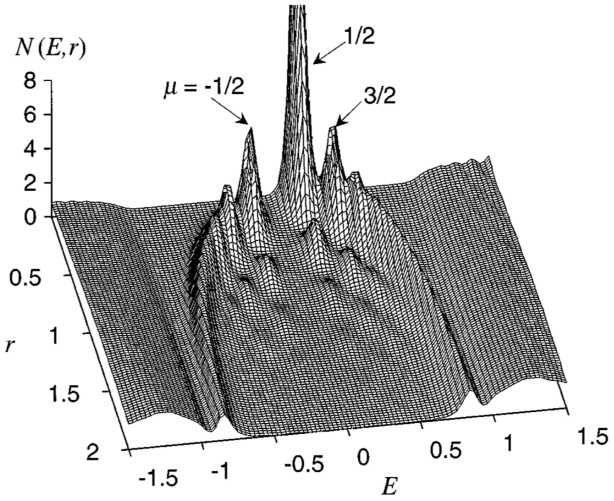

Figure 1.6: Local density of state in units of the normal-state density of states at the Fermi surface at $T = 0.05T_c$ and $k_F\xi_0 = 8$ [28]. E and r are normalized by Δ_0 and ξ_0, respectively.

calculated using them [12, 16]. Recently, the augmented Eilenberger (or AQC) equations with the quantum corrections of the first-order in δ were derived to study the vortex-core [8, 9, 21, 31] and surface [32] charging. These standard and augmented Eilenberger equations are valid for superconductors which can be described by small values of the quasiclassical parameter, but not for those whose values of δ fall near the quantum limit. Therefore, one may want to investigate the vortex-core charge in type-II superconductors near the quantum limit. Hayashi *et al.* also studied the carrier density in type-II superconductors near the quantum limit based on the BdG equations, and found that the carrier density at the core center increases monotonically as a function of the quasiclassical parameter (see Fig. 1.7) and the Friedel oscillation appears at low temperatures [33]. Thus, the BdG equations are suitable for studying the vortex states in superconductors near the quantum limit. However, the calculations performed by Hayashi *et al.* did not include Maxwell's equations, which are necessary for transparent interpretation. Therefore, the charge density they calculated does not meet the necessary charge neutrality condition. Machida *et al.* calculated the vortex-core charge by solving the BdG equations with the Poisson equation self-consistently, and showed that the charge density satisfies the neutrality condition. The vortex-core charge is suppressed due to the screening effect, and the decay length of the charge density around the vortex core increases monotonically as the quasiclassical parameter approaches the quantum limit [34]. On the other hand, they did not calculate the charge density at the vortex center as a function of the quasiclassical parameter and temperature. Therefore, one may wonder that the vortex-core charge increases monotonically even near the quantum limit, or it is suppressed by the screening effect and has a peak as a function of δ.

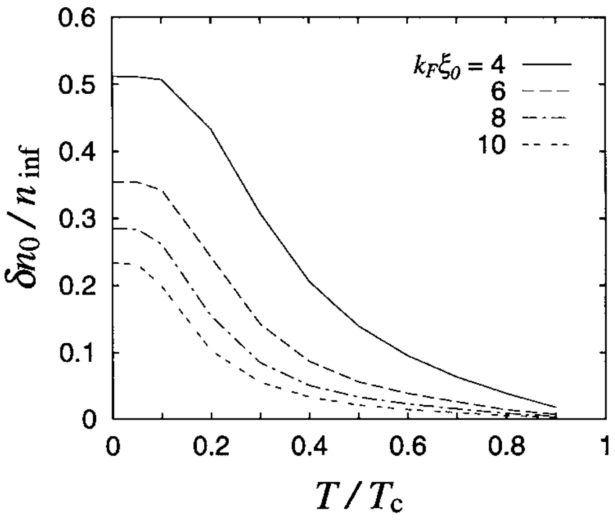

Figure 1.7: Carrier density difference $\delta n_0 \equiv |n_0 - n_{\rm inf}|$ between the vortex center n_0 and far away from the core $n_{\rm inf}$ in units of the carrier density far away from the core $n_{\rm inf}$ as a function of temperature calculated for $k_{\rm F}\xi_0 = 4, 6, 8$ and 10 [33].

1.3 Purpose of the thesis

The main purpose of this thesis is to construct a numerical method based on the AQC equations for studying the temperature and magnetic field dependence of the vortex-core charge in the Abrikosov lattice [23] of type-II superconductors microscopically, to study the forces responsible for the charging in the Abrikosov lattice, and to clarify the temperature and magnetic field dependence of the vortex-core charge in the Abrikosov lattice within the AQC equations and the δ-dependence of the vortex-core charging near the quantum limit using the BdG equations.

To these ends, we calculate the temperature and magnetic field dependence of the vortex-core charge in a two-dimensional s-wave superconductor due to the Lorentz and PPG forces using the AQC equations of superconductivity in the Matsubara formalism. We can neglect the SDOS pressure terms in superconductors with a cylindrical Fermi surface [8]. A method proposed recently by Sharma in Ref. [35] may be more useful, but her formulation still only incorporates the Lorentz force. We here perform the numerical calculation of the vortex-core charging combining the methods in Refs. [8] and [22]. We also study the charge redistribution around the vortex core based on the BdG equations to clarify the δ-dependence of the vortex-core charging near the quantum limit. These calculations will be very useful for experimental researchers.

This thesis is organized as follows. In Sect. 2, we present the formalism based on the AQC equations with the Lorentz and PPG forces in the Matsubara formalism and based on the BdG equations, and show that the PPG force can be neglected in the Meissner state. In Sect. 3, we give numerical results for the charging in the Abrikosov lattice and an isolated vortex near the quantum limit of an s-wave superconductor with a cylindrical

Fermi surface, and discuss the vortex-core charging due to the PPG force. In Sect. 4, we provide a conclusion.

2 Formulation

2.1 Augmented quasiclassical equations

We consider clean s-wave superconductors in equilibrium, and then the main part of the AQC equations with the PPG and Lorentz forces in the Matsubara formalism are given by [8, 9]

$$\begin{aligned}\left[i\varepsilon_n\hat{\tau}_3 - \hat{\Delta}\hat{\tau}_3, \hat{g}\right] + i\hbar\boldsymbol{v}_{\mathrm{F}}\cdot\boldsymbol{\partial}\hat{g} + \frac{i\hbar}{2}e(\boldsymbol{v}_{\mathrm{F}}\times\boldsymbol{B})\cdot\frac{\partial}{\partial\boldsymbol{p}_{\mathrm{F}}}\left\{\hat{\tau}_3, \hat{g}\right\} \\ - \frac{i\hbar}{2}\boldsymbol{\partial}\hat{\Delta}\hat{\tau}_3\cdot\frac{\partial\hat{g}}{\partial\boldsymbol{p}_{\mathrm{F}}} - \frac{i\hbar}{2}\frac{\partial\hat{g}}{\partial\boldsymbol{p}_{\mathrm{F}}}\cdot\boldsymbol{\partial}\hat{\Delta}\hat{\tau}_3 = \hat{0},\end{aligned} \tag{2.1}$$

where $\hat{g} = \hat{g}(\varepsilon_n, \boldsymbol{p}_{\mathrm{F}}, \boldsymbol{r})$ and $\hat{\Delta} = \hat{\Delta}(\boldsymbol{r})$ are the quasiclassical Green's functions in the Matsubara formalism and the pair potential, respectively, $\varepsilon_n = (2n+1)\pi k_{\mathrm{B}}T$ is the fermion Matsubara energy ($n = 0, \pm1, \cdots$) with k_{B} and T denoting the Boltzmann constant and temperature, respectively, $\boldsymbol{v}_{\mathrm{F}}$ and $\boldsymbol{p}_{\mathrm{F}}$ are the Fermi velocity and momentum, respectively, $e < 0$ is the electron charge, $\boldsymbol{B} = \boldsymbol{B}(\boldsymbol{r})$ is the magnetic-flux density, and the commutators are given by $[\hat{a}, \hat{b}] \equiv \hat{a}\hat{b} - \hat{b}\hat{a}$, and $\{\hat{a}, \hat{b}\} \equiv \hat{a}\hat{b} + \hat{b}\hat{a}$. The first and second terms in Eq. (2.1) correspond to the standard Eilenberger equations [7, 13–15], the third term is the Lorentz force [16, 17], and the fourth and fifth terms represent the PPG force [8, 9, 18]. We also assume spin-singlet pairing without spin paramagnetism. The matrices $\hat{g}$, $\hat{\Delta}$ and $\hat{\tau}_3$ are then given by [13]

$$\hat{g} = \begin{bmatrix} g & -if \\ i\bar{f} & -\bar{g} \end{bmatrix}, \quad \hat{\Delta} = \begin{bmatrix} 0 & \Delta \\ \Delta^* & 0 \end{bmatrix}, \quad \hat{\tau}_3 = \begin{bmatrix} 1 & 0 \\ 0 & -1 \end{bmatrix}, \tag{2.2}$$

where the barred functions are defined generally by $\bar{X}(\varepsilon_n, \boldsymbol{p}_{\mathrm{F}}, \boldsymbol{r}) \equiv X^*(\varepsilon_n, -\boldsymbol{p}_{\mathrm{F}}, \boldsymbol{r})$. The operator $\boldsymbol{\partial}$ is also defined by

$$\boldsymbol{\partial} \equiv \begin{cases} \boldsymbol{\nabla} & \text{on } g \text{ or } \bar{g} \\ \boldsymbol{\nabla} - i\dfrac{2e\boldsymbol{A}}{\hbar} & \text{on } f \text{ or } \Delta \\ \boldsymbol{\nabla} + i\dfrac{2e\boldsymbol{A}}{\hbar} & \text{on } \bar{f} \text{ or } \Delta^* \end{cases}, \tag{2.3}$$

where $\boldsymbol{A} = \boldsymbol{A}(\boldsymbol{r})$ is the vector potential.

With the procedure in Ref. [3], we expand g and f formally in terms of δ as $g = g_0 + g_1 + \cdots$ and $f = f_0 + f_1 + \cdots$, where g_0 and f_0 are the Green's functions of the standard Eilenberger equations. The standard Eilenberger equations with the normalization

condition $g_0 = \mathrm{sgn}(\varepsilon_n)\left(1 - f_0\bar{f}_0\right)^{1/2}$ are then given by [7, 13–15, 36]

$$\varepsilon_n f_0 + \frac{1}{2}\hbar \boldsymbol{v}_\mathrm{F} \cdot \left(\boldsymbol{\nabla} - i\frac{2e\boldsymbol{A}}{\hbar}\right) f_0 = \Delta g_0, \tag{2.4a}$$

$$\Delta = 2\Gamma_0 \pi k_\mathrm{B} T \sum_{n=0}^{n_\mathrm{c}} \langle f_0 \rangle_\mathrm{F}, \tag{2.4b}$$

$$\boldsymbol{j} = -i2\pi e N(0) k_\mathrm{B} T \sum_{n=0}^{n_\mathrm{c}} \langle \boldsymbol{v}_\mathrm{F}(g_0 - g_0^*) \rangle_\mathrm{F}, \tag{2.4c}$$

where $\boldsymbol{j}$ is the current density, Γ_0 is the dimensionless coupling constant responsible for the Cooper pairing defined by

$$\frac{1}{\Gamma_0} = \ln\frac{T}{T_\mathrm{c}} + 2\pi k_\mathrm{B} T \sum_{n=0}^{n_\mathrm{c}} \frac{1}{\varepsilon_n}, \tag{2.5}$$

ε_c is the cutoff determined from $\varepsilon_\mathrm{c} = (2n_\mathrm{c} + 1)\pi k_\mathrm{B} T$ and $\varepsilon_\mathrm{c} = 20 k_\mathrm{B} T_\mathrm{c}$, $\langle \cdots \rangle_\mathrm{F}$ is the Fermi surface average normalized as $\langle 1 \rangle_\mathrm{F} = 1$, μ_0 is the permeability of vacuum, and $N(0)$ is the normal density of states (DOS) per spin and unit volume at the Fermi energy. Eq. (2.4) forms a set of self-consistent equations for f_0, Δ, and $\boldsymbol{A}$ by using Ampère's laws, $\boldsymbol{\nabla} \times \boldsymbol{\nabla} \times \boldsymbol{A} = \mu_0 \boldsymbol{j}$.

We obtain the equation for g_1 from the expansion of Eq. (2.1) up to the first-order in δ as [8, 9]

$$\boldsymbol{v}_\mathrm{F} \cdot \boldsymbol{\nabla} g_1 = -e(\boldsymbol{v}_\mathrm{F} \times \boldsymbol{B}) \cdot \frac{\partial g_0}{\partial \boldsymbol{p}_\mathrm{F}} - \frac{i}{2}\boldsymbol{\partial}\Delta^* \cdot \frac{\partial f_0}{\partial \boldsymbol{p}_\mathrm{F}} - \frac{i}{2}\boldsymbol{\partial}\Delta \cdot \frac{\partial \bar{f}_0}{\partial \boldsymbol{p}_\mathrm{F}}, \tag{2.6}$$

with $g_1 = -\bar{g}_1$. The first term in Eq. (2.6) is the Lorentz force, and the second and third terms are the PPG force. We decompose the PPG force into the radial, angular, and vector potential parts, including $(\partial\Delta/\partial r)\hat{\boldsymbol{r}}$, $(\partial\Delta/\partial\theta)(\hat{\boldsymbol{\theta}}/r)$, and $-2ie\boldsymbol{A}\Delta/\hbar$, respectively, which are defined by

$$-\frac{i}{2}\frac{\partial\Delta^*}{\partial r}\hat{\boldsymbol{r}} \cdot \frac{\partial f_0}{\partial \boldsymbol{p}_\mathrm{F}} - \frac{i}{2}\frac{\partial\Delta}{\partial r}\hat{\boldsymbol{r}} \cdot \frac{\partial \bar{f}_0}{\partial \boldsymbol{p}_\mathrm{F}}, \quad \text{radial parts}, \tag{2.7a}$$

$$-\frac{i}{2r}\frac{\partial\Delta^*}{\partial\theta}\hat{\boldsymbol{\theta}} \cdot \frac{\partial f_0}{\partial \boldsymbol{p}_\mathrm{F}} - \frac{i}{2r}\frac{\partial\Delta}{\partial\theta}\hat{\boldsymbol{\theta}} \cdot \frac{\partial \bar{f}_0}{\partial \boldsymbol{p}_\mathrm{F}}, \quad \text{angular parts}, \tag{2.7b}$$

$$\frac{e}{\hbar}\Delta^*\boldsymbol{A} \cdot \frac{\partial f_0}{\partial \boldsymbol{p}_\mathrm{F}} - \frac{e}{\hbar}\Delta\boldsymbol{A} \cdot \frac{\partial \bar{f}_0}{\partial \boldsymbol{p}_\mathrm{F}}, \quad \text{vector potential parts}, \tag{2.7c}$$

where r and θ are the radius and the azimuth angle, respectively, in the cylindrical coordinate system $(r\cos\theta, r\sin\theta)$. The contribution of the spatial derivative and vector potential terms to the PPG force come from paramagnetic and diamagnetic supercurrents, respectively. Therefore, we call the spatial derivative terms (Eqs. (2.7a) and (2.7b)) and vector potential terms (Eq. (2.7c)) the paramagnetic (PM) and diamagnetic (DM) terms,

respectively. The expression for the electric field $\boldsymbol{E} = \boldsymbol{E}(\boldsymbol{r})$ is also obtained as [8,9]

$$-\lambda_{\mathrm{TF}}^2 \boldsymbol{\nabla}^2 \boldsymbol{E} + \boldsymbol{E} = i\frac{\pi k_{\mathrm{B}} T}{e} \sum_{n=0}^{n_{\mathrm{c}}} \langle \boldsymbol{\nabla}(g_1 - g_1^*) \rangle_{\mathrm{F}} \,, \tag{2.8}$$

where $\lambda_{\mathrm{TF}} \equiv \sqrt{\epsilon_0 d/2e^2 N(0)}$ is the Thomas–Fermi screening length with ϵ_0 and d denoting the permittivity of vacuum and the thickness, respectively [21,32,37]. Using this equation, we can calculate the electric field and charge density microscopically. See Appendix. A for details on the derivation of the AQC equations.

2.2 Meissner state

Kita derived the Hall coefficient due to the Lorentz force acting on equilibrium supercurrents in the Meissner state based on the AQC equations with only the Lorentz force, and showed that it has a finite value in s- and d-wave superconductors [3]. One may predict that the PPG force also acts on supercurrents even in the Meissner state and causes the Hall effect near a surface, since the charging in an isolated vortex of type-II superconductors is dominated by the angular parts which arise from the phase of the pair potential in the PPG force terms. However, contrary to its expectations, it is shown below that the PPG force does not act on supercurrents in the Meissner state. To this end, we derive an expression for the Hall electric field in the Meissner state by solving the AQC equations with the Lorentz and PPG forces to study the action of the PPG force on supercurrents. We first assume the form of the pair potential and the anomalous quasiclassical Green's function as $\Delta(\boldsymbol{r}) = |\Delta(\boldsymbol{r})| \mathrm{e}^{i\varphi(\boldsymbol{r})}$ and $f_0(\varepsilon_n, \boldsymbol{p}_{\mathrm{F}}, \boldsymbol{r}) = \tilde{f}_0(\varepsilon_n, \boldsymbol{p}_{\mathrm{F}}, \boldsymbol{r}) \mathrm{e}^{i\varphi(\boldsymbol{r})}$, respectively, substitute them into Eq. (2.4a), and neglect the spatial derivative of $\tilde{f}_0$. Then the Doppler-shifted quasiclassical Green's functions in the standard Eilenberger equations are given by

$$g_0 = \frac{\tilde{\varepsilon}_n}{\sqrt{\tilde{\varepsilon}_n^2 + |\Delta|^2}}, \tag{2.9a}$$

$$\tilde{f}_0 = \frac{|\Delta|}{\sqrt{\tilde{\varepsilon}_n^2 + |\Delta|^2}}, \tag{2.9b}$$

where $\tilde{\varepsilon}_n$ is defined by $\tilde{\varepsilon}_n \equiv \varepsilon_n + im\boldsymbol{v}_{\mathrm{F}} \cdot \boldsymbol{v}_{\mathrm{s}}$ with $\boldsymbol{v}_{\mathrm{s}} \equiv (\hbar/2m)(\boldsymbol{\nabla}\varphi - 2e\boldsymbol{A}/\hbar)$ and m denoting the superfluid velocity and the electron mass, respectively. We also substitute Eq. (2.9) into Eq. (2.6) and then obtain the g_1 equation as

$$\boldsymbol{v}_{\mathrm{F}} \cdot \boldsymbol{\nabla} g_1 = -e(\boldsymbol{v}_{\mathrm{F}} \times \boldsymbol{B}) \cdot \frac{\partial}{\partial \boldsymbol{p}_{\mathrm{F}}} \frac{\tilde{\varepsilon}_n}{\sqrt{\tilde{\varepsilon}_n^2 + |\Delta|^2}}. \tag{2.10}$$

The PPG force terms in Eq. (2.6) all cancel each other out without the low energy excitations, since the Doppler shift method is an approximation that neglects the low energy excitations such as the vortex and surface bound states (see Fig. 2.1). Fig. 2.1

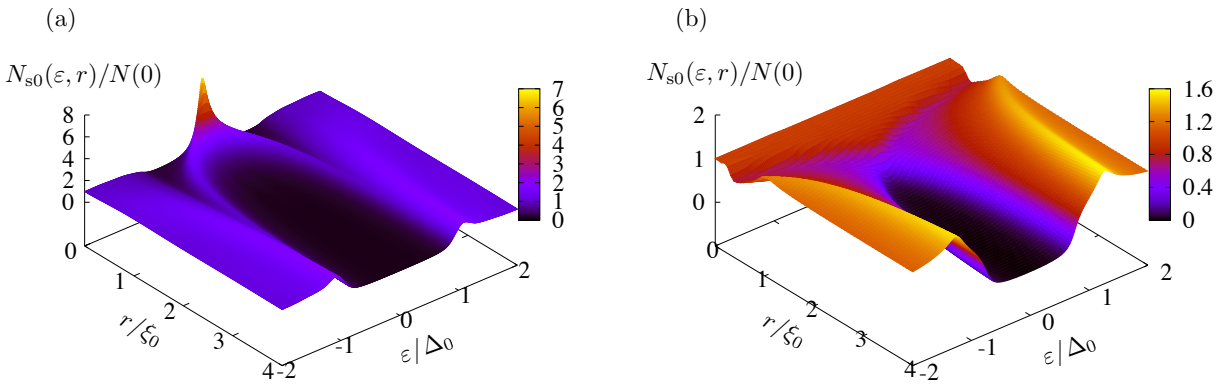

Figure 2.1: LDOS obtained from the Eilenberger equations (a) and the Doppler-shifted Green's function (b) in an isolated vortex of s-wave superconductors with a cylindrical Fermi surface in the high-κ limit. $r = 0$ is the vortex center.

plots the superconducting LDOS $N_{s0}(\varepsilon, r)$ obtained from the Eilenberger equations and the Doppler-shifted Green's function in an isolated vortex of s-wave superconductors with a cylindrical Fermi surface in the high-κ limit. $N_{s0}(\varepsilon, r)$ is calculated using Eq. (A.87). Thus, we see that the low energy excitations are important for the PPG force to work. It is now clear that the larger low-energy excitation at low temperatures is one of the factors that lead to the larger vortex-core charge due to the PPG force (Fig. 1.2).

To study the action of the PPG force on supercurrents in the Meissner state, we next assume that the gap amplitude is spatially constant as $|\Delta(\boldsymbol{r})| = |\Delta|$, and obtain g_0, f_0, and $\boldsymbol{v}_{\rm F} \cdot \boldsymbol{\nabla} g_1$ up to the first-order in $\boldsymbol{v}_{\rm s}$ as

$$g_0 = \frac{\varepsilon_n}{\sqrt{\varepsilon_n^2 + |\Delta|^2}} + im\boldsymbol{v}_{\rm F} \cdot \boldsymbol{v}_{\rm s} \frac{|\Delta|^2}{(\varepsilon_n^2 + |\Delta|^2)^{3/2}}, \tag{2.11a}$$

$$\tilde{f}_0 = \frac{|\Delta|}{\sqrt{\varepsilon_n^2 + |\Delta|^2}} - im\boldsymbol{v}_{\rm F} \cdot \boldsymbol{v}_{\rm s} \frac{\varepsilon_n |\Delta|}{(\varepsilon_n^2 + |\Delta|^2)^{3/2}}, \tag{2.11b}$$

$$\boldsymbol{v}_{\rm F} \cdot \boldsymbol{\nabla} g_1 = -ie(\boldsymbol{v}_{\rm F} \times \boldsymbol{B}) \cdot \frac{\partial}{\partial \boldsymbol{p}_{\rm F}} m\boldsymbol{v}_{\rm F} \cdot \boldsymbol{v}_{\rm s} \frac{|\Delta|^2}{(\varepsilon_n^2 + |\Delta|^2)^{3/2}}. \tag{2.11c}$$

Substituting Eqs. (2.11a) and (2.11b) into Eqs. (2.4c) and (2.4b), respectively, and using $\langle \boldsymbol{v}_{\rm F} \rangle_{\rm F} = \boldsymbol{0}$, we obtain the gap equation and the London equation as [13]

$$1 = 2\pi\Gamma_0 k_{\rm B} T \sum_{n=0}^{\infty} \frac{1}{\sqrt{\varepsilon_n^2 + |\Delta|^2}}, \tag{2.12a}$$

$$\boldsymbol{\nabla}^2 \boldsymbol{B} = \frac{1}{\lambda_{\rm L}^2} \boldsymbol{B}, \tag{2.12b}$$

where $\lambda_{\rm L}$ is the London penetration depth at finite temperatures $\lambda_{\rm L} \equiv \lambda_0 \langle v_{\rm F} \rangle_{\rm F} [2\langle (1 - Y) v_{{\rm F}x}^2 \rangle_{\rm F}]^{-1/2}$, λ_0 is the magnetic penetration depth $\lambda_0 \equiv [\mu_0 N(0) e^2 \langle v_{\rm F}^2 \rangle_{\rm F}]^{-1/2}$, and Y de-

notes the Yosida function [3, 13, 38] defined by

$$Y \equiv 1 - 2\pi k_{\mathrm{B}} T \sum_{n=0}^{\infty} \frac{|\Delta|^2}{(\varepsilon_n^2 + |\Delta|^2)^{3/2}}. \tag{2.13}$$

Furthermore, considering the region outside the vortex core or a surface without any spatial variation in the gap amplitude, substituting Eq. (2.11c) into Eq. (2.8), and using $g_1 = -\bar{g}_1$, we then obtain the equation for the electric field in the Meissner state as

$$-\lambda_{\mathrm{TF}}^2 \boldsymbol{\nabla}^2 \boldsymbol{E} + \boldsymbol{E} = \boldsymbol{B} \times \underline{R}_{\mathrm{H}} \boldsymbol{j}, \tag{2.14}$$

where $\underline{R}_{\mathrm{H}}$ is the equilibrium Hall coefficient tensor. The current density and the Hall coefficient tensor in the Meissner state given by

$$\boldsymbol{j} = meN(0)(1-Y)\langle \boldsymbol{v}_{\mathrm{F}} \boldsymbol{v}_{\mathrm{F}} \rangle_{\mathrm{F}} \boldsymbol{v}_{\mathrm{s}}, \tag{2.15a}$$

$$\underline{R}_{\mathrm{H}} = \frac{1}{2eN(0)} \left\langle \frac{\partial}{\partial \boldsymbol{p}_{\mathrm{F}}} \boldsymbol{v}_{\mathrm{F}} \right\rangle_{\mathrm{F}} \langle \boldsymbol{v}_{\mathrm{F}} \boldsymbol{v}_{\mathrm{F}} \rangle_{\mathrm{F}}^{-1}. \tag{2.15b}$$

This Hall coefficient is the same as that obtained in Ref. [3], despite considering the PPG force. Therefore, the Lorentz force acts on supercurrents in the Meissner state as shown in the previous study [3], but the PPG force does not. It can also be shown that the PPG force does not act on the shielding currents in anisotropic [32] and chiral [21] superconductors based on the corresponding AQC equations if $\boldsymbol{v}_{\mathrm{F}} \cdot \boldsymbol{\nabla} \tilde{f}_0$ is zero.

2.3 Bogoliubov–de Gennes equations

For simplicity, we consider spin-singlet s-wave superconductors with a cylindrical Fermi surface and adopt the same method in Refs. [34, 39], and [6] to solve the BdG equations self-consistently. We also neglect the vector potential when calculating the vortex-core charge. These assumptions are valid, as will be shown below, based on the AQC equations, the vortex-core charging comes from the pair-potential gradient force acting on the paramagnetic supercurrents [31]. Nevertheless, it is imperative to confirm the validity of these assumptions within the BdG equations, as a future work.

Then, for clean s-wave superconductors in equilibrium, the BdG equations are given by

$$\left[-\frac{\hbar^2}{2m} \boldsymbol{\nabla}^2 + e\Phi(\boldsymbol{r}) - \mu \right] u_n(\boldsymbol{r}) - \Delta(\boldsymbol{r}) v_n(\boldsymbol{r}) = E_n u_n(\boldsymbol{r}), \tag{2.16a}$$

$$-\left[-\frac{\hbar^2}{2m} \boldsymbol{\nabla}^2 + e\Phi(\boldsymbol{r}) - \mu \right] v_n(\boldsymbol{r}) - \Delta^*(\boldsymbol{r}) u_n(\boldsymbol{r}) = E_n v_n(\boldsymbol{r}), \tag{2.16b}$$

where $\Phi(\boldsymbol{r})$ and μ are the electrostatic and chemical potentials, $u_n(\boldsymbol{r})$ and $v_n(\boldsymbol{r})$ are Bogoliubov wave functions labeled by the quantum number n. The pair potential is determined by

$$\Delta(\boldsymbol{r}) = \Gamma_0 \sum_n u_n(\boldsymbol{r}) v_n^*(\boldsymbol{r}) (1 - 2f_{\mathrm{F}}(E_n)), \tag{2.17}$$

where $f_{\rm F}(E_n)=1/(\mathrm{e}^{E_n/k_{\rm B}T}+1)$ is Fermi distribution function at temperature T. We solve self-consistently Eqs. (2.16) and (2.17) together with the following Poisson equation:

$$\begin{aligned}-\epsilon_0\boldsymbol{\nabla}^2\Phi(\boldsymbol{r}) &= \rho(\boldsymbol{r}) \\ &= e\left(n(\boldsymbol{r})-n_0\right) \\ &= 2e\sum_n\left[|u_n(\boldsymbol{r})|^2 f_{\rm F}(E_n)+|v_n(\boldsymbol{r})|^2(1-f_{\rm F}(E_n))\right]-en_0, \end{aligned} \tag{2.18}$$

where $n(\boldsymbol{r})$ is the particle density and n_0 is the particle density at a sufficient distance from the vortex center.

We next consider a two-dimensional superconductor with an isolated vortex, neglect the kinetic term with the z direction, and use $\Delta(\boldsymbol{r})=\Delta(r)\mathrm{e}^{-i\theta}$ as the form of the pair potential with the cylindrical coordinates (r,θ). The Bogoliubov wave functions, $u_n(\boldsymbol{r})$ and $v_n(\boldsymbol{r})$, which are classified in terms of the angular momentum l, are expanded as

$$u_n(\boldsymbol{r})=u_{nl}(r)e^{il\theta}=\sum_i c_i^{nl}\phi_i^l(r)\mathrm{e}^{il\theta}, \tag{2.19a}$$

$$v_n(\boldsymbol{r})=v_{nl}(r)e^{i(l+1)\theta}=\sum_i d_i^{nl}\phi_i^{l+1}(r)\mathrm{e}^{i(l+1)\theta}, \tag{2.19b}$$

where ϕ_i^l is given by $\phi_i^l(r)=\sqrt{2}J_l(\alpha_i^l r/R)/RJ_{l+1}(\alpha_i^l)$, $J_l(x)$ is the Bessel function of l-th order, α_i^l is the i-th zero of J_l, R is radius of a vortex, and i is integer ranging from $i=1$ to N with N denoting the cutoff depending on the temperature and quasiclassical parameter. We can rewrite the BdG equations to eigenvalue problem for $2N\times 2N$ matrices with simplified forms:

$$\begin{pmatrix}\underline{K}^l & \underline{\Delta} \\ \underline{\Delta}^{\rm T} & -\underline{\bar{K}}^{l+1}\end{pmatrix}\begin{pmatrix}\boldsymbol{c}^{n,l}\\ \boldsymbol{d}^{n,l}\end{pmatrix}=E_{n,l}\begin{pmatrix}\boldsymbol{c}^{n,l}\\ \boldsymbol{d}^{n,l}\end{pmatrix}, \tag{2.20a}$$

$$(\underline{K}^l)_{ij}\equiv\left[\frac{\hbar^2}{2m}\left(\frac{\alpha_j^l}{R}\right)^2-\mu\right]\delta_{ij}-\int_0^R rdr\phi_i^l(r)\Phi(r)\phi_j^l(r), \tag{2.20b}$$

$$(\underline{\bar{K}}^{l+1})_{ij}\equiv\left[\frac{\hbar^2}{2m}\left(\frac{\alpha_j^l}{R}\right)^2-\mu\right]\delta_{ij}-\int_0^R rdr\phi_i^{l+1}(r)\Phi(r)\phi_j^{l+1}(r), \tag{2.20c}$$

$$(\underline{\Delta}^l)_{ij}\equiv-\int_0^R rdr\phi_i^l(r)\Delta(r)\phi_j^{l+1}(r), \tag{2.20d}$$

$$\boldsymbol{c}^{n,l}\equiv[c_1^{n,l},c_2^{n,l},\cdots]^{\rm T},\qquad \boldsymbol{d}^{n,l}\equiv[d_1^{n,l},d_2^{n,l},\cdots]^{\rm T}. \tag{2.20e}$$

Similarly, by expanding with the orthogonal function system, the pair potential and the number of particles can be expressed as

$$\Delta(r)=\Gamma_0\sum_{n,l}\sum_{i,j}c_i^{n,l}\phi_i^l(r)d_j^{n,l}\phi_j^{l+1}(r)\left(1-2f_{\rm F}(E_{n,l})\right), \tag{2.21}$$

$$n(r) = 2\sum_{n,l}\sum_{i,j}\Big[\Big(c_i^{n,l}\phi_i^l(r)c_j^{n,l}\phi_j^l(r) - d_i^{n,l}\phi_i^{l+1}(r)d_j^{n,l}\phi_j^{l+1}(r)\Big) f_{\rm F}(E_{n,l}) + d_i^{n,l}\phi_i^{l+1}(r)d_j^{n,l}\phi_j^{l+1}(r)\Big]. \tag{2.22}$$

The normalization condition,

$$\int d^3r \left(|u_n(\boldsymbol{r})|^2 + |v_{n'}(\boldsymbol{r})|^2\right) = \delta_{nn'}, \tag{2.23}$$

is also translated as

$$\begin{aligned} 1 &= 2\pi\int_0^R rdr \sum_{i=1}^{\infty}\sum_{j=1}^{\infty}\left(c_i^{n,l}c_j^{n,l}\phi_i^l(r)\phi_j^l + d_i^{n,l}d_j^{n,l}\phi_i^{l+1}(r)\phi_j^{l+1}\right) \\ &= 2\pi\sum_{i=1}^{\infty}\left((c_i^{n,l})^2 + (d_i^{n,l})^2\right). \end{aligned} \tag{2.24}$$

We finally estimate the coupling constant Γ_0 by assuming a uniform system at absolute zero. In a uniform system, each component of the matrix is diagonalized as

$$(\underline{\Delta})_{i,j} = \Delta_0\delta_{ij}, \tag{2.25a}$$

$$(\underline{K})_{i,j} = \left[\frac{\hbar^2}{2m}\left(\frac{\alpha_j^l}{R}\right)^2 - \mu\right]\delta_{ij} \equiv \xi_j^{n,l}\delta_{ij}. \tag{2.25b}$$

Thus, the BdG equations are written as

$$\left(\begin{array}{ccc|ccc} \xi_1^{n,l} & & 0 & \Delta_0 & & 0 \\ & \xi_2^{n,l} & & & \Delta_0 & \\ 0 & & \ddots & 0 & & \ddots \\ \hline \Delta_0 & & 0 & -\xi_1^{n,l} & & 0 \\ & \Delta_0 & & & -\xi_2^{n,l} & \\ 0 & & \ddots & 0 & & \ddots \end{array}\right)\left(\begin{array}{c} c_1^{n,l} \\ c_2^{n,l} \\ \vdots \\ \hline d_1^{n,l} \\ d_2^{n,l} \\ \vdots \end{array}\right) = E_{n,l}\left(\begin{array}{c} c_1^{n,l} \\ c_2^{n,l} \\ \vdots \\ \hline d_1^{n,l} \\ d_2^{n,l} \\ \vdots \end{array}\right),$$

$$\Longrightarrow \left(\begin{array}{cccccc} \xi_1^{n,l} & \Delta_0 & & & & 0 \\ \Delta_0 & -\xi_1^{n,l} & & & & \\ & & \ddots & & & \\ & & & \xi_i^{n,l} & \Delta_0 & \\ & & & \Delta_0 & -\xi_i^{n,l} & \\ 0 & & & & & \ddots \end{array}\right)\left(\begin{array}{c} c_1^{n,l} \\ d_1^{n,l} \\ \vdots \\ c_i^{n,l} \\ d_i^{n,l} \\ \vdots \end{array}\right) = E_{n,l}\left(\begin{array}{c} c_1^{n,l} \\ d_1^{n,l} \\ \vdots \\ c_i^{n,l} \\ d_i^{n,l} \\ \vdots \end{array}\right), \tag{2.26}$$

which is a two-line, two-column eigenvalue equation:

$$\begin{pmatrix} \xi_i^{n,l} & \Delta_0 \\ \Delta_0 & -\xi_i^{n,l} \end{pmatrix}\begin{pmatrix} c_i^{n,l} \\ d_i^{n,l} \end{pmatrix} = E_{n,l}\begin{pmatrix} c_i^{n,l} \\ d_i^{n,l} \end{pmatrix}. \tag{2.27}$$

The eigenvalues and eigenfunctions of this expression are

$$E_{n,l} = \pm\sqrt{(\xi_i^{n,l})^2 + \Delta_0^2}, \tag{2.28a}$$

$$c_i^{n,l} = \sqrt{\frac{1}{4\pi}\left(1 \pm \frac{\xi_i^{n,l}}{E_{n,l}}\right)}, \qquad d_i^{n,l} = \sqrt{\frac{1}{4\pi}\left(1 \mp \frac{\xi_i^{n,l}}{E_{n,l}}\right)}. \tag{2.28b}$$

Since the Fermi distribution function at $T=0$ is a step function, Eq. (2.21) becomes

$$\Delta_0 = \Gamma_0 \sum_{n,l} \sum_{i,j} c_i^{n,l} d_j^{n,l} \phi_i^l(r) \phi_j^l(r)(1 - 2\theta(-E_{n,l})). \tag{2.29}$$

Furthermore, by operating $\int_0^R r dr$ to both sides of Eq. (2.29) and using Eq. (2.28), we can obtain the coupling constant as

$$\begin{aligned} \frac{1}{\Gamma_0} &= \frac{1}{2\pi R^2} \sum_{n,l} \sum_{i} \frac{(1 - 2\theta(-E_{n,l}))}{E_{n,l}} \\ &= \frac{1}{2\pi R^2} \left(\sum_{0 \le E_{n,l}} \frac{1}{E_{n,l}} - \sum_{E_{n,l}<0} \frac{1}{E_{n,l}} \right) \\ &= \frac{1}{2\pi R^2} \sum_{0 \le |E_{n,l}| < E_c} \frac{1}{|E_{n,l}|}, \end{aligned} \tag{2.30}$$

where E_c is the energy cutoff, and we set $E_c = 10\Delta_0$. $\sum_{0 \le |E_{n,l}| < E_c}$ denotes the summation of all positive quantum numbers n, l, and i that satisfy $0 \le |E_{n,l}| < E_c$.

3 Numerical Results

3.1 Numerical procedures

We solve Eqs. (2.4), (2.6), and (2.8) numerically for a triangular vortex lattice of an s-wave superconductor with a cylindrical Fermi surface by combing the methods in Refs. [8] and [22]. We choose the magnetic field to be along the axial direction of the cylinder. We can also express the corresponding vector potential in terms of the average flux density $\bar{\boldsymbol{B}} = (0, 0, \bar{B})$ as $\boldsymbol{A}(\boldsymbol{r}) = (\bar{\boldsymbol{B}} \times \boldsymbol{r})/2 + \tilde{\boldsymbol{A}}(\boldsymbol{r})$, where $\tilde{\boldsymbol{A}}$ denotes the spatial variation of the flux density. Functions $\tilde{\boldsymbol{A}}(\boldsymbol{r})$ and $\Delta(\boldsymbol{r})$ for the triangular lattice have the following periodic boundary conditions [40–42]:

$$\tilde{\boldsymbol{A}}(\boldsymbol{r} + \boldsymbol{R}) = \tilde{\boldsymbol{A}}(\boldsymbol{r}), \tag{3.1a}$$

$$\Delta(\boldsymbol{r} + \boldsymbol{R}) = \Delta(\boldsymbol{r}) \mathrm{e}^{i\frac{|e|}{\hbar}\bar{\boldsymbol{B}}\cdot(\boldsymbol{r}\times\boldsymbol{R}) + i\frac{|e|}{\hbar}\bar{\boldsymbol{B}}\times(\boldsymbol{a}_1 - \boldsymbol{a}_2)\cdot\boldsymbol{R} + i\pi n_1 n_2}, \tag{3.1b}$$

where $\boldsymbol{R} = n_1\boldsymbol{a}_1 + n_2\boldsymbol{a}_2$ with the integers n_1 and n_2, and $\boldsymbol{a}_1 = a_2(\sqrt{3}/2, 1/2, 0)$ and $\boldsymbol{a}_2 = a_2(0, 1, 0)$ are the basic vectors of the triangular lattice with the length a_2 determined

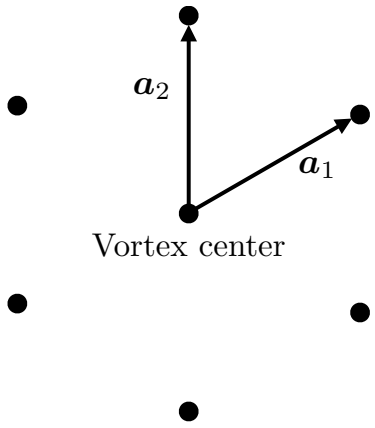

Figure 3.1: Schematic representation of a vortex-lattice.

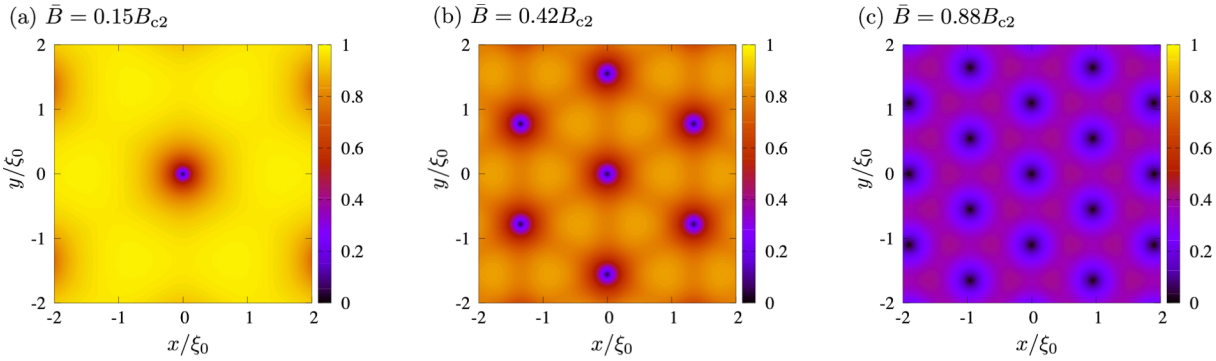

Figure 3.2: Gap amplitude $|\Delta(\boldsymbol{r})|$ at temperature $T = 0.2T_c$ in units of the zero temperature gap Δ_0 on a square grid with x and y ranging from $[-2\xi_0, +2\xi_0]$ for the average flux densities (a) $\bar{B} = 0.15B_{c2}$, (b) $\bar{B} = 0.42B_{c2}$, and (c) $\bar{B} = 0.88B_{c2}$.

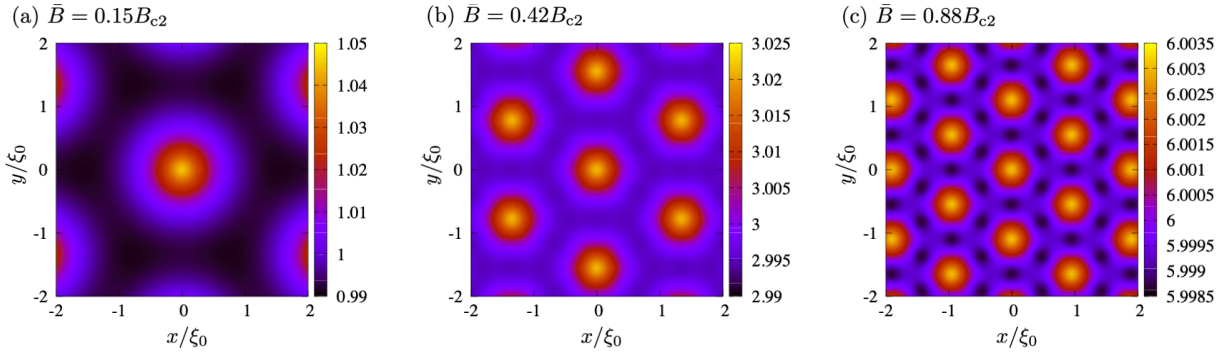

Figure 3.3: Magnetic-flux density $B(\boldsymbol{r})$ at temperature $T = 0.2T_c$ in units of $B_0 \equiv \hbar/2|e|\xi_0^2$ on a square grid with x and y ranging from $[-2\xi_0, +2\xi_0]$ for the average flux densities (a) $\bar{B} = 0.15B_{c2}$, (b) $\bar{B} = 0.42B_{c2}$, and (c) $\bar{B} = 0.88B_{c2}$.

by the flux-quantization condition $(\boldsymbol{a}_1 \times \boldsymbol{a}_2) \cdot \bar{\boldsymbol{B}} = h/2|e|$. We first solve the standard Eilenberger equations (2.4) self-consistently for the vortex lattice using the Riccati method [13, 30, 43, 44], and substitute the solution into the right-hand side of Eq. (2.6), which is solved by using the standard Runge–Kutta method. Here, we have chosen the following initial conditions:

$$\Delta(\boldsymbol{r}) = \Delta_T \sqrt{1 - \frac{\bar{B}}{B_{c2}}}\tilde{\psi}^s, \qquad \tilde{\boldsymbol{A}}(\boldsymbol{r}) = \boldsymbol{0}, \tag{3.2}$$

where Δ_T is the energy gap obtained by solving the weak-coupling gap equation [Eq. (2.12a)], $B_{c2} = \mu_0 H_{c2}$ is the upper critical field obtained from the Helfand–Werthamer theory [45, 46], and $\tilde{\psi}^s$ denotes the Abrikosov's solution of the linearized GL equations in a symmetric gauge without prefactors [13, 41]. Then, we have used the periodic conditions of the Green's functions:

$$g_0(\varepsilon_n, R_z(n\pi/3)\boldsymbol{p}_F, R_z(n\pi/3)\boldsymbol{r}) = g_0(\varepsilon_n, \boldsymbol{p}_F, \boldsymbol{r}), \tag{3.3a}$$

$$f_0(\varepsilon_n, R_z(n\pi/3)\boldsymbol{p}_F, R_z(n\pi/3)\boldsymbol{r}) = f_0(\varepsilon_n, \boldsymbol{p}_F, \boldsymbol{r})\mathrm{e}^{-in\pi/3}, \tag{3.3b}$$

where $R_z(\theta)$ is a rotation operator that rotates the vortex center by an angle θ around the z-axis, and n is an integer. Next, the electric field is obtained by substituting the solution of Eq. (2.6) into Eq. (2.8) and solving Eq. (2.8), and then the charge density ρ is calculated from Gauss' law $\rho = \epsilon_0 d\boldsymbol{\nabla} \cdot \boldsymbol{E}$ numerically. We choose the parameters as $\lambda_{TF} = 0.03\xi_0$, $\lambda_0 = 5\xi_0$ and $\delta = 0.03$. The average magnetic flux density, which is a parameter, is normalized by using the upper critical field B_{c2}.

To study the δ-dependence of the vortex-core charge in s-wave superconductors with a cylindrical Fermi surface near quantum limit, we also solve the eigenvalue equation [Eq. (2.20)] obtained form the BdG equations together with the gap [Eq. (2.21)] and Poisson equations [Eqs. (2.18) and (2.22)] self-consistently and numerically. We use $\Phi = 0$ and $\Delta = \Delta_T \tanh r/\xi_0$ when we first solve Eq. (2.20).

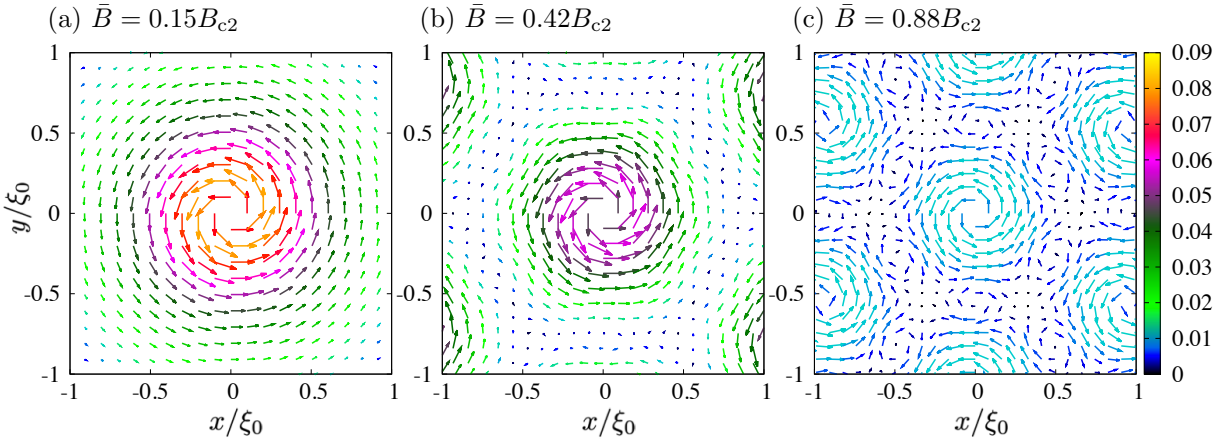

Figure 3.4: Supercurrent $\boldsymbol{j}(\boldsymbol{r}) = (j_x(\boldsymbol{r}), j_y(\boldsymbol{r}))$ at temperature $T = 0.2T_c$ in units of $j_0 \equiv \hbar\mu_0/2|e|\xi_0^3$, on a square grid with x and y ranging from $[-\xi_0, +\xi_0]$, for the average flux densities (a) $\bar{B} = 0.15B_{c2}$ and (b) $\bar{B} = 0.42B_{c2}$ (c) $\bar{B} = 0.88B_{c2}$.

3.2 Vortex-core charging in the Abrikosov lattice

Figs. 3.2, 3.3, and 3.4 show the spatial variations of the gap amplitude $|\Delta(\boldsymbol{r})|$, the z-component of the magnetic-flux density $B(\boldsymbol{r})$, the current density $\boldsymbol{j}(\boldsymbol{r})$, respectively, at temperature $T = 0.2T_c$ for the average flux densities from $\bar{B} = 0.15B_{c2}$ to $\bar{B} = 0.88B_{c2}$. We find that the gap amplitude away from the vortex core and its slope at the core become small together, and the $B/\bar{B}$ at the core is also small, i.e. the flux density becomes spatially uniform at strong magnetic fields compared with weak fields. We also see in Figs. 3.2, 3.3, and 3.4 that the distance between the two vortices becomes closer and each vortex has the strong six-fold symmetrical anisotropy at strong magnetic fields. Thus, we have reproduced the results in the previous work proposed by Ichioka *et al.* [42].

Figs. 3.5 and 3.6 show the spatial dependence of the charge density $\rho(\boldsymbol{r})$ and the electric field $\boldsymbol{E}(\boldsymbol{r})$ due to the Lorentz force, and the spatial derivative terms of the pair potential and the terms for the product of the vector and pair potential in the PPG force, respectively, at temperature $T = 0.2T_c$ for the average flux densities from $\bar{B} = 0.15B_{c2}$ to $\bar{B} = 0.88B_{c2}$. We see that the charges are accumulated at the core where the pair potential is zero. The charge redistribution due to the Lorentz force and the PM terms in the PPG force are very similar, but the charge due to the PM terms in the PPG force is larger at weak magnetic fields compared to that due to the Lorentz force. On the other hand, the charge due to the DM terms in the PPG force has an opposite sign and almost the same magnitude as that due to the Lorentz force. We also find that larger charge accumulates between two neighboring vortices at strong magnetic fields since the distance between the two vortices becomes smaller and circulating supercurrents in the opposite direction from that around the core are generated between the two vortices at strong magnetic fields as found in Fig. 3.4(c). We also see in Fig. 3.6 that the Hall electric fields are orthogonal to

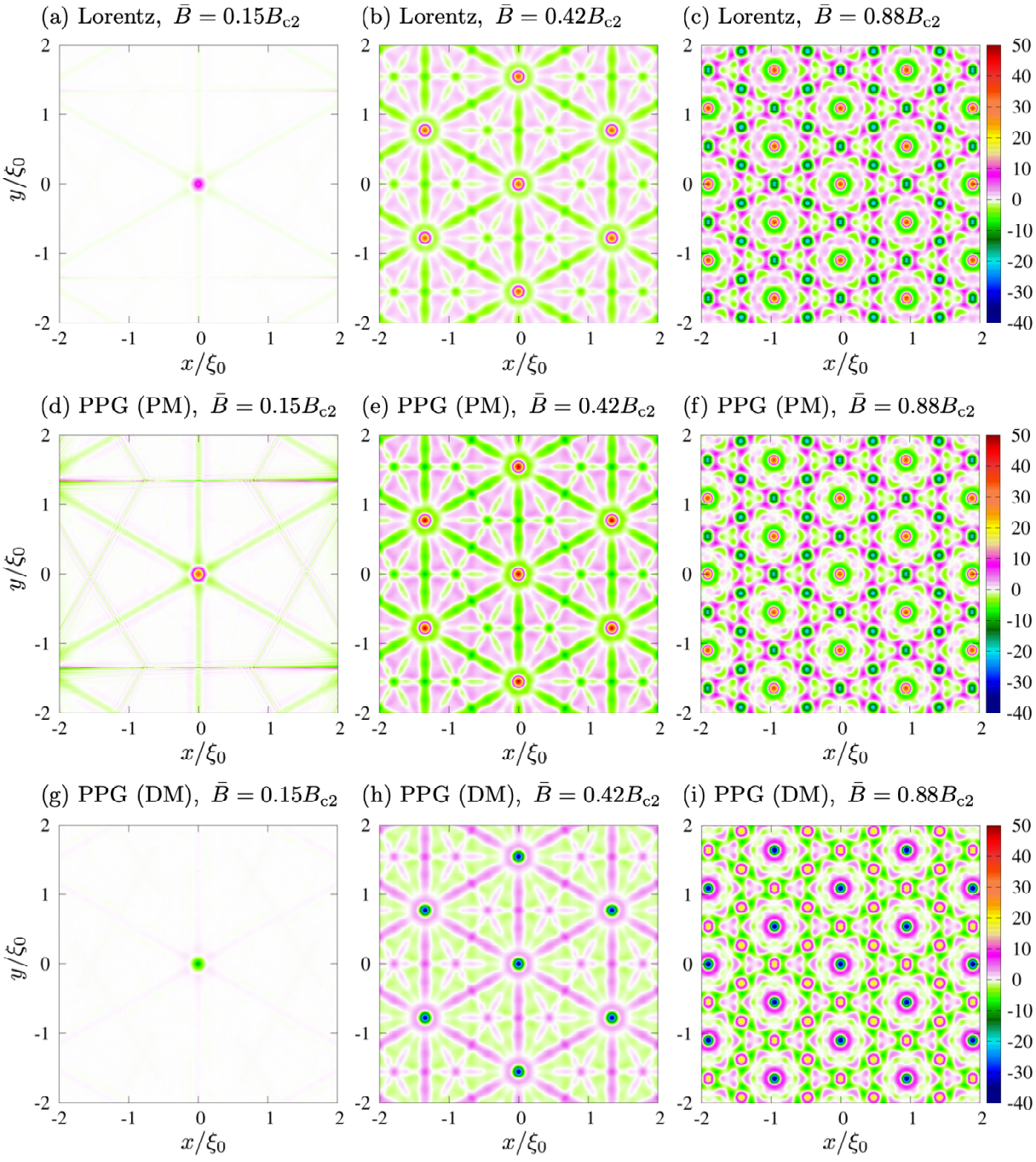

Figure 3.5: Charge density $\rho(\boldsymbol{r})$ due to the Lorentz force ((a), (b), and (c)), and the paramagnetic ((d), (e), and (f)) and diamagnetic ((g), (h), and (i)) terms in the PPG force at temperature $T = 0.2T_c$ in units of $\rho_0 \equiv \Delta_0\epsilon_0 d/|e|\xi_0^2$ on a square grid with x and y ranging from $[-2\xi_0, +2\xi_0]$ for the average flux densities $\bar{B} = 0.15B_{c2}$, $\bar{B} = 0.42B_{c2}$, and $\bar{B} = 0.88B_{c2}$ from right to left, respectively. PM and DM denote paramagnetic and diamagnetic, respectively.

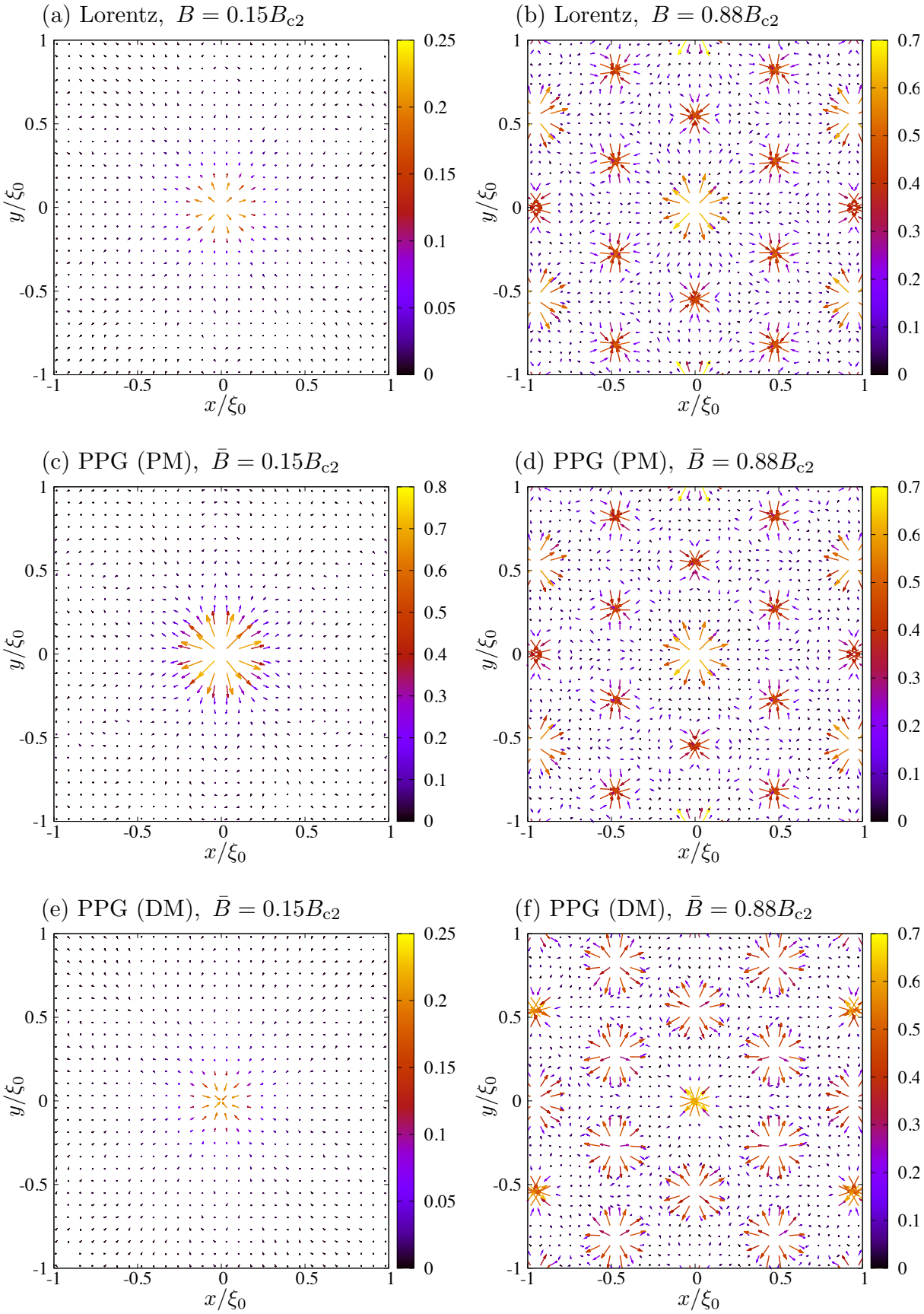

Figure 3.6: Electric field $\boldsymbol{E}(\boldsymbol{r})$ due to the Lorentz force ((a) and (b)), and the paramagnetic ((c) and (d)) and diamagnetic ((e) and (f)) terms in the PPG force at temperature $T = 0.2T_c$ in units of $E_0 \equiv \Delta_0/|e|\xi_0$ on a square grid with x and y ranging from $[-\xi_0, +\xi_0]$ for the average flux densities $\bar{B} = 0.15B_{c2}$, $\bar{B} = 0.42B_{c2}$, and $\bar{B} = 0.88B_{c2}$ from right to left, respectively. PM and DM denote paramagnetic and diamagnetic, respectively.

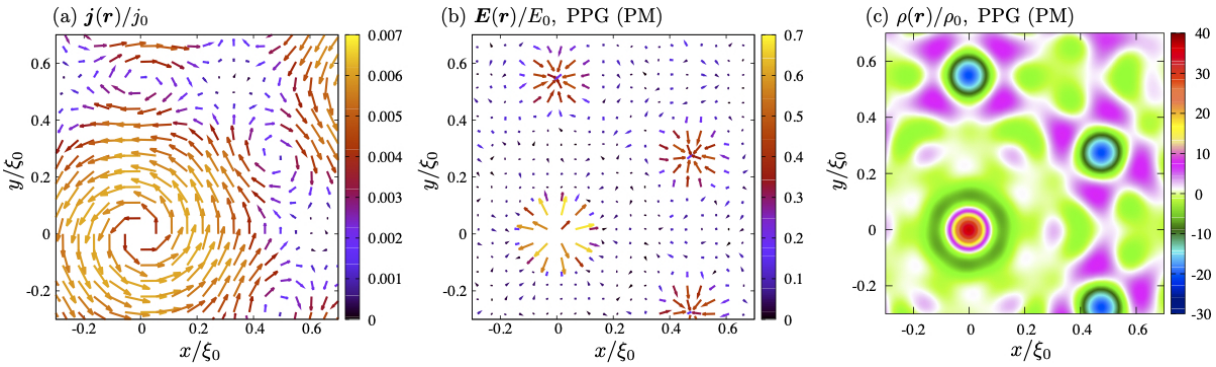

Figure 3.7: Zoomed-in plots of (a) the current density $\boldsymbol{j}(\boldsymbol{r})$, (b) the electric field $\boldsymbol{E}(\boldsymbol{r})$ (b), and (c) the charge density $\rho(\boldsymbol{r})$ due to the PM terms in the PPG force for temperature $T = 0.2T_c$ and the average flux density $\bar{B} = 0.88B_{c2}$ on a square grid with x and y ranging from $[-0.3\xi_0, 0.7\xi_0]$ in units of $j_0 \equiv \hbar\mu_0/2|e|\xi_0^3$ $E_0 \equiv \Delta_0/|e|\xi_0$, and $\rho_0 \equiv \Delta_0\epsilon_0 d/|e|\xi_0^2$, respectively.

supercurrents and strong around the core and between two neighboring vortices at strong magnetic fields. To make it clear to understand the relationship between the supercurrent, electric field, and charge redistribution, the zoomed-in plots of Figs. 3.4(c), 3.5(f) and 3.6(d) are shown in Fig. 3.7.

Fig. 3.8 shows the charge density at the vortex center as a function of the magnetic field for temperatures $T = 0.2T_c$ and $T = 0.5T_c$, respectively. It is shown that the vortex-core charge due to the Lorentz force has a large peak of upper convexity as seen in the previous work [22]. However, the vortex-core charge due to the Lorentz force obtained by us is about 10 times larger than that calculated in the previous study [22], even if the same quasiclassical parameter is used. This is because the method in the previous study neglected the component perpendicular to the Fermi velocity of in $\boldsymbol{\nabla} g_1$. We have here adopted a direct method to solve the equation for g_1 [Eq. (2.6)] used in Refs. [8, 9]. We also note that the vortex-core charge has the λ_{TF}-dependence and is not linear as a function of δ using $\delta = \lambda_{TF}/\xi_0$, even within the AQC theory. On the other hand, the vortex-core charge due to the DM terms in the PPG force has an opposite sign and almost the same magnitude as that due to the Lorentz force at all temperatures and magnetic fields within our calculation. Therefore, the charge due to the Lorentz force and the DM terms in the PPG force almost cancel each other out. Consequently, the total charge is almost the same as that due to the PM terms in the PPG force. We also find that the vortex-core charge due to the PM and DM terms, respectively, in the PPG force also has a peak at about half the upper critical field as a function of the magnetic field. This may be due to the fact that the PM and DM supercurrents also have peaks because it is expected that the magnetic field dependence of the charge due to the PPG force is the same as that of the supercurrents. Based on this, we can find in Fig. 3.9 that both the charge due to all the PPG force terms and the total supercurrents around the core

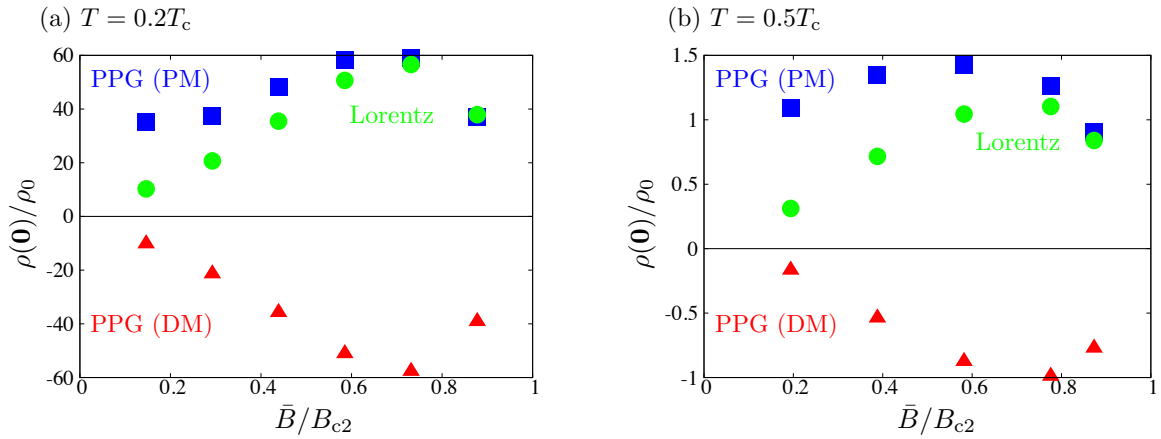

Figure 3.8: Charge density at the vortex center $\rho(\mathbf{0})$ due to the Lorentz force (green circular points), and the paramagnetic (blue square points) and diamagnetic (red triangular points) terms in the PPG force in units of $\rho_0 \equiv \Delta_0\epsilon_0 d/|e|\xi_0^2$ as a function of the magnetic field calculated for temperatures (a) $T = 0.2T_c$ and (b) $T = 0.5T_c$. PM and DM denote paramagnetic and diamagnetic, respectively.

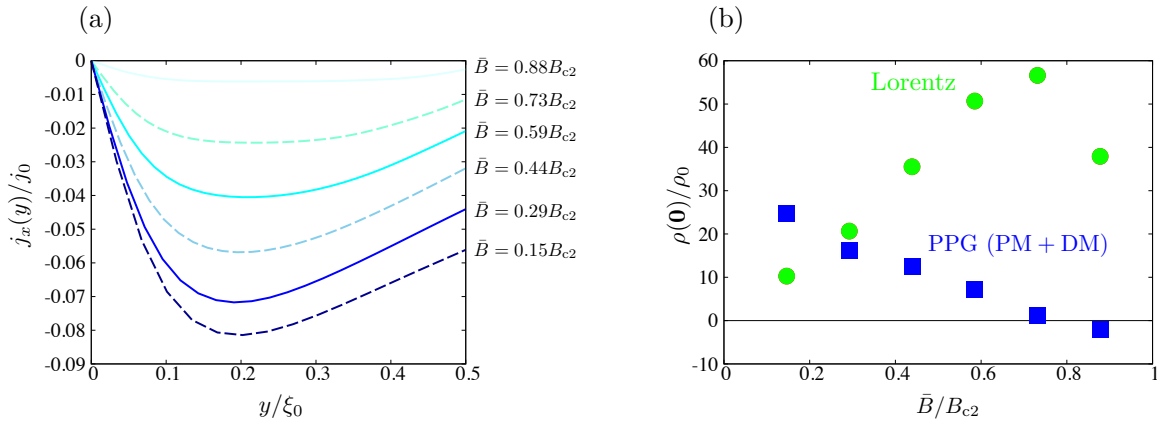

Figure 3.9: (a) The x-component of a supercurrent $j_x(\boldsymbol{r})$ in units of $j_0 \equiv \hbar\mu_0/2|e|\xi_0^3$ over $y \leq 0.5\xi_0$ at $x = 0$ for several $\bar{B}$, and (b) charge density at the vortex center $\rho(\mathbf{0})$ due to the Lorentz force (green circular points), and the PPG force (blue square points) in units of $\rho_0 \equiv \Delta_0\epsilon_0 d/|e|\xi_0^2$ as a function of the magnetic field calculated for $T = 0.2T_c$. PM and DM denote paramagnetic and diamagnetic, respectively.

decrease monotonically with an increase in magnetic field. We can also explain that the peak of the total charge originates from the competition between the charges due to the PPG force, which is dominant at weak fields, and the Lorentz force, which is dominant at strong fields as shown in Fig. 3.9(b). Thus, measurements should be performed at low temperatures and about half the upper critical field to detect the vortex-core charge experimentally.

Fig. 3.10 shows the λ_0 dependence of the charge density at the vortex center due the Lorentz and PPG forces [8] and the spatial dependence of the magnetic-flux density with an isolated vortex in a two-dimensional s-wave superconductor at temperature $T = 0.2T_c$. As λ_0 becomes larger, the wider and more gently the magnetic flux penetrates, so the magnetic-flux density at the vortex center becomes smaller. Therefore, $\rho(0)$ due to the Lorentz force rapidly decreases as λ_0 is increased. On the other hand, even in the high-κ

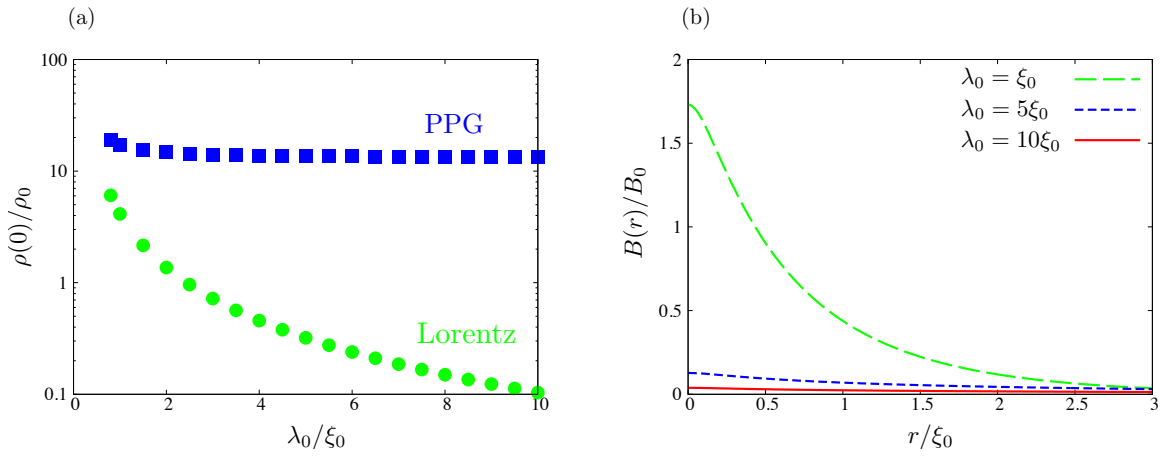

Figure 3.10: (a) Magnetic-penetration-depth dependence of the charge density $\rho(r)$ at the vortex center due to the Lorentz and PPG forces and (b) the spatial dependence of the magnetic-flux density $B(\boldsymbol{r})$ with an isolated vortex s-wave superconductors at temperature $T = 0.2T_c$ in units of $\rho_0 \equiv \Delta_0\epsilon_0 d/|e|\xi_0^2$ and $B_0 \equiv \hbar/2|e|\xi_0^2$, respectively.

limit, which can be regarded as a zero field, the PPG force charging is relatively large, if it is a vortex state where low-energy excitation occurs.

We next calculate the order of magnitude for the accumulated charge around a vortex to compare our result with the vortex-core charge measured by the NMR/NQR [47]. We choose the core region of radius $0.2\xi_0$ and the thickness $d = 10$ Å to roughly estimate the peak value of the accumulated charge Q. The vortex-core charge in YBCO at $T = 0.2T_c$ and $B = 0.73B_{c2}$ is given by $Q \sim 10^{-3}|e|$ for the following appropriate parameters: $k_F^{-1} \simeq 1.0$ Å, $\Delta_0 \simeq 28$ meV [48], and $\xi_0 \simeq 30$ Å [47]. The amount of charge that we estimate based on our present calculation is an order of magnitude larger than the charge reported in Ref. [22], owing to the difference in the method and the Thomas–Fermi screening length described above. The order of magnitude of the estimated charge in YBCO using our calculation is roughly consistent with the experimental results measured by Kumagai *et al.* [47].

We finally discuss what the vortex-core charging due to the PPG force is. The vortex-core charge due to the PPG force at weak magnetic fields has the following characteristics: (i) the dominant contribution from the angular parts, i.e. the angular derivatives of the cylindrical coordinates around the vortex core [21], (ii) the PPG force acts on only supercurrents in the vortex state in the core, and (iii) it is relatively large even in the high-κ limit and in the isolated vortex system [8,9]. The PPG force terms are dominated by the angular parts arising from the phase of the pair potential, and they all cancel each other out away from the core as seen in Subsect. 2.2. Therefore, the presence of supercurrents is essential to PPG force charging in the vortex state. Furthermore, since the vortex-core charge is relatively large even in the high-κ limit and in the isolated vortex system, the large vortex-charging is caused by the PPG force acting on circulating supercurrents in

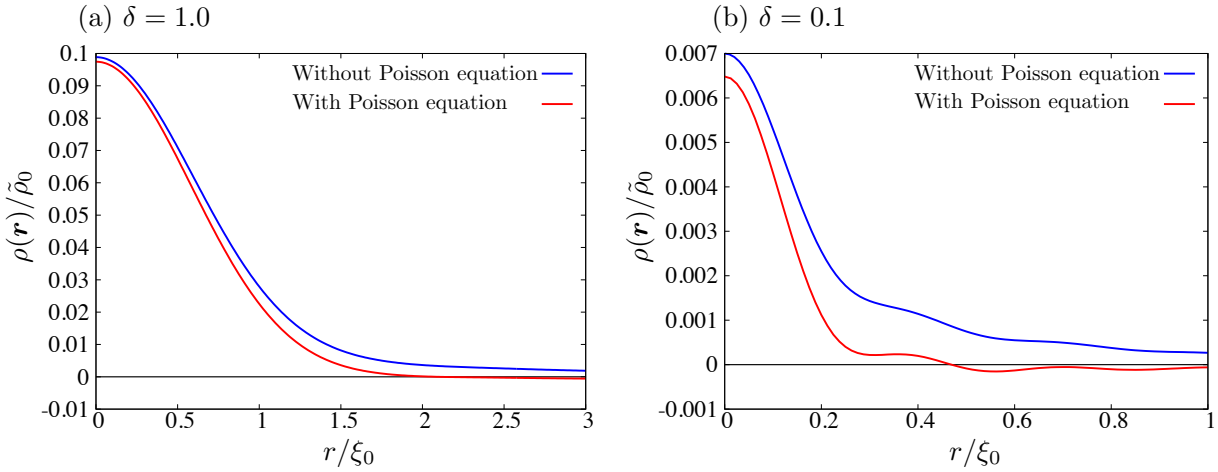

Figure 3.11: Charge density at the vortex center $\rho(\mathbf{0})$ without the Poisson equation (blue line), with the Poisson equation (red line) in units of $\tilde{\rho}_0 \equiv \varepsilon_{\rm F}\epsilon_0 k_{\rm F}^2 d/|e|$ calculated for $T = 0.2T_{\rm c}$ at (a) $\delta = 1.0$ and (b) $\delta = 0.1$.

the vortex state even in an area that can be considered zero magnetic field as seen in Fig. 3.10. Thus, we can deduce that the vortex-core charging due to the PPG force is the anomalous Hall effect on supercurrents in the vortex state.

3.3 Charging in an isolated vortex near the quantum limit without the vector potential

Fig. 3.11 plots the spatial variations of the charge density around an isolated vortex core at temperature $T = 0.2T_{\rm c}$ for the quasiclassical parameters $\delta = 0.1$ and 1 based on the BdG equations with and without the Poisson equation, simultaneously. We confirm that the charge density satisfies the neutral condition by solving the BdG equations with the Poisson equation self-consistently, and the Friedel-like oscillation of the charge density around the core obtained from the BdG equations with the Poisson equation is stronger than that without the Poisson equation. Thus, we have reproduced the result proposed by Machida *et al.* [34]. We also see that the Friedel-like oscillation cannot be found in the quantum limit. This may be because the period of the oscillation is longer and number of the energy peaks in the LDOS decreases [49] as the quasiclassical parameter approaches the quantum limit $\delta = 1$.

Fig. 3.12 plots the quasiclassical parameter dependence of the vortex-core charge at temperature $T = 0.2T_{\rm c}$ based on the BdG equations with and without the Poisson equation, simultaneously. The charge density at the vortex center increases almost linearly within $0.1 \leq \delta \leq 1$ and the vortex-core charge with the quantum limit $\delta = 1$ is more than 10 times larger than that with $\delta = 0.03$ that we used above when solving the AQC equations. Hayashi *et al.* showed the δ-linear behavior of the vortex-core charge based on the BdG equations without the Poisson equation [33]. We find that this δ-linear be-

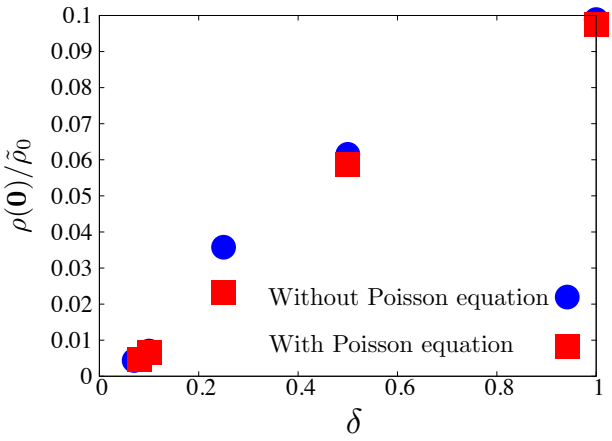

Figure 3.12: Charge density at the vortex center $\rho(\mathbf{0})$ without the Poisson equation (blue circular points), with the Poisson equation (red square points) in units of $\tilde{\rho}_0 \equiv \varepsilon_{\rm F}\epsilon_0 k_{\rm F}^2 d/|e|$ as a function of δ calculated for $T = 0.2T_{\rm c}$.

havior of the vortex-core charge does not change even if we solve he BdG equations with the Poisson equation self-consistently. We here note that the δ-dependence of the charge density at the core is calculated in units of $\tilde{\rho}_0 \equiv \varepsilon_{\rm F}\epsilon_0 k_{\rm F}^2 d/|e|$, assuming that $k_{\rm F}$ is constant and considering ξ_0 changes since it is expected that $k_{\rm F}^{-1}$ of a wide range of materials is about 1 Å. Therefore, to measure the vortex-core charge, we should choose a material that is close to the quantum limit and has a short coherence length.

4 Conclusion

We have developed a numerical method for the study of electric charging in the vortex lattice state of type-II superconductors based on the AQC equations with the Lorentz and PPG forces. Using it, we have calculated the charge distribution in the vortex lattice of s-wave superconductors with a cylindrical Fermi surface. We have shown that the vortex-core charge due to the Lorentz force and the terms for the product of the vector and pair potential coming from DM supercurrents in the PPG force almost cancel each other out, and the total vortex-core charge becomes almost the same as that due to the spatial derivative terms of the pair potential coming from PM supercurrents in the PPG force. We have also found that low temperatures and magnetic fields about half the upper critical field are suitable for the experimental measurement of electric charge in the vortex core. Moreover, we have shown that the PPG force does not contribute to the charging in the Meissner state. On the other hand, the PPG force contributes to the vortex-core charging even at zero field such as the isolated vortex system and the high-κ limit, and is dominated by the terms of the pair potential phase, which are related to supercurrents. Therefore, it can be understood that the vortex-core charging due to the PPG force is caused by the anomalous Hall effect on supercurrents in the vortex state. We again emphasize that only the Lorentz force acts on supercurrents away from the vortex core and the Lorentz force may be important for transport phenomena [18, 50].

We have also studied the coherence length dependence of the vortex-core charging in an isolated vortex of s-wave superconductors neglecting the vector potential. We have shown that the vortex-core charge increases almost linearly within the large quasiclassical parameter region. Therefore, we should choose superconductors near the quantum limit when we measure the vortex-core charge.

There still remains many interesting problems in relation to the study of vortex lattice systems using the AQC equations. For example, we can use the method developed in this thesis, together with the AC response theory based on the standard Eilenberger equations [10, 11] to calculate the flux-flow Hall effect in the Abrikosov lattice, and to also study the vortex lattice in ^{3}He [51–55].

Kumagai *et al.* estimated the vortex-core charge in cuprate superconductors by the NMR/NQR measurements. However, they used the local electric field gradient obtained from changes in the nuclear quadrupole resonance frequency to estimate the vortex-core charge experimentally. To the best of our knowledge, direct observation of the vortex-core charge such as the atomic force microscopy measurement has not been achieved yet. The temperature, magnetic field, and quasiclassical parameter dependence of the vortex-core charge calculated in this thesis will be very useful when experimental researchers choose the external parameters and a material to try to measure the vortex-core charge directly. I hope that our present study will stimulate more detailed experiments on vortex-core charging.

Appendix

A Derivation of Augmented Quasiclassical Equations in Matsubara formalism

Using the static gauge $\boldsymbol{E}(\boldsymbol{r}) = -\boldsymbol{\nabla}\Phi(\boldsymbol{r})$ and $\boldsymbol{B}(\boldsymbol{r}) = \boldsymbol{\nabla} \times \boldsymbol{A}(\boldsymbol{r})$, we can also derive the AQC equations of superconductivity with the Lorentz and PPG forces, and SDOS pressure, following the procedure in Ref. [9, 13, 17].

A.1 Matsubara Green's functions and Gor'kov equations

As a starting point, we introduce the Heisenberg representations of the creation and annihilation operators for electrons by

$$\begin{cases} \hat{\psi}_1(1) \equiv e^{\tau_1 \hat{\mathcal{H}}} \hat{\psi}(\xi_1) e^{-\tau_1 \hat{\mathcal{H}}} \\ \hat{\psi}_2(1) \equiv e^{\tau_1 \hat{\mathcal{H}}} \hat{\psi}^\dagger(\xi_1) e^{-\tau_1 \hat{\mathcal{H}}} \end{cases}, \tag{A.1}$$

where the variable ξ is defined explicitly as $\xi \equiv (\boldsymbol{r}, \alpha)$ with $\boldsymbol{r}$ and α denoting the space and spin coordinates, the argument 1 in the round brackets denotes $1 \equiv (\xi_1, \tau_1)$, and the variable τ_1 lies in $0 \leq \tau_1 \leq 1/k_{\mathrm{B}}T$ with k_{B} and T denoting the Boltzmann constant and temperature, respectively. Using them, we define the Matsubara Green's function:

$$\begin{aligned} G_{ij}(1,2) &\equiv -\theta(\tau_1 - \tau_2)\langle \hat{\psi}_i(1)\hat{\psi}_{3-j}(2)\rangle + \theta(\tau_2 - \tau_1)\langle \hat{\psi}_{3-j}(2)\hat{\psi}_i(1)\rangle \\ &\equiv -\langle \hat{T}_\tau \hat{\psi}_i(1)\hat{\psi}_{3-j}(2)\rangle, \end{aligned} \tag{A.2}$$

where $\theta(\tau)$ is the step function, $\langle \cdots \rangle$ denotes the grand-canonical average, and T_τ means ordering in τ: the $\hat{\psi}$ under T_τ are placed from left to right in order decreasing "time" τ. [56]. The elements of $G_{ij}(1,2)$ satisfy

$$G_{ij}(1,2) = -G_{3-j,3-i}(2,1) = G^*_{ji}(\xi_2\tau_1, \xi_1\tau_2), \tag{A.3}$$

where the superscript * is the complex conjugate. The Matsubara Green's function can be expanded as

$$G_{ij}(1,2) = k_{\mathrm{B}}T \sum_{n=-\infty}^{\infty} G_{ij}(\xi_1, \xi_2; \varepsilon_n) e^{-i\varepsilon_n(\tau_1 - \tau_2)}, \tag{A.4}$$

where $\varepsilon_n = (2n+1)\pi k_{\mathrm{B}}T$ is the fermion Matsubara energy ($n = 0, \pm 1, \ldots$). We separate the spin variable $\alpha = \uparrow, \downarrow$ from $\xi = (\boldsymbol{r}, \alpha)$ to write the four new notation for each G_{ij} as

$$G_{11}(\xi_1, \xi_2; \varepsilon_n) = G_{\alpha_1,\alpha_2}(\boldsymbol{r}_1, \boldsymbol{r}_2; \varepsilon_n), \tag{A.5a}$$

$$G_{12}(\xi_1, \xi_2; \varepsilon_n) = F_{\alpha_1,\alpha_2}(\boldsymbol{r}_1, \boldsymbol{r}_2; \varepsilon_n), \tag{A.5b}$$

$$G_{21}(\xi_1, \xi_2; \varepsilon_n) = -\bar{F}_{\alpha_1,\alpha_2}(\boldsymbol{r}_1, \boldsymbol{r}_2; \varepsilon_n), \tag{A.5c}$$

$$G_{22}(\xi_1, \xi_2; \varepsilon_n) = -\bar{G}_{\alpha_1,\alpha_2}(\boldsymbol{r}_1, \boldsymbol{r}_2; \varepsilon_n). \tag{A.5d}$$

Then, we express the spin degrees of freedom as the 2×2 matrix

$$\underline{G}(\boldsymbol{r}_1, \boldsymbol{r}_2; \varepsilon_n) \equiv \begin{bmatrix} G_{\uparrow\uparrow}(\boldsymbol{r}_1, \boldsymbol{r}_2; \varepsilon_n) & G_{\uparrow\downarrow}(\boldsymbol{r}_1, \boldsymbol{r}_2; \varepsilon_n) \\ G_{\downarrow\uparrow}(\boldsymbol{r}_1, \boldsymbol{r}_2; \varepsilon_n) & G_{\downarrow\downarrow}(\boldsymbol{r}_1, \boldsymbol{r}_2; \varepsilon_n) \end{bmatrix}. \tag{A.6}$$

In matrix notation, $\underline{G}$ and $\underline{F}$ satisfy the following symmetry relations: [13]

$$\underline{G}(\boldsymbol{r}_1, \boldsymbol{r}_2; \varepsilon_n) = \underline{G}^\dagger(\boldsymbol{r}_2, \boldsymbol{r}_1; -\varepsilon_n) = \bar{\underline{G}}^{\mathrm{T}}(\boldsymbol{r}_2, \boldsymbol{r}_1; -\varepsilon_n), \tag{A.7a}$$

$$\underline{F}(\boldsymbol{r}_1, \boldsymbol{r}_2; \varepsilon_n) = -\bar{\underline{F}}^\dagger(\boldsymbol{r}_2, \boldsymbol{r}_1; -\varepsilon_n) = -\underline{F}^{\mathrm{T}}(\boldsymbol{r}_2, \boldsymbol{r}_1; -\varepsilon_n), \tag{A.7b}$$

where † and $^{\mathrm{T}}$ denote the Hermitian conjugate and transpose, respectively. It follows from these symmetry relations that $\bar{\underline{G}}(\boldsymbol{r}_1, \boldsymbol{r}_2; \varepsilon_n) = \underline{G}^*(\boldsymbol{r}_1, \boldsymbol{r}_2; \varepsilon_n)$ and $\bar{\underline{F}}(\boldsymbol{r}_1, \boldsymbol{r}_2; \varepsilon_n) = \underline{F}^*(\boldsymbol{r}_1, \boldsymbol{r}_2; \varepsilon_n)$ hold. Using $\underline{G}$ and $\underline{F}$, we define the Nambu matrix as a 4×4 matrix,

$$\hat{G}(\boldsymbol{r}_1, \boldsymbol{r}_2; \varepsilon_n) \equiv \begin{bmatrix} \underline{G}(\boldsymbol{r}_1, \boldsymbol{r}_2; \varepsilon_n) & \underline{F}(\boldsymbol{r}_1, \boldsymbol{r}_2; \varepsilon_n) \\ -\underline{F}^*(\boldsymbol{r}_1, \boldsymbol{r}_2; \varepsilon_n) & -\underline{G}^*(\boldsymbol{r}_1, \boldsymbol{r}_2; \varepsilon_n) \end{bmatrix}. \tag{A.8}$$

In the mean-field approximation, the Nambu Green's function satisfy the Gor'kov equations: [13, 19]

$$\begin{aligned} &\begin{bmatrix} (i\varepsilon_n - \hat{\mathcal{K}}_1)\underline{\sigma}_0 & \underline{0} \\ \underline{0} & (i\varepsilon_n + \hat{\mathcal{K}}_1^*)\underline{\sigma}_0 \end{bmatrix} \hat{G}(\boldsymbol{r}_1, \boldsymbol{r}_2; \varepsilon_n) \\ &\quad - \int d^3 r_3 \hat{\mathcal{U}}_{\mathrm{BdG}}(\boldsymbol{r}_1, \boldsymbol{r}_3) \hat{G}(\boldsymbol{r}_3, \boldsymbol{r}_2; \varepsilon_n) = \hat{\delta}(\boldsymbol{r}_1 - \boldsymbol{r}_2), \end{aligned} \tag{A.9}$$

where $\underline{\sigma}_0$ and $\underline{0}$ denote the 2×2 unit and zero matrices, respectively. Operator $\hat{\mathcal{K}}_1$ is defined by

$$\hat{\mathcal{K}}_1 \equiv \frac{1}{2m} \left[-i\hbar \frac{\partial}{\partial \boldsymbol{r}_1} - e\boldsymbol{A}(\boldsymbol{r}_1) \right]^2 + e\Phi(\boldsymbol{r}_1) - \mu, \tag{A.10}$$

where m is the electron mass, $e < 0$ is the electron charge, and μ is the chemical potential. Matrix $\hat{\mathcal{U}}_{\mathrm{BdG}}(\boldsymbol{r}_1, \boldsymbol{r}_3)$ denotes

$$\hat{\mathcal{U}}_{\mathrm{BdG}}(\boldsymbol{r}_1, \boldsymbol{r}_2) \equiv \begin{bmatrix} \underline{\mathcal{U}}_{\mathrm{HF}}(\boldsymbol{r}_1, \boldsymbol{r}_2) & \underline{\Delta}(\boldsymbol{r}_1, \boldsymbol{r}_2) \\ -\underline{\Delta}^*(\boldsymbol{r}_1, \boldsymbol{r}_2) & -\underline{\mathcal{U}}^*_{\mathrm{HF}}(\boldsymbol{r}_1, \boldsymbol{r}_2) \end{bmatrix}, \tag{A.11}$$

where matrices $\underline{\mathcal{U}}_{\mathrm{HF}}(\boldsymbol{r}_1, \boldsymbol{r}_2)$ and $\underline{\Delta}(\boldsymbol{r}_1, \boldsymbol{r}_2)$ are the Hartree–Fock and pair potentials, respectively, and have the following definitions;

$$\begin{aligned} \underline{\mathcal{U}}_{\mathrm{HF}}(\boldsymbol{r}_1, \boldsymbol{r}_2) \equiv{}& \delta(\boldsymbol{r}_1 - \boldsymbol{r}_2)\underline{\sigma}_0 \mathrm{Tr} \int d^3 r_3 \mathcal{V}(\boldsymbol{r}_1 - \boldsymbol{r}_3) k_{\mathrm{B}} T \sum_{n=-\infty}^{\infty} \underline{G}(\boldsymbol{r}_3, \boldsymbol{r}_3; \varepsilon_n) \mathrm{e}^{-i\varepsilon_n 0_-} \\ &- \mathcal{V}(\boldsymbol{r}_1 - \boldsymbol{r}_2) k_{\mathrm{B}} T \sum_{n=-\infty}^{\infty} \underline{G}(\boldsymbol{r}_1, \boldsymbol{r}_2; \varepsilon_n) \mathrm{e}^{-i\varepsilon_n 0_-}, \end{aligned} \tag{A.12}$$

$$\underline{\Delta}(\boldsymbol{r}_1, \boldsymbol{r}_2) \equiv \mathcal{V}(\boldsymbol{r}_1 - \boldsymbol{r}_2) k_{\mathrm{B}} T \sum_{n=-\infty}^{\infty} \underline{F}(\boldsymbol{r}_1, \boldsymbol{r}_2; \varepsilon_n), \tag{A.13}$$

where 0_- denotes an extra infinitesimal negative constant. Finally, matrix $\hat{\delta}(\boldsymbol{r}_1 - \boldsymbol{r}_2)$ on the right-hand side of Eq. (A.9) is defined by

$$\hat{\delta}(\boldsymbol{r}_1 - \boldsymbol{r}_2) \equiv \begin{bmatrix} \delta(\boldsymbol{r}_1 - \boldsymbol{r}_2)\underline{\sigma}_0 & \underline{0} \\ \underline{0} & \delta(\boldsymbol{r}_1 - \boldsymbol{r}_2)\underline{\sigma}_0 \end{bmatrix}. \tag{A.14}$$

A.2 Gauge-covariant Wigner transform

Eq. (A.9) has an important property called *gauge invariance* [13].

We introduce the gauge transformation in terms of a continuously differentiable function $\chi(\boldsymbol{r})$ by

$$\begin{cases} \boldsymbol{A}(\boldsymbol{r}_1) = \boldsymbol{A}'(\boldsymbol{r}_1) + \dfrac{\partial \chi(\boldsymbol{r}_1)}{\partial \boldsymbol{r}_1} \\ \hat{\psi}_1(1) = \hat{\psi}'_1(1)\mathrm{e}^{ie\chi(\boldsymbol{r}_1)/\hbar} \\ \hat{\psi}_2(1) = \hat{\psi}'_2(1)\mathrm{e}^{-ie\chi(\boldsymbol{r}_1)/\hbar} \end{cases}, \tag{A.15a}$$

where a prime $'$ distinguishes f' from f as different functions. The corresponding variations of the Green's function (A.8) and potential (A.11) are expressible in terms of the matrix

$$\hat{\Theta}(\boldsymbol{r}_1) \equiv \begin{bmatrix} \underline{\sigma}_0 e^{ie\chi(\boldsymbol{r}_1)/\hbar} & \underline{0} \\ \underline{0} & \underline{\sigma}_0 e^{-ie\chi(\boldsymbol{r}_1)/\hbar} \end{bmatrix}, \tag{A.16}$$

as

$$\hat{G}(\boldsymbol{r}_1, \boldsymbol{r}_2; \varepsilon_n) = \hat{\Theta}(\boldsymbol{r}_1)\hat{G}'(\boldsymbol{r}_1, \boldsymbol{r}_2; \varepsilon_n)\hat{\Theta}^*(\boldsymbol{r}_2), \tag{A.17a}$$

$$\hat{\mathcal{U}}_{\mathrm{BdG}}(\boldsymbol{r}_1, \boldsymbol{r}_2) = \hat{\Theta}(\boldsymbol{r}_1)\hat{\mathcal{U}}'_{\mathrm{BdG}}(\boldsymbol{r}_1, \boldsymbol{r}_2)\hat{\Theta}^*(\boldsymbol{r}_2). \tag{A.17b}$$

Moreover, using

$$[\mp i\hbar\frac{\partial}{\partial \boldsymbol{r}_1} - e\boldsymbol{A}(\boldsymbol{r}_1)]^2 e^{\pm ie\chi(\boldsymbol{r}_1)/\hbar} = e^{\pm ie\chi(\boldsymbol{r}_1)/\hbar}[\mp i\hbar\frac{\partial}{\partial \boldsymbol{r}_1} - e\boldsymbol{A}'(\boldsymbol{r}_1)]^2, \tag{A.18}$$

the $\hat{\mathcal{K}}_1$ term of Eq. (A.9) is expressible as

$$\begin{bmatrix} -\hat{\mathcal{K}}_1\underline{\sigma}_0 & \underline{0} \\ \underline{0} & \hat{\mathcal{K}}_1^*\underline{\sigma}_0 \end{bmatrix} \hat{\Theta}(\boldsymbol{r}_1) = \hat{\Theta}(\boldsymbol{r}_1) \begin{bmatrix} -\hat{\mathcal{K}}'_1\underline{\sigma}_0 & \underline{0} \\ \underline{0} & \hat{\mathcal{K}}'^*_1\underline{\sigma}_0 \end{bmatrix}. \tag{A.19}$$

Substituting Eqs. (A.17a) and (A.17b) into Eq. (A.9), then use Eq. (A.19), and multiply the resulting equation by $\hat{\Theta}^*(\boldsymbol{r}_1)$ and $\hat{\Theta}(\boldsymbol{r}_2)$ from left and right, respectively. We then realize that the resulting equation in terms of $\boldsymbol{A}'(\boldsymbol{r}_1)$, $\hat{G}'(\boldsymbol{r}_1, \boldsymbol{r}_2; \varepsilon_n)$ and $\hat{\mathcal{U}}'_{\mathrm{BdG}}(\boldsymbol{r}_1, \boldsymbol{r}_2)$ is identical in form to Eq. (A.9). This is *gauge invariance*, implying that there is an arbitrariness in the choice of vector potential.

The original *Wigner transform* [57] may be defined, for example, in terms of the Nambu matrix (A.8) as follows: Let us introduce the "center-of-mass" and "relative" coordinates as

$$\boldsymbol{r}_{12} = \frac{\boldsymbol{r}_1 + \boldsymbol{r}_2}{2}, \qquad \bar{\boldsymbol{r}}_{12} \equiv \boldsymbol{r}_1 - \boldsymbol{r}_2. \tag{A.20}$$

The Wigner transform is defined as the Fourier transform with respect to the relative coordinates,

$$\hat{G}(\varepsilon_n, \boldsymbol{p}, \boldsymbol{r}_{12}) \equiv \int d^3\bar{r}_{12} e^{-i\boldsymbol{p}\cdot\bar{\boldsymbol{r}}_{12}/\hbar} \hat{G}(\boldsymbol{r}_1, \boldsymbol{r}_2; \varepsilon_n), \tag{A.21}$$

where $\hat{G}$'s on both sides are different functions distinguished by their arguments. However, the original Wigner transform breaks the gauge invariance with respect to the center-of-mass coordinate when applied to the Green's functions of charged systems. Therefore, we apply an extended version for describing superconductors [13, 16]. The *gauge-covariant Wigner transform* for the Green's functions Eq. (A.8) is defined by

$$\begin{aligned}\hat{G}(\varepsilon_n, \boldsymbol{p}, \boldsymbol{r}_{12}) &\equiv \int d^3\bar{r}_{12} e^{-i\boldsymbol{p}\cdot\bar{\boldsymbol{r}}_{12}/\hbar} \hat{\Gamma}(\boldsymbol{r}_{12}, \boldsymbol{r}_1) \hat{G}(\boldsymbol{r}_1, \boldsymbol{r}_2; \varepsilon_n) \hat{\Gamma}(\boldsymbol{r}_2, \boldsymbol{r}_{12}) \\ &\equiv \begin{bmatrix} \underline{G}(\varepsilon_n, \boldsymbol{p}, \boldsymbol{r}_{12}) & \underline{F}(\varepsilon_n, \boldsymbol{p}, \boldsymbol{r}_{12}) \\ -\underline{F}^*(\varepsilon_n, -\boldsymbol{p}, \boldsymbol{r}_{12}) & -\underline{G}^*(\varepsilon_n, -\boldsymbol{p}, \boldsymbol{r}_{12}) \end{bmatrix},\end{aligned} \tag{A.22a}$$

the inverse relation

$$\hat{G}(\boldsymbol{r}_1, \boldsymbol{r}_2; \varepsilon_n) = \hat{\Gamma}(\boldsymbol{r}_1, \boldsymbol{r}_{12}) \int \frac{d^3p}{(2\pi\hbar)^3} e^{i\boldsymbol{p}\cdot\bar{\boldsymbol{r}}_{12}/\hbar} \hat{G}(\varepsilon_n, \boldsymbol{p}, \boldsymbol{r}_{12}) \hat{\Gamma}(\boldsymbol{r}_{12}, \boldsymbol{r}_2). \tag{A.22b}$$

Here, matrix $\hat{\Gamma}$ is given by

$$\hat{\Gamma}(\boldsymbol{r}_1, \boldsymbol{r}_2) \equiv \begin{bmatrix} \underline{\sigma}_0 e^{iI(\boldsymbol{r}_1, \boldsymbol{r}_2)} & \underline{0} \\ \underline{0} & \underline{\sigma}_0 e^{-iI(\boldsymbol{r}_1, \boldsymbol{r}_2)} \end{bmatrix}, \tag{A.23}$$

with the line integral

$$I(\boldsymbol{r}_1, \boldsymbol{r}_2) \equiv \frac{e}{\hbar} \int_{\boldsymbol{r}_2}^{\boldsymbol{r}_1} \boldsymbol{A}(\boldsymbol{s}) \cdot d\boldsymbol{s}, \tag{A.24}$$

where $\boldsymbol{s}$ denotes a straight-line path from $\boldsymbol{r}_2$ to $\boldsymbol{r}_1$.

Using Eq. (A.17a) and

$$\hat{\Gamma}(\boldsymbol{r}_1, \boldsymbol{r}_2) = \hat{\Theta}(\boldsymbol{r}_1) \hat{\Gamma}'(\boldsymbol{r}_1, \boldsymbol{r}_2) \hat{\Theta}^*(\boldsymbol{r}_2), \tag{A.25}$$

it follows easily that $\hat{G}(\varepsilon_n, \boldsymbol{p}, \boldsymbol{r}_{12})$ changes under the gauge transformation,

$$\hat{G}(\varepsilon_n, \boldsymbol{p}, \boldsymbol{r}_{12}) = \hat{\Theta}(\boldsymbol{r}_{12}) \hat{G}'(\varepsilon_n, \boldsymbol{p}, \boldsymbol{r}_{12}) \hat{\Theta}^*(\boldsymbol{r}_{12}). \tag{A.26}$$

Thus, only the center-of-mass coordinate is relevant to the variation of $\hat{G}(\varepsilon_n, \boldsymbol{p}, \boldsymbol{r}_{12})$ under the gauge transformation.

Similarly, we transform the mean-field potential (A.11)

$$\begin{aligned}\hat{\mathcal{U}}_{\mathrm{BdG}}(\boldsymbol{p}, \boldsymbol{r}_{12}) &\equiv \int d^3\bar{r}_{12} e^{-i\boldsymbol{p}\cdot\bar{\boldsymbol{r}}_{12}/\hbar} \hat{\Gamma}(\boldsymbol{r}_{12}, \boldsymbol{r}_1) \hat{\mathcal{U}}_{\mathrm{BdG}}(\boldsymbol{r}_1, \boldsymbol{r}_2) \hat{\Gamma}(\boldsymbol{r}_2, \boldsymbol{r}_{12}) \\ &\equiv \begin{bmatrix} \underline{\mathcal{U}}_{\mathrm{HF}}(\boldsymbol{p}, \boldsymbol{r}_{12}) & \underline{\Delta}(\boldsymbol{p}, \boldsymbol{r}_{12}) \\ -\underline{\Delta}^*(-\boldsymbol{p}, \boldsymbol{r}_{12}) & -\underline{\mathcal{U}}^*_{\mathrm{HF}}(-\boldsymbol{p}, \boldsymbol{r}_{12}) \end{bmatrix},\end{aligned} \tag{A.27a}$$

whose inverse reads

$$\hat{\mathcal{U}}_{\mathrm{BdG}}(\boldsymbol{r}_1,\boldsymbol{r}_2)=\hat{\Gamma}(\boldsymbol{r}_1,\boldsymbol{r}_{12})\int\frac{d^3p}{(2\pi\hbar)^3}e^{i\boldsymbol{p}\cdot\bar{\boldsymbol{r}}_{12}/\hbar}\hat{\mathcal{U}}_{\mathrm{BdG}}(\boldsymbol{p},\boldsymbol{r}_{12})\hat{\Gamma}(\boldsymbol{r}_{12},\boldsymbol{r}_2). \tag{A.27b}$$

Note that potentials $\underline{\mathcal{U}}_{\mathrm{HF}}(\boldsymbol{p},\boldsymbol{r}_{12})$ and $\underline{\Delta}(\boldsymbol{p},\boldsymbol{r}_{12})$ satisfy the following relations: $\underline{\mathcal{U}}_{\mathrm{HF}}(\boldsymbol{p},\boldsymbol{r}_{12})=\underline{\mathcal{U}}^{\dagger}_{\mathrm{HF}}(\boldsymbol{p},\boldsymbol{r}_{12})$ and $\underline{\Delta}(\boldsymbol{p},\boldsymbol{r}_{12})=-\underline{\Delta}^{\mathrm{T}}(-\boldsymbol{p},\boldsymbol{r}_{12})$.

A.3 Kinetic-energy terms in the Wigner representation

Let us express the kinetic-energy terms of Gor'kov equation (A.9) in the Wigner representation.

First, we prepare the functions:

$$\mathcal{E}_1(u)\equiv\int_0^1 d\eta \mathrm{e}^{\eta u}=\frac{\mathrm{e}^u-1}{u}=\sum_{n=1}^{\infty}\frac{u^{n-1}}{n!}, \tag{A.28}$$

$$\mathcal{E}_2(u)\equiv\int_0^1 d\eta\int_0^{\eta}d\zeta \mathrm{e}^{\zeta u}=\frac{\mathrm{e}^u-1-u}{u^2}=\sum_{n=2}^{\infty}\frac{u^{n-2}}{n!}, \tag{A.29}$$

with which we can express basic phase factors (A.24) as

$$\begin{aligned} I(\boldsymbol{r}_1,\boldsymbol{r}_{12})&=\frac{e}{\hbar}\int_{\boldsymbol{r}_{12}}^{\boldsymbol{r}_1}\boldsymbol{A}(\boldsymbol{s})\cdot d\boldsymbol{s}\\ &=\frac{e}{\hbar}\mathcal{E}_1\left(\frac{\bar{\boldsymbol{r}}_{12}}{2}\cdot\frac{\partial}{\partial\boldsymbol{r}_{12}}\right)\boldsymbol{A}(\boldsymbol{r}_{12})\cdot\frac{\bar{\boldsymbol{r}}_{12}}{2}, \end{aligned} \tag{A.30a}$$

$$I(\boldsymbol{r}_{12},\boldsymbol{r}_2)=\frac{e}{\hbar}\mathcal{E}_1\left(-\frac{\bar{\boldsymbol{r}}_{12}}{2}\cdot\frac{\partial}{\partial\boldsymbol{r}_{12}}\right)\boldsymbol{A}(\boldsymbol{r}_{12})\cdot\frac{\bar{\boldsymbol{r}}_{12}}{2}. \tag{A.30b}$$

Using $\partial/\partial\boldsymbol{r}_1=\partial/\partial\bar{\boldsymbol{r}}_{12}+(1/2)\partial/\partial\boldsymbol{r}_{12}$ and Eq. (A.30), $(\partial/\partial\boldsymbol{r}_1)I(\boldsymbol{r}_1,\boldsymbol{r}_{12})$ and $(\partial/\partial\boldsymbol{r}_1)I(\boldsymbol{r}_{12},\boldsymbol{r}_1)$ become

$$\begin{aligned} \frac{\partial}{\partial\boldsymbol{r}_1}I(\boldsymbol{r}_1,\boldsymbol{r}_{12})&=\frac{e}{\hbar}\boldsymbol{A}(\boldsymbol{r}_1)-\frac{e}{2\hbar}\boldsymbol{A}(\boldsymbol{r}_{12})\\ &\quad-\frac{e}{4\hbar}\left[2\mathcal{E}_1\left(\frac{\bar{\boldsymbol{r}}_{12}}{2}\cdot\frac{\partial}{\partial\boldsymbol{r}_{12}}\right)-\mathcal{E}_2\left(\frac{\bar{\boldsymbol{r}}_{12}}{2}\cdot\frac{\partial}{\partial\boldsymbol{r}_{12}}\right)\right]\boldsymbol{B}(\boldsymbol{r}_{12})\times\bar{\boldsymbol{r}}_{12}, \end{aligned} \tag{A.31a}$$

$$\frac{\partial}{\partial\boldsymbol{r}_1}I(\boldsymbol{r}_{12},\boldsymbol{r}_2)=\frac{e}{2\hbar}\boldsymbol{A}(\boldsymbol{r}_{12})-\frac{e}{4\hbar}\mathcal{E}_2\left(-\frac{\bar{\boldsymbol{r}}_{12}}{2}\cdot\frac{\partial}{\partial\boldsymbol{r}_{12}}\right)\boldsymbol{B}(\boldsymbol{r}_{12})\times\bar{\boldsymbol{r}}_{12}. \tag{A.31b}$$

Now, we focus on the kinetic-energy term in Eq. (A.9) given by

$$\begin{bmatrix}\hat{\mathcal{K}}_1\underline{\sigma}_0 & \underline{0}\\ \underline{0} & -\hat{\mathcal{K}}_1^*\underline{\sigma}_0\end{bmatrix}\hat{G}(\boldsymbol{r}_1,\boldsymbol{r}_2;\varepsilon_n)=\begin{bmatrix}\hat{\mathcal{K}}_1\underline{G}(\boldsymbol{r}_1,\boldsymbol{r}_2;\varepsilon_n) & \hat{\mathcal{K}}_1\underline{F}(\boldsymbol{r}_1,\boldsymbol{r}_2;\varepsilon_n)\\ \hat{\mathcal{K}}_1^*\underline{F}^*(\boldsymbol{r}_1,\boldsymbol{r}_2;\varepsilon_n) & \hat{\mathcal{K}}_1^*\underline{G}^*(\boldsymbol{r}_1,\boldsymbol{r}_2;\varepsilon_n)\end{bmatrix}. \tag{A.32}$$

To perform the calculation of the kinetic-energy term $\hat{\mathcal{K}}_1\underline{G}(\boldsymbol{r}_1,\boldsymbol{r}_2;\varepsilon_n)$, as a first, we obtain

$$
\begin{aligned}
&\left[-i\hbar\frac{\partial}{\partial\boldsymbol{r}_1}-e\boldsymbol{A}(\boldsymbol{r}_1)\right]\mathrm{e}^{iI(\boldsymbol{r}_1,\boldsymbol{r}_{12})}\mathrm{e}^{iI(\boldsymbol{r}_{12},\boldsymbol{r}_2)}\underline{G}(\varepsilon_n,\boldsymbol{p},\boldsymbol{r}_{12})\\
&=\mathrm{e}^{iI(\boldsymbol{r}_1,\boldsymbol{r}_{12})}\mathrm{e}^{iI(\boldsymbol{r}_{12},\boldsymbol{r}_2)}\left[\hbar\frac{\partial I(\boldsymbol{r}_1,\boldsymbol{r}_{12})}{\partial\boldsymbol{r}_1}+\hbar\frac{\partial I(\boldsymbol{r}_{12},\boldsymbol{r}_2)}{\partial\boldsymbol{r}_1}-i\hbar\frac{\partial}{\partial\boldsymbol{r}_1}-e\boldsymbol{A}(\boldsymbol{r}_1)\right]\underline{G}(\varepsilon_n,\boldsymbol{p},\boldsymbol{r}_{12})\\
&\approx\mathrm{e}^{iI(\boldsymbol{r}_1,\boldsymbol{r}_{12})}\mathrm{e}^{iI(\boldsymbol{r}_{12},\boldsymbol{r}_2)}\left[e\boldsymbol{A}(\boldsymbol{r}_1)-\frac{e}{2}\boldsymbol{A}(\boldsymbol{r}_{12})-\frac{3e}{8}\boldsymbol{B}(\boldsymbol{r}_{12})\times\bar{\boldsymbol{r}}_{12}\right.\\
&\qquad\left.+\frac{e}{2}\boldsymbol{A}(\boldsymbol{r}_{12})-\frac{e}{8}\boldsymbol{B}(\boldsymbol{r}_{12})\times\bar{\boldsymbol{r}}_{12}-i\hbar\frac{\partial}{\partial\boldsymbol{r}_1}-e\boldsymbol{A}(\boldsymbol{r}_1)\right]\underline{G}(\varepsilon_n,\boldsymbol{p},\boldsymbol{r}_{12})\\
&=\mathrm{e}^{iI(\boldsymbol{r}_1,\boldsymbol{r}_{12})}\mathrm{e}^{iI(\boldsymbol{r}_{12},\boldsymbol{r}_2)}\left[-i\hbar\frac{\partial}{\partial\bar{\boldsymbol{r}}_{12}}-\frac{i\hbar}{2}\frac{\partial}{\partial\boldsymbol{r}_{12}}-\frac{e}{2}\boldsymbol{B}(\boldsymbol{r}_{12})\times\bar{\boldsymbol{r}}_{12}\right]\underline{G}(\varepsilon_n,\boldsymbol{p},\boldsymbol{r}_{12}).
\end{aligned}
\tag{A.33}
$$

Here, we have neglected spatial derivatives of both $\boldsymbol{E}$ and $\boldsymbol{B}$, which amounts to assuming $\mathcal{E}_1\to 1$ and $\mathcal{E}_2\to 1/2$. In addition, we also neglect the terms of the second-order in $\boldsymbol{\partial}_{\boldsymbol{r}_{12}}$, $\boldsymbol{E}$, and $\boldsymbol{B}$ except that of $\boldsymbol{\partial}^2_{\boldsymbol{r}_{12}}$, we then expand Φ around $\boldsymbol{r}_{12}$ up to the first order in $\bar{\boldsymbol{r}}_{12}$ as $\Phi(\boldsymbol{r}_1)\approx\Phi(\boldsymbol{r}_{12})-\boldsymbol{E}(\boldsymbol{r}_{12})\cdot\bar{\boldsymbol{r}}_{12}/2$. By these procedure, we thereby obtain $\hat{\mathcal{K}}_1\underline{G}(\boldsymbol{r}_1,\boldsymbol{r}_2;\varepsilon_n)$ as

$$
\begin{aligned}
\hat{\mathcal{K}}_1\underline{G}(\boldsymbol{r}_1,\boldsymbol{r}_2;\varepsilon_n)&=\left[\frac{1}{2m}\left(-i\hbar\frac{\partial}{\partial\boldsymbol{r}_1}-e\boldsymbol{A}(\boldsymbol{r}_1)\right)^2+e\Phi(\boldsymbol{r}_1)-\mu\right]\underline{G}(\boldsymbol{r}_1,\boldsymbol{r}_2;\varepsilon_n)\\
&\approx\mathrm{e}^{iI(\boldsymbol{r}_1,\boldsymbol{r}_{12})}\mathrm{e}^{iI(\boldsymbol{r}_{12},\boldsymbol{r}_2)}\int\frac{d^3p}{(2\pi\hbar)^3}\left\{\frac{1}{2m}\left[-i\hbar\frac{\partial}{\partial\bar{\boldsymbol{r}}_{12}}-\frac{i\hbar}{2}\frac{\partial}{\partial\boldsymbol{r}_{12}}-\frac{e}{2}\boldsymbol{B}(\boldsymbol{r}_{12})\times\bar{\boldsymbol{r}}_{12}\right]^2\right.\\
&\qquad\left.+e\Phi(\boldsymbol{r}_1)-\mu\right\}\mathrm{e}^{i\boldsymbol{p}\cdot\bar{\boldsymbol{r}}_{12}/\hbar}\underline{G}(\varepsilon_n,\boldsymbol{p},\boldsymbol{r}_{12})\\
&\approx\mathrm{e}^{iI(\boldsymbol{r}_1,\boldsymbol{r}_{12})}\mathrm{e}^{iI(\boldsymbol{r}_{12},\boldsymbol{r}_2)}\int\frac{d^3p}{(2\pi\hbar)^3}\left\{\frac{1}{2m}\left[-\hbar^2\frac{\partial^2}{\partial\bar{\boldsymbol{r}}_{12}^2}-\hbar^2\frac{\partial}{\partial\bar{\boldsymbol{r}}_{12}}\cdot\frac{\partial}{\partial\boldsymbol{r}_{12}}-\frac{\hbar^2}{4}\frac{\partial^2}{\partial\boldsymbol{r}_{12}^2}\right.\right.\\
&\qquad\left.\left.+i\hbar e(\boldsymbol{B}(\boldsymbol{r}_{12})\times\bar{\boldsymbol{r}}_{12})\cdot\frac{\partial}{\partial\bar{\boldsymbol{r}}_{12}}\right]+e\Phi(\boldsymbol{r}_1)-\mu\right\}\mathrm{e}^{i\boldsymbol{p}\cdot\bar{\boldsymbol{r}}_{12}/\hbar}\underline{G}(\varepsilon_n,\boldsymbol{p},\boldsymbol{r}_{12})\\
&\approx\mathrm{e}^{iI(\boldsymbol{r}_1,\boldsymbol{r}_{12})}\mathrm{e}^{iI(\boldsymbol{r}_{12},\boldsymbol{r}_2)}\int\frac{d^3p}{(2\pi\hbar)^3}\mathrm{e}^{i\boldsymbol{p}\cdot\bar{\boldsymbol{r}}_{12}/\hbar}\\
&\qquad\times\left[\frac{p^2}{2m}-i\hbar\frac{\boldsymbol{p}}{2m}\cdot\frac{\partial}{\partial\boldsymbol{r}_{12}}-\frac{\hbar^2}{8m}\frac{\partial^2}{\partial\boldsymbol{r}_{12}^2}+e\Phi(\boldsymbol{r}_{12})-\mu\right]\underline{G}(\varepsilon_n,\boldsymbol{p},\boldsymbol{r}_{12})\\
&+\mathrm{e}^{iI(\boldsymbol{r}_1,\boldsymbol{r}_{12})}\mathrm{e}^{iI(\boldsymbol{r}_{12},\boldsymbol{r}_2)}\int\frac{d^3p}{(2\pi\hbar)^3}\left[-\frac{e\boldsymbol{p}}{2m}\cdot(\boldsymbol{B}(\boldsymbol{r}_{12})\times\bar{\boldsymbol{r}}_{12})-e\boldsymbol{E}(\boldsymbol{r}_{12})\cdot\frac{\bar{\boldsymbol{r}}_{12}}{2}\right]\mathrm{e}^{i\boldsymbol{p}\cdot\bar{\boldsymbol{r}}_{12}/\hbar}\underline{G}(\varepsilon_n,\boldsymbol{p},\boldsymbol{r}_{12})\\
&\approx\mathrm{e}^{iI(\boldsymbol{r}_1,\boldsymbol{r}_{12})+iI(\boldsymbol{r}_{12},\boldsymbol{r}_2)}\int\frac{d^3p}{(2\pi\hbar)^3}\mathrm{e}^{i\boldsymbol{p}\cdot\bar{\boldsymbol{r}}_{12}/\hbar}\times\left\{\frac{p^2}{2m}+e\Phi(\boldsymbol{r}_{12})-\mu-\frac{\hbar^2}{8m}\frac{\partial^2}{\partial\boldsymbol{r}_{12}^2}\right.\\
&\left.-\frac{i\hbar}{2}\frac{\boldsymbol{p}}{m}\cdot\frac{\partial}{\partial\boldsymbol{r}_{12}}-\frac{i\hbar}{2}e\frac{\boldsymbol{p}}{m}\cdot\left[\boldsymbol{B}(\boldsymbol{r}_{12})\times\frac{\partial}{\partial\boldsymbol{p}}\right]-\frac{i\hbar}{2}e\boldsymbol{E}(\boldsymbol{r}_{12})\cdot\frac{\partial}{\partial\boldsymbol{p}}\right\}\underline{G}(\varepsilon_n,\boldsymbol{p},\boldsymbol{r}_{12}).
\end{aligned}
\tag{A.34a}
$$

Note that

$$
\int d^3p\;\bar{\boldsymbol{r}}_{12}\mathrm{e}^{i\boldsymbol{p}\cdot\bar{\boldsymbol{r}}_{12}/\hbar}G(\boldsymbol{p},\boldsymbol{r}_{12},\varepsilon_n)=i\hbar\int d^3p\;\mathrm{e}^{i\boldsymbol{p}\cdot\bar{\boldsymbol{r}}_{12}/\hbar}\frac{\partial}{\partial\boldsymbol{p}}G(\boldsymbol{p},\boldsymbol{r}_{12},\varepsilon_n),
$$

because of the Green's functions equal to 0 at $p_x, p_y, p_z \to \pm\infty$. In the same way, we can transform another each submatrix on the right-hand side of Eq. (A.32) as

$$\begin{aligned}
&\hat{\mathcal{K}}_1 \underline{F}(\boldsymbol{r}_1, \boldsymbol{r}_2; \varepsilon_n) \\
&\approx \mathrm{e}^{iI(\boldsymbol{r}_1, \boldsymbol{r}_{12}) - iI(\boldsymbol{r}_{12}, \boldsymbol{r}_2)} \int \frac{d^3p}{(2\pi\hbar)^3} \mathrm{e}^{i\boldsymbol{p}\cdot\bar{\boldsymbol{r}}_{12}/\hbar} \times \left\{ \frac{p^2}{2m} + e\Phi(\boldsymbol{r}_{12}) - \mu - \frac{\hbar^2}{8m} \left[\frac{\partial}{\partial \boldsymbol{r}} - i\frac{2e}{\hbar} \boldsymbol{A}(\boldsymbol{r}_{12}) \right]^2 \right. \\
&\left. - \frac{i\hbar}{2} \frac{\boldsymbol{p}}{m} \cdot \left[\frac{\partial}{\partial \boldsymbol{r}_{12}} - i\frac{2e}{\hbar} \boldsymbol{A}(\boldsymbol{r}_{12}) \right] - \frac{i\hbar}{4} e \frac{\boldsymbol{p}}{m} \cdot \left[\boldsymbol{B}(\boldsymbol{r}_{12}) \times \frac{\partial}{\partial \boldsymbol{p}} \right] - \frac{i\hbar}{2} e\boldsymbol{E}(\boldsymbol{r}_{12}) \cdot \frac{\partial}{\partial \boldsymbol{p}} \right\} \underline{F}(\varepsilon_n, \boldsymbol{p}, \boldsymbol{r}_{12}),
\end{aligned} \tag{A.34b}$$

$$\begin{aligned}
&\hat{\mathcal{K}}_1^* \underline{F}^*(\boldsymbol{r}_1, \boldsymbol{r}_2; \varepsilon_n) \\
&\approx \mathrm{e}^{-iI(\boldsymbol{r}_1, \boldsymbol{r}_{12}) + iI(\boldsymbol{r}_{12}, \boldsymbol{r}_2)} \int \frac{d^3p}{(2\pi\hbar)^3} \mathrm{e}^{i\boldsymbol{p}\cdot\bar{\boldsymbol{r}}_{12}/\hbar} \left\{ \frac{p^2}{2m} + e\Phi(\boldsymbol{r}_{12}) - \mu - \frac{\hbar^2}{8m} \left[\frac{\partial}{\partial \boldsymbol{r}} + i\frac{2e}{\hbar} \boldsymbol{A}(\boldsymbol{r}_{12}) \right]^2 \right. \\
&\left. - \frac{i\hbar}{2} \frac{\boldsymbol{p}}{m} \cdot \left[\frac{\partial}{\partial \boldsymbol{r}_{12}} + i\frac{2e}{\hbar} \boldsymbol{A}(\boldsymbol{r}_{12}) \right] + i\frac{i\hbar}{4} e \frac{\boldsymbol{p}}{m} \cdot \left[\boldsymbol{B}(\boldsymbol{r}_{12}) \times \frac{\partial}{\partial \boldsymbol{p}} \right] - \frac{i\hbar}{2} e\boldsymbol{E}(\boldsymbol{r}_{12}) \cdot \frac{\partial}{\partial \boldsymbol{p}} \right\} \underline{F}^*(\varepsilon_n, -\boldsymbol{p}, \boldsymbol{r}_{12}),
\end{aligned} \tag{A.34c}$$

$$\begin{aligned}
&\hat{\mathcal{K}}_1^* \underline{G}^*(\boldsymbol{r}_1, \boldsymbol{r}_2; \varepsilon_n) \\
&\approx \mathrm{e}^{-iI(\boldsymbol{r}_1, \boldsymbol{r}_{12}) - iI(\boldsymbol{r}_{12}, \boldsymbol{r}_2)} \int \frac{d^3p}{(2\pi\hbar)^3} \mathrm{e}^{i\boldsymbol{p}\cdot\bar{\boldsymbol{r}}_{12}/\hbar} \times \left\{ \frac{p^2}{2m} + e\Phi(\boldsymbol{r}_{12}) - \mu - \frac{\hbar^2}{8m} \frac{\partial^2}{\partial \boldsymbol{r}_{12}^2} \right. \\
&\left. - \frac{i\hbar}{2} \frac{\boldsymbol{p}}{m} \cdot \frac{\partial}{\partial \boldsymbol{r}_{12}} + i\frac{i\hbar}{2} e \frac{\boldsymbol{p}}{m} \cdot \left[\boldsymbol{B}(\boldsymbol{r}_{12}) \times \frac{\partial}{\partial \boldsymbol{p}} \right] - \frac{i\hbar}{2} e\boldsymbol{E}(\boldsymbol{r}_{12}) \cdot \frac{\partial}{\partial \boldsymbol{p}} \right\} \underline{G}^*(\varepsilon_n, -\boldsymbol{p}, \boldsymbol{r}_{12}).
\end{aligned} \tag{A.34d}$$

Thus, using the gauge-invariant differential operator

$$\boldsymbol{\partial}_{12} \equiv \begin{cases} \dfrac{\partial}{\partial \boldsymbol{r}_{12}} & \text{on } \underline{G}\ ,\ \underline{G}^* \\ \dfrac{\partial}{\partial \boldsymbol{r}_{12}} - i\dfrac{2e\boldsymbol{A}}{\hbar} & \text{on } \underline{F} \\ \dfrac{\partial}{\partial \boldsymbol{r}_{12}} + i\dfrac{2e\boldsymbol{A}}{\hbar} & \text{on } \underline{F}^* \end{cases}, \tag{A.35}$$

the kinetic-energy terms in the Wigner representation translated as

$$\begin{aligned}
&\int d^3\bar{r}_{12} \mathrm{e}^{-i\boldsymbol{p}\cdot\bar{\boldsymbol{r}}_{12}/\hbar} \hat{\Gamma}(\boldsymbol{r}_{12}, \boldsymbol{r}_1) \begin{bmatrix} (i\varepsilon_n - \hat{\mathcal{K}}_1)\underline{\sigma}_0 & \underline{0} \\ \underline{0} & (i\varepsilon_n + \hat{\mathcal{K}}_1^*)\underline{\sigma}_0 \end{bmatrix} \hat{G}(\boldsymbol{r}_1, \boldsymbol{r}_2; \varepsilon_n) \hat{\Gamma}(\boldsymbol{r}_2, \boldsymbol{r}_{12}) \\
&= -\left[\frac{p^2}{2m} + e\Phi(\boldsymbol{r}_{12}) - \mu - \frac{i\hbar}{2} \frac{\boldsymbol{p}}{m} \cdot \boldsymbol{\partial}_{12} - \frac{\hbar^2}{8m} \boldsymbol{\partial}_{12}^2 - \frac{i\hbar}{2} e\boldsymbol{E}(\boldsymbol{r}_{12}) \cdot \frac{\partial}{\partial \boldsymbol{p}} \right] \hat{\tau}_3 \hat{G}(\varepsilon_n, \boldsymbol{p}, \boldsymbol{r}_{12}) \\
&+ \frac{i\hbar}{8} e \frac{\boldsymbol{p}}{m} \cdot \left[\boldsymbol{B}(\boldsymbol{r}_{12}) \times \frac{\partial}{\partial \boldsymbol{p}} \right] \left[3\hat{G}(\varepsilon_n, \boldsymbol{p}, \boldsymbol{r}_{12}) + \hat{\tau}_3 \hat{G}(\varepsilon_n, \boldsymbol{p}, \boldsymbol{r}_{12}) \hat{\tau}_3 \right] + i\varepsilon_n \hat{G}(\varepsilon_n, \boldsymbol{p}, \boldsymbol{r}_{12}).
\end{aligned} \tag{A.36}$$

A.4 Self-energy terms in the Wigner representation

We consider the Wigner representation of the self-energy terms in Eq. (A.9). Let us introduce matrices:

$$\underline{J}(\boldsymbol{r}_1,\boldsymbol{r}_2;\varepsilon_n) \equiv \int d^3r_3 \underline{\mathcal{U}}_{\rm HF}(\boldsymbol{r}_1,\boldsymbol{r}_3)\underline{G}(\boldsymbol{r}_3,\boldsymbol{r}_2;\varepsilon_n), \tag{A.37a}$$

$$\underline{K}(\boldsymbol{r}_1,\boldsymbol{r}_2;\varepsilon_n) \equiv \int d^3r_3 \underline{\Delta}(\boldsymbol{r}_1,\boldsymbol{r}_3)\underline{F}^*(\boldsymbol{r}_3,\boldsymbol{r}_2;\varepsilon_n), \tag{A.37b}$$

$$\underline{L}(\boldsymbol{r}_1,\boldsymbol{r}_2;\varepsilon_n) \equiv \int d^3r_3 \underline{\mathcal{U}}_{\rm HF}(\boldsymbol{r}_1,\boldsymbol{r}_3)\underline{F}(\boldsymbol{r}_3,\boldsymbol{r}_2;\varepsilon_n), \tag{A.37c}$$

$$\underline{M}(\boldsymbol{r}_1,\boldsymbol{r}_2;\varepsilon_n) \equiv \int d^3r_3 \underline{\Delta}(\boldsymbol{r}_1,\boldsymbol{r}_3)\underline{G}^*(\boldsymbol{r}_3,\boldsymbol{r}_2;\varepsilon_n). \tag{A.37d}$$

Using them, the self-energy terms in Eq. (A.9) is expressed as

$$\begin{aligned}
&\int d^3r_3 \hat{\mathcal{U}}_{\rm BdG}(\boldsymbol{r}_1,\boldsymbol{r}_3)\hat{G}(\boldsymbol{r}_3,\boldsymbol{r}_2;\varepsilon_n) \\
&= \begin{bmatrix} \underline{J}(\boldsymbol{r}_1,\boldsymbol{r}_2;\varepsilon_n) - \underline{K}(\boldsymbol{r}_1,\boldsymbol{r}_2;\varepsilon_n) & \underline{L}(\boldsymbol{r}_1,\boldsymbol{r}_2;\varepsilon_n) - \underline{M}(\boldsymbol{r}_1,\boldsymbol{r}_2;\varepsilon_n) \\ \underline{L}^*(\boldsymbol{r}_1,\boldsymbol{r}_2;\varepsilon_n) - \underline{M}^*(\boldsymbol{r}_1,\boldsymbol{r}_2;\varepsilon_n) & \underline{J}^*(\boldsymbol{r}_1,\boldsymbol{r}_2;\varepsilon_n) - \underline{K}^*(\boldsymbol{r}_1,\boldsymbol{r}_2;\varepsilon_n). \end{bmatrix}
\end{aligned} \tag{A.38}$$

Firstly, let us focus on Eq. (A.37a). Substituting Eqs. (A.22b) and (A.27b) into Eq. (A.37a) gives

$$\begin{aligned}
\underline{J}(\boldsymbol{r}_1,\boldsymbol{r}_2;\varepsilon_n) = {\rm e}^{iI(\boldsymbol{r}_1,\boldsymbol{r}_{12})+iI(\boldsymbol{r}_{12},\boldsymbol{r}_2)} \int \frac{d^3p}{(2\pi\hbar)^3} \int \frac{d^3p'}{(2\pi\hbar)^3} \int d^3r_3 \\
\times {\rm e}^{i\phi_{123}+i\boldsymbol{p}\cdot\bar{\boldsymbol{r}}_{13}/\hbar+i\boldsymbol{p}'\cdot\bar{\boldsymbol{r}}_{32}/\hbar} \underline{\mathcal{U}}_{\rm HF}(\boldsymbol{p},\boldsymbol{r}_{13})\underline{G}(\varepsilon_n,\boldsymbol{p}',\boldsymbol{r}_{32}).
\end{aligned} \tag{A.39}$$

Here, the phase integral ϕ_{123} is defined by

$$\phi_{123} \equiv \frac{e}{\hbar}\oint_{C_{123}} \boldsymbol{A}(\boldsymbol{s})\cdot d\boldsymbol{s} = \frac{e}{\hbar}\int_{S_{123}} \boldsymbol{B}(\boldsymbol{r})\cdot d\boldsymbol{S}, \tag{A.40}$$

where we used the Stokes theorem. Next, perform a variable transformation shown in Fig. A.2 :

$$\begin{aligned}
&\boldsymbol{r} \equiv \boldsymbol{r}_{12} + \left(u-\frac{1}{2}\right)\bar{\boldsymbol{r}}_{32} + \left(v-\frac{1}{2}\right)\bar{\boldsymbol{r}}_{13} \quad (0\le u\le 1,\ 0\le v\le u), \\
&d\boldsymbol{S} = (\bar{\boldsymbol{r}}_{32}\times\bar{\boldsymbol{r}}_{13})dudv, \\
&S_1 \ :\ \frac{1}{2}\le u\le 1,\ \frac{1}{2}\le v\le u, \\
&S_2 \ :\ 0\le u\le \frac{1}{2},\ 0\le v\le u, \\
&S_3 \ :\ \frac{1}{2}\le u\le 1,\ 0\le v\le \frac{1}{2}.
\end{aligned} \tag{A.41}$$

Furthermore, since we are considering short-range interactions, we expand at a point at the center-of-mass coordinate $\boldsymbol{r}_{12}$ and use the approximation $\boldsymbol{B}(\boldsymbol{r}) \approx \boldsymbol{B}(\boldsymbol{r}_{12})$, ϕ_{123}

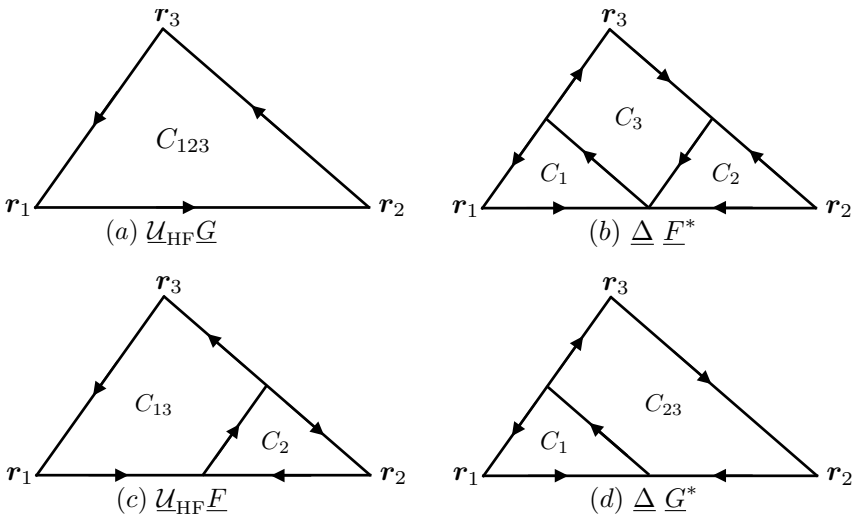

Figure A.1: Paths of the phase integrals.

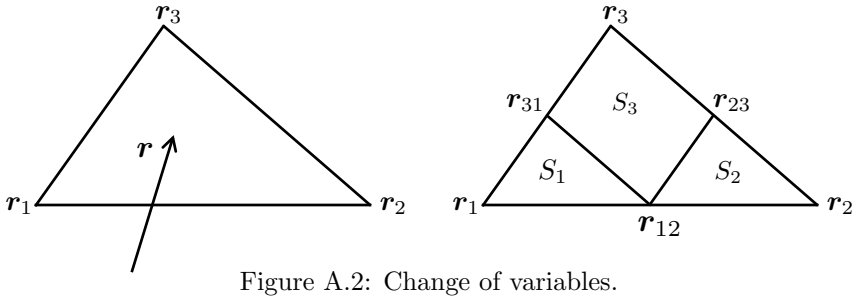

Figure A.2: Change of variables.

becomes

$$\phi_{123} \approx \frac{e}{\hbar}\boldsymbol{B}(\boldsymbol{r}_{12})\cdot(\bar{\boldsymbol{r}}_{32}\times\bar{\boldsymbol{r}}_{13})\int_0^1\int_0^u dv\ du = \frac{e}{2\hbar}\boldsymbol{B}(\boldsymbol{r}_{12})\cdot(\bar{\boldsymbol{r}}_{32}\times\bar{\boldsymbol{r}}_{13}). \tag{A.42}$$

By the same procedure as the standard Wigner transformation [58], $\underline{J}(\boldsymbol{r}_1,\boldsymbol{r}_2;\varepsilon_n)$ can be expressed as

$$\begin{aligned}\underline{J}(\boldsymbol{r}_1,\boldsymbol{r}_2;\varepsilon_n) \approx{}& \mathrm{e}^{iI(\boldsymbol{r}_1,\boldsymbol{r}_{12})+iI(\boldsymbol{r}_{12},\boldsymbol{r}_2)}\int\frac{d^3p}{(2\pi\hbar)^3}\mathrm{e}^{i\boldsymbol{p}\cdot\bar{\boldsymbol{r}}_{12}/\hbar}\underline{\mathcal{U}}_{\rm HF}(\boldsymbol{p},\boldsymbol{r}_{12})\\ &\times\mathrm{e}^{(i\hbar/2)e\boldsymbol{B}(\boldsymbol{r}_{12})\cdot(\overleftarrow{\boldsymbol{\partial}}_{\boldsymbol{p}}\times\overrightarrow{\boldsymbol{\partial}}_{\boldsymbol{p}})}\mathrm{e}^{(i\hbar/2)\overleftarrow{\boldsymbol{\partial}}_{12}\cdot\overrightarrow{\boldsymbol{\partial}}_{\boldsymbol{p}}-(i\hbar/2)\overleftarrow{\boldsymbol{\partial}}_{\boldsymbol{p}}\cdot\overrightarrow{\boldsymbol{\partial}}_{12}}\underline{G}(\varepsilon_n,\boldsymbol{p},\boldsymbol{r}_{12}).\end{aligned} \tag{A.43}$$

Note that the left (right) arrow on each differential operator acts on the left potential (right Green's function). We similarly introduce the phase integral $\phi_1+\phi_2+\phi_3$, $\phi_{13}+\phi_2$, and $\phi_1+\phi_{23}$,

$$\begin{aligned}\phi_1+\phi_2+\phi_3 \equiv{}& \frac{e}{\hbar}\oint_{C_1}\boldsymbol{A}(\boldsymbol{s})\cdot d\boldsymbol{s}+\frac{e}{\hbar}\oint_{C_2}\boldsymbol{A}(\boldsymbol{s})\cdot d\boldsymbol{s}+\frac{e}{\hbar}\oint_{C_3}\boldsymbol{A}(\boldsymbol{s})\cdot d\boldsymbol{s}\\ \approx{}& \frac{e}{\hbar}\boldsymbol{B}(\boldsymbol{r}_{12})\cdot(\bar{\boldsymbol{r}}_{32}\times\bar{\boldsymbol{r}}_{13})\left[\int_{\frac12}^1\int_{\frac12}^u dv\ du+\int_0^{\frac12}\int_0^u dv\ du-\int_{\frac12}^1\int_0^{\frac12} dv\ du\right]\\ ={}& 0,\end{aligned} \tag{A.44}$$

$$\begin{aligned}\phi_{13}+\phi_2 &\equiv \frac{e}{\hbar}\oint_{C_{13}}\boldsymbol{A}(\boldsymbol{s})\cdot d\boldsymbol{s}+\frac{e}{\hbar}\oint_{C_2}\boldsymbol{A}(\boldsymbol{s})\cdot d\boldsymbol{s}\\ &\approx \frac{e}{\hbar}\boldsymbol{B}(\boldsymbol{r}_{12})\cdot(\bar{\boldsymbol{r}}_{32}\times\bar{\boldsymbol{r}}_{13})\left[\int_{\frac{1}{2}}^{1}\int_{0}^{u}dv\;du-\int_{0}^{\frac{1}{2}}\int_{0}^{u}dv\;du\right]\\ &= \frac{e}{4\hbar}\boldsymbol{B}(\boldsymbol{r}_{12})\cdot(\bar{\boldsymbol{r}}_{32}\times\bar{\boldsymbol{r}}_{13}),\end{aligned}\tag{A.45}$$

$$\begin{aligned}\phi_{1}+\phi_{23} &\equiv \frac{e}{\hbar}\oint_{C_{1}}\boldsymbol{A}(\boldsymbol{s})\cdot d\boldsymbol{s}+\frac{e}{\hbar}\oint_{C_{23}}\boldsymbol{A}(\boldsymbol{s})\cdot d\boldsymbol{s}\\ &\approx \frac{e}{\hbar}\boldsymbol{B}(\boldsymbol{r}_{12})\cdot(\bar{\boldsymbol{r}}_{32}\times\bar{\boldsymbol{r}}_{13})\left[\int_{\frac{1}{2}}^{1}\int_{\frac{1}{2}}^{u}dv\;du-\int_{\frac{1}{2}}^{1}\int_{0}^{\frac{1}{2}}dv\;du-\int_{0}^{\frac{1}{2}}\int_{0}^{u}dv\;du\right]\\ &= -\frac{e}{4\hbar}\boldsymbol{B}(\boldsymbol{r}_{12})\cdot(\bar{\boldsymbol{r}}_{32}\times\bar{\boldsymbol{r}}_{13}),\end{aligned}\tag{A.46}$$

with the integral paths given by Fig. A.1. Substituting Eqs. (A.22b) and (A.27b) into Eqs. (A.37b), (A.37c), and (A.37d), the matrices $\underline{K}(\boldsymbol{r}_1,\boldsymbol{r}_2;\varepsilon_n)$, $\underline{L}(\boldsymbol{r}_1,\boldsymbol{r}_2;\varepsilon_n)$, and $\underline{M}(\boldsymbol{r}_1,\boldsymbol{r}_2;\varepsilon_n)$ are given by

$$\begin{aligned}\underline{K}(\boldsymbol{r}_1,\boldsymbol{r}_2;\varepsilon_n) &= \mathrm{e}^{iI(\boldsymbol{r}_1,\boldsymbol{r}_{12})+iI(\boldsymbol{r}_{12},\boldsymbol{r}_2)}\int\frac{d^3p}{(2\pi\hbar)^3}\int\frac{d^3p'}{(2\pi\hbar)^3}\int d^3r_3\\ &\quad\times\mathrm{e}^{i(\phi_1+\phi_2+\phi_3)-2iI(\boldsymbol{r}_{13},\boldsymbol{r}_{12})-2iI(\boldsymbol{r}_{12},\boldsymbol{r}_{32})+i\boldsymbol{p}\cdot\bar{\boldsymbol{r}}_{13}/\hbar+i\boldsymbol{p}'\cdot\bar{\boldsymbol{r}}_{32}/\hbar}\underline{\Delta}(\boldsymbol{p},\boldsymbol{r}_{13})\underline{F}^*(\varepsilon_n,-\boldsymbol{p}',\boldsymbol{r}_{32})\\ &\approx \mathrm{e}^{iI(\boldsymbol{r}_1,\boldsymbol{r}_{12})+iI(\boldsymbol{r}_{12},\boldsymbol{r}_2)}\int\frac{d^3p}{(2\pi\hbar)^3}\mathrm{e}^{i\boldsymbol{p}\cdot\bar{\boldsymbol{r}}_{12}/\hbar}\\ &\quad\times\underline{\Delta}(\boldsymbol{p},\boldsymbol{r}_{12})\mathrm{e}^{(i\hbar/2)\overleftarrow{\boldsymbol{\partial}}_{12}\cdot\overrightarrow{\boldsymbol{\partial}}_{\boldsymbol{p}}-(i\hbar/2)\overleftarrow{\boldsymbol{\partial}}_{\boldsymbol{p}}\cdot\overrightarrow{\boldsymbol{\partial}}_{12}}\underline{F}^*(\varepsilon_n,-\boldsymbol{p},\boldsymbol{r}_{12}),\end{aligned}\tag{A.47}$$

$$\begin{aligned}\underline{L}(\boldsymbol{r}_1,\boldsymbol{r}_2;\varepsilon_n) &= \mathrm{e}^{iI(\boldsymbol{r}_1,\boldsymbol{r}_{12})-iI(\boldsymbol{r}_{12},\boldsymbol{r}_2)}\int\frac{d^3p}{(2\pi\hbar)^3}\int\frac{d^3p'}{(2\pi\hbar)^3}\int d^3r_3\\ &\quad\times\mathrm{e}^{i(\phi_{13}+\phi_2)-2iI(\boldsymbol{r}_{32},\boldsymbol{r}_{12})+i\boldsymbol{p}\cdot\bar{\boldsymbol{r}}_{13}/\hbar+i\boldsymbol{p}'\cdot\bar{\boldsymbol{r}}_{32}/\hbar}\underline{\mathcal{U}}_{\mathrm{HF}}(\boldsymbol{p},\boldsymbol{r}_{13})\underline{F}(\varepsilon_n,\boldsymbol{p}',\boldsymbol{r}_{32})\\ &\approx \mathrm{e}^{iI(\boldsymbol{r}_1,\boldsymbol{r}_{12})-iI(\boldsymbol{r}_{12},\boldsymbol{r}_2)}\int\frac{d^3p}{(2\pi\hbar)^3}\mathrm{e}^{i\boldsymbol{p}\cdot\bar{\boldsymbol{r}}_{12}/\hbar}\\ &\quad\times\underline{\mathcal{U}}_{\mathrm{HF}}(\boldsymbol{p},\boldsymbol{r}_{12})\mathrm{e}^{(i\hbar/4)e\boldsymbol{B}(\mathrm{r}_{12})\cdot(\overleftarrow{\boldsymbol{\partial}}_{\boldsymbol{p}}\times\overrightarrow{\boldsymbol{\partial}}_{\boldsymbol{p}})}\mathrm{e}^{(i\hbar/2)\overleftarrow{\boldsymbol{\partial}}_{12}\cdot\overrightarrow{\boldsymbol{\partial}}_{\boldsymbol{p}}-(i\hbar/2)\overleftarrow{\boldsymbol{\partial}}_{\boldsymbol{p}}\cdot\overrightarrow{\boldsymbol{\partial}}_{12}}\underline{F}(\varepsilon_n,\boldsymbol{p},\boldsymbol{r}_{12}),\end{aligned}\tag{A.48}$$

$$\begin{aligned}\underline{M}(\boldsymbol{r}_1,\boldsymbol{r}_2;\varepsilon_n) &= \mathrm{e}^{iI(\boldsymbol{r}_1,\boldsymbol{r}_{12})-iI(\boldsymbol{r}_{12},\boldsymbol{r}_2)}\int\frac{d^3p}{(2\pi\hbar)^3}\int\frac{d^3p'}{(2\pi\hbar)^3}\int d^3r_3\\ &\quad\times\mathrm{e}^{i(\phi_1+\phi_{23})-2iI(\boldsymbol{r}_{13},\boldsymbol{r}_{12})+i\boldsymbol{p}\cdot\bar{\boldsymbol{r}}_{13}/\hbar+i\boldsymbol{p}'\cdot\bar{\boldsymbol{r}}_{32}/\hbar}\underline{\Delta}(\boldsymbol{p},\boldsymbol{r}_{13})\underline{G}^*(\varepsilon_n,-\boldsymbol{p}',\boldsymbol{r}_{32})\\ &\approx \mathrm{e}^{iI(\boldsymbol{r}_1,\boldsymbol{r}_{12})-iI(\boldsymbol{r}_{12},\boldsymbol{r}_2)}\int\frac{d^3p}{(2\pi\hbar)^3}\mathrm{e}^{i\boldsymbol{p}\cdot\bar{\boldsymbol{r}}_{12}/\hbar}\\ &\quad\times\underline{\Delta}(\boldsymbol{p},\boldsymbol{r}_{12})\mathrm{e}^{-(i\hbar/4)e\boldsymbol{B}(\mathrm{r}_{12})\cdot(\overleftarrow{\boldsymbol{\partial}}_{\boldsymbol{p}}\times\overrightarrow{\boldsymbol{\partial}}_{\boldsymbol{p}})}\mathrm{e}^{(i\hbar/2)\overleftarrow{\boldsymbol{\partial}}_{12}\cdot\overrightarrow{\boldsymbol{\partial}}_{\boldsymbol{p}}-(i\hbar/2)\overleftarrow{\boldsymbol{\partial}}_{\boldsymbol{p}}\cdot\overrightarrow{\boldsymbol{\partial}}_{12}}\underline{G}^*(\varepsilon_n,-\boldsymbol{p},\boldsymbol{r}_{12}).\end{aligned}\tag{A.49}$$

Since substituting Eqs. (A.43), (A.47), (A.48), and (A.49) into Eq. (A.38), we finally obtain the self-energy terms of the Gor'kov equation in the Wigner representation as

$$\begin{aligned}
&\int d^3\bar{r}_{12}\mathrm{e}^{-i\boldsymbol{p}\cdot\bar{\boldsymbol{r}}_{12}}\hat{\Gamma}(\boldsymbol{r}_{12},\boldsymbol{r}_1)\int d^3r_3\hat{\mathcal{U}}_{\mathrm{BdG}}(\boldsymbol{r}_1,\boldsymbol{r}_3)\hat{G}(\boldsymbol{r}_3,\boldsymbol{r}_2;\varepsilon_n)\hat{\Gamma}(\boldsymbol{r}_2,\boldsymbol{r}_{12})\\
&\approx\hat{\Delta}(\boldsymbol{p},\boldsymbol{r}_{12})\circ\hat{G}(\varepsilon_n,\boldsymbol{p},\boldsymbol{r}_{12})+\mathcal{U}_{\mathrm{HF}}(\boldsymbol{p})\hat{\tau}_3\circ\hat{G}(\varepsilon_n,\boldsymbol{p},\boldsymbol{r}_{12})\\
&\quad+\frac{i\hbar}{8}e\boldsymbol{B}(\boldsymbol{r}_{12})\cdot\left\{\left(\boldsymbol{v}-\frac{\boldsymbol{p}}{m}\right)\times\frac{\partial}{\partial\boldsymbol{p}}\left[3\hat{G}(\varepsilon_n,\boldsymbol{p},\boldsymbol{r})+\hat{\tau}_3\hat{G}(\varepsilon_n,\boldsymbol{p},\boldsymbol{r})\hat{\tau}_3\right]\right\}.
\end{aligned}\tag{A.50}$$

We have expanded the Hartree–Fock potential formally as $\underline{\mathcal{U}}_{\mathrm{HF}}(\boldsymbol{p},\boldsymbol{r})=\mathcal{U}_{\mathrm{HF}}(\boldsymbol{p})\underline{\sigma}_0+O(\underline{\Delta}^2(\boldsymbol{p},\boldsymbol{r}))$ with $\mathcal{U}_{\mathrm{HF}}(\boldsymbol{p})$ denoting the Hartree–Fock potential in the homogeneous normal state, also have neglected all terms of the product of two momentum derivatives of the pair potential and Green's function. $\hat{\tau}_3$ is defined by

$$\hat{\tau}_3\equiv\begin{bmatrix}\underline{\sigma}_0 & \underline{0}\\ \underline{0} & -\underline{\sigma}_0\end{bmatrix},\tag{A.51}$$

the operator $\circ$ is given by

$$\hat{a}(\boldsymbol{p},\boldsymbol{r})\circ\hat{b}(\boldsymbol{p},\boldsymbol{r})\equiv\hat{a}(\boldsymbol{p},\boldsymbol{r})\exp\left[\frac{i\hbar}{2}\left(\overleftarrow{\boldsymbol{\partial}}\cdot\overrightarrow{\boldsymbol{\partial}}_{\boldsymbol{p}}-\overleftarrow{\boldsymbol{\partial}}_{\boldsymbol{p}}\cdot\overrightarrow{\boldsymbol{\partial}}\right)\right]\hat{b}(\boldsymbol{p},\boldsymbol{r}),\tag{A.52}$$

$\boldsymbol{v}$ is the velocity in the normal state given by

$$\boldsymbol{v}=\frac{\partial\varepsilon_{\boldsymbol{p}}}{\partial\boldsymbol{p}},\quad\varepsilon_{\boldsymbol{p}}=\frac{p^2}{2m}+\mathcal{U}_{\mathrm{HF}}(\boldsymbol{p}).\tag{A.53}$$

A.5 Augmented quasiclassical equations with the Lorentz and PPG forces

Using Eqs. (A.9), (A.36), and (A.50), we obtain the Gor'kov equations in the Wigner representation as

$$\begin{aligned}
&\left\{i\varepsilon_n\hat{1}-\left[\xi_{\boldsymbol{p}}-i\frac{\hbar\boldsymbol{v}}{2}\cdot\boldsymbol{\partial}-\frac{\hbar^2\boldsymbol{\partial}^2}{8m^*}-\frac{i\hbar}{2}e\boldsymbol{E}(\boldsymbol{r})\cdot\frac{\partial}{\partial\boldsymbol{p}}\right]\hat{\tau}_3\right\}\hat{G}(\varepsilon_n,\boldsymbol{p},\boldsymbol{r})\\
&\quad-\hat{\Delta}(\boldsymbol{p},\boldsymbol{r})\circ\hat{G}(\varepsilon_n,\boldsymbol{p},\boldsymbol{r})+\frac{i\hbar}{8}e\boldsymbol{v}\cdot\left[\boldsymbol{B}(\boldsymbol{r})\times\frac{\partial}{\partial\boldsymbol{p}}\right]\left[3\hat{G}(\varepsilon_n,\boldsymbol{p},\boldsymbol{r})+\hat{\tau}_3\hat{G}(\varepsilon_n,\boldsymbol{p},\boldsymbol{r})\hat{\tau}_3\right]=\hat{1},
\end{aligned}\tag{A.54}$$

where $\xi_{\boldsymbol{p}}$ is defined by $\xi_{\boldsymbol{p}}\equiv\varepsilon_{\boldsymbol{p}}+e\Phi(\boldsymbol{r})-\mu$ with $\varepsilon_{\boldsymbol{p}}$ denoting the single-particle energy, m^* is the effective mass defined by $m^*\equiv p/v$, $\hat{1}$ denotes the 4×4 unit matrix, $\boldsymbol{\partial}$ is given by

$$\boldsymbol{\partial}\equiv\begin{cases}\dfrac{\partial}{\partial\boldsymbol{r}} & :\text{on }\underline{G}\text{ or }\underline{G}^*\\ \dfrac{\partial}{\partial\boldsymbol{r}}-i\dfrac{2e}{\hbar}\boldsymbol{A}(\boldsymbol{r}) & :\text{on }\underline{F}\\ \dfrac{\partial}{\partial\boldsymbol{r}}+i\dfrac{2e}{\hbar}\boldsymbol{A}(\boldsymbol{r}) & :\text{on }\underline{F}^*\end{cases}.\tag{A.55}$$

We take Hermitian conjugate of Eq. (A.54), use symmetries $\hat{\mathcal{U}}^\dagger_{\rm BdG}(\boldsymbol{p},\boldsymbol{r}) = \hat{\mathcal{U}}_{\rm BdG}(\boldsymbol{p},\boldsymbol{r})$ and $\hat{G}^\dagger(\varepsilon_n,\boldsymbol{p},\boldsymbol{r}) = \hat{G}(-\varepsilon_n,\boldsymbol{p},\boldsymbol{r})$, and replace $\varepsilon_n \to -\varepsilon_n$ to obtain

$$\hat{G}(\varepsilon_n,\boldsymbol{p},\boldsymbol{r})\left\{i\varepsilon_n\hat{1} - \hat{\tau}_3\left[\xi_{\boldsymbol{p}} + i\frac{\hbar\boldsymbol{v}}{2}\cdot\boldsymbol{\partial} - \frac{\hbar^2\boldsymbol{\partial}^2}{8m^*} + \frac{i\hbar}{2}e\boldsymbol{E}(\boldsymbol{r})\cdot\frac{\partial}{\partial\boldsymbol{p}}\right]\right\}$$
$$- \hat{G}(\varepsilon_n,\boldsymbol{p},\boldsymbol{r})\circ\hat{\Delta}(\boldsymbol{p},\boldsymbol{r}) - \frac{i\hbar}{8}e\boldsymbol{v}\cdot\left[\boldsymbol{B}(\boldsymbol{r})\times\frac{\partial}{\partial\boldsymbol{p}}\right]\left[3\hat{G}(\varepsilon_n,\boldsymbol{p},\boldsymbol{r}) + \hat{\tau}_3\hat{G}(\varepsilon_n,\boldsymbol{p},\boldsymbol{r})\hat{\tau}_3\right] = \hat{1}. \tag{A.56}$$

We next operate $\hat{\tau}_3$ from the left- and right-hand sides of Eq. (A.56), and the resulting equation is subtracted from Eq. (A.54) and added to Eq. (A.54). Then, we obtain the following two equations:

$$\left[i\varepsilon_n\hat{\tau}_3 - \hat{\Delta}(\boldsymbol{p},\boldsymbol{r})\hat{\tau}_3, \hat{\tau}_3\hat{G}(\varepsilon_n,\boldsymbol{p},\boldsymbol{r})\right]_\circ + i\hbar\boldsymbol{v}\cdot\boldsymbol{\partial}\hat{\tau}_3\hat{G}(\varepsilon_n,\boldsymbol{p},\boldsymbol{r})$$
$$+ i\hbar e\boldsymbol{E}\cdot\frac{\partial}{\partial\boldsymbol{p}}\hat{\tau}_3\hat{G}(\varepsilon_n,\boldsymbol{p},\boldsymbol{r}) + \frac{i\hbar}{2}e\boldsymbol{v}\cdot\left(\boldsymbol{B}\times\frac{\partial}{\partial\boldsymbol{p}}\right)\left\{\hat{\tau}_3,\hat{\tau}_3\hat{G}(\varepsilon_n,\boldsymbol{p},\boldsymbol{r})\right\} = \hat{0}, \tag{A.57a}$$

$$\frac{1}{2}\left\{i\varepsilon_n\hat{\tau}_3 - \hat{\Delta}(\boldsymbol{p},\boldsymbol{r})\hat{\tau}_3, \hat{\tau}_3\hat{G}(\varepsilon_n,\boldsymbol{p},\boldsymbol{r})\right\}_\circ - \xi_{\boldsymbol{p}}\hat{\tau}_3\hat{G}(\varepsilon_n,\boldsymbol{p},\boldsymbol{r}) - \hat{1}$$
$$+ \frac{\hbar^2\boldsymbol{\partial}^2}{8m^*}\hat{\tau}_3\hat{G}(\varepsilon_n,\boldsymbol{p},\boldsymbol{r}) + \frac{i\hbar}{8}e\boldsymbol{v}\cdot\left(\boldsymbol{B}\times\frac{\partial}{\partial\boldsymbol{p}}\right)\left[\hat{\tau}_3,\hat{\tau}_3\hat{G}(\varepsilon_n,\boldsymbol{p},\boldsymbol{r})\right] = \hat{0}, \tag{A.57b}$$

with $[\hat{a},\hat{b}]_\circ \equiv \hat{a}\circ\hat{b} - \hat{b}\circ\hat{a}$ and $\{\hat{a},\hat{b}\}_\circ \equiv \hat{a}\circ\hat{b} + \hat{b}\circ\hat{a}$. Now, in terms of Eq. (A.22a), we introduce the quasiclassical Green's function,

$$\hat{g}(\varepsilon_n,\boldsymbol{p}_{\rm F},\boldsymbol{r}) \equiv {\rm P}\int_{-\infty}^{\infty}\frac{d\xi_{\boldsymbol{p}}}{\pi}i\hat{\tau}_3\hat{G}(\varepsilon_n,\boldsymbol{p},\boldsymbol{r})$$
$$\equiv \begin{bmatrix} \underline{g}(\varepsilon_n,\boldsymbol{p}_{\rm F},\boldsymbol{r}) & -i\underline{f}(\varepsilon_n,\boldsymbol{p}_{\rm F},\boldsymbol{r}) \\ -i\underline{f}^*(\varepsilon_n,-\boldsymbol{p}_{\rm F},\boldsymbol{r}) & -\underline{g}^*(\varepsilon_n,-\boldsymbol{p}_{\rm F},\boldsymbol{r}) \end{bmatrix} \tag{A.58}$$

where P denotes the principal value. It follows that the upper elements $\underline{g}$ and $\underline{f}$ satisfy $\underline{g}(\varepsilon_n,\boldsymbol{p}_{\rm F},\boldsymbol{r}) = -\underline{g}^\dagger(-\varepsilon_n,\boldsymbol{p}_{\rm F},\boldsymbol{r})$, $\underline{f}(\varepsilon_n,\boldsymbol{p}_{\rm F},\boldsymbol{r}) = -\underline{f}^{\rm T}(-\varepsilon_n,-\boldsymbol{p}_{\rm F},\boldsymbol{r})$. To derive the equation for $\hat{g}$ from Eq. (A.57a), we express $\boldsymbol{\partial}_{\boldsymbol{p}} = \boldsymbol{\partial}_{\boldsymbol{p}_\parallel} + \boldsymbol{v}(\partial/\partial\xi)$ with $\boldsymbol{p}_\parallel$ denoting the component on the energy surface $\xi = \xi_{\boldsymbol{p}}$, set $\boldsymbol{p} = \boldsymbol{p}_{\rm F}$ except for the argument of $\hat{G}$, integrate Eq. (A.57a) over $-\varepsilon_{\rm c} \le \xi_{\boldsymbol{p}} \le \varepsilon_{\rm c}$, and use $\boldsymbol{v}\times\boldsymbol{\partial}_{\boldsymbol{p}_\parallel} = \boldsymbol{v}\times\boldsymbol{\partial}_{\boldsymbol{p}}$ and

$${\rm P}\int_{-\infty}^{\infty}d\xi_{\boldsymbol{p}}\frac{\partial}{\partial\xi_{\boldsymbol{p}}}\hat{G}(\varepsilon_n,\boldsymbol{p},\boldsymbol{r}) = \hat{0}. \tag{A.59}$$

We also neglect terms with $e\boldsymbol{E}\cdot\boldsymbol{\partial}_{\boldsymbol{p}_\parallel}$ and take the limit $\varepsilon_{\rm c}\to\infty$. We thereby obtain the AQC equations with the Lorentz and PPG forces in the equilibrium Matsubara formalism for clean superconductors :

$$\left[i\varepsilon_n\hat{\tau}_3 - \hat{\Delta}(\boldsymbol{p}_{\rm F},\boldsymbol{r})\hat{\tau}_3, \hat{g}(\varepsilon_n,\boldsymbol{p}_{\rm F},\boldsymbol{r})\right]_\circ + i\hbar\boldsymbol{v}_{\rm F}\cdot\boldsymbol{\partial}\hat{g}(\varepsilon_n,\boldsymbol{p}_{\rm F},\boldsymbol{r})$$
$$+ \frac{i\hbar}{2}e\boldsymbol{v}_{\rm F}\cdot\left(\boldsymbol{B}\times\frac{\partial}{\partial\boldsymbol{p}_{\rm F}}\right)\{\hat{\tau}_3,\hat{g}(\varepsilon_n,\boldsymbol{p}_{\rm F},\boldsymbol{r})\} = \hat{0}. \tag{A.60}$$

We also include the effects of impurity scatterings in the self-consistent Born approximation by [9]

$$\hat{\sigma}_{\rm imp}(\varepsilon_n, \boldsymbol{r}) \equiv -i\frac{\hbar}{2\tau}\int \frac{d\Omega_{\mathbf{p}}}{4\pi}\hat{g}(\varepsilon_n, \boldsymbol{p}_{\rm F}, \boldsymbol{r})\hat{\tau}_3, \tag{A.61}$$

where $\Omega_{\boldsymbol{p}}$ denotes the solid angle of momentum. Then, the AQC equations including impurity scatterings in the Matsubara formalism are given by

$$\begin{aligned}&\left[i\varepsilon_n\hat{\tau}_3 - \hat{\Delta}(\boldsymbol{p}_{\rm F}, \boldsymbol{r})\hat{\tau}_3 - \hat{\sigma}_{\rm imp}(\varepsilon_n, \boldsymbol{r})\hat{\tau}_3, \hat{g}(\varepsilon_n, \boldsymbol{p}_{\rm F}, \boldsymbol{r})\right]_\circ \\ &\quad + i\hbar\boldsymbol{v}_{\rm F}\cdot\boldsymbol{\partial}\hat{g}(\varepsilon_n, \boldsymbol{p}_{\rm F}, \boldsymbol{r}) + \frac{i\hbar}{2}e\boldsymbol{v}_{\rm F}\cdot\left(\boldsymbol{B}\times\frac{\partial}{\partial\boldsymbol{p}_{\rm F}}\right)\{\hat{\tau}_3, \hat{g}(\varepsilon_n, \boldsymbol{p}_{\rm F}, \boldsymbol{r})\} = \hat{0}.\end{aligned} \tag{A.62}$$

With the same procedure on Eq. (A.60), from Eq. (A.57b), we obtain the equation for

$$\hat{g}^{(1)}(\varepsilon_n, \boldsymbol{p}_{\rm F}, \boldsymbol{r}) \equiv {\rm P}\int_{-\infty}^{\infty}\frac{d\xi_{\boldsymbol{p}}}{\pi}i\left[\xi_{\boldsymbol{p}}\hat{\tau}_3\hat{G}(\varepsilon_n, \boldsymbol{p}, \boldsymbol{r}) + \hat{1}\right], \tag{A.63}$$

as

$$\begin{aligned}\hat{g}^{(1)}(\varepsilon_n, \boldsymbol{p}_{\rm F}, \boldsymbol{r}) &= \frac{1}{2}\left\{i\varepsilon_n\hat{\tau}_3 - \hat{\Delta}(\boldsymbol{p}_{\rm F}, \boldsymbol{r})\hat{\tau}_3, \hat{g}(\varepsilon_n, \boldsymbol{p}_{\rm F}, \boldsymbol{r})\right\}_\circ \\ &\quad + \frac{\hbar^2\boldsymbol{\partial}^2}{8m^*}\hat{g}(\varepsilon_n, \boldsymbol{p}_{\rm F}, \boldsymbol{r}) + \frac{i\hbar}{8}e\boldsymbol{v}_{\rm F}\cdot\left(\boldsymbol{B}\times\frac{\partial}{\partial\boldsymbol{p}_{\rm F}}\right)\left[\hat{\tau}_3, \hat{g}(\varepsilon_n, \boldsymbol{p}_{\rm F}, \boldsymbol{r})\right].\end{aligned} \tag{A.64}$$

Neglecting the second and third terms in Eq. (A.64) to take the leading-order as

$$\hat{g}^{(1)}(\varepsilon_n, \boldsymbol{p}_{\rm F}, \boldsymbol{r}) \approx \frac{1}{2}\left\{i\varepsilon_n\hat{\tau}_3 - \hat{\Delta}(\boldsymbol{p}_{\rm F}, \boldsymbol{r})\hat{\tau}_3, \hat{g}(\varepsilon_n, \boldsymbol{p}_{\rm F}, \boldsymbol{r})\right\}, \tag{A.65}$$

we use it to calculate the terms of the slope in the DOS.

A.6 Local density of states

The LDOS in the superconducting state can be expressed as

$$\begin{aligned}N_{\rm s}(\varepsilon, \boldsymbol{r}) &\equiv -{\rm Tr}\int\frac{d^3p}{(2\pi\hbar)^3}\frac{1}{2\pi}{\rm Im}\underline{G}^{\rm R}(\varepsilon, \boldsymbol{p}, \boldsymbol{r}) \\ &= -{\rm Tr}\int_{-\infty}^{\infty}d\xi_{\boldsymbol{p}}N(\xi_{\boldsymbol{p}} + \mu - e\Phi(\boldsymbol{r}))\int\frac{d\Omega_{\boldsymbol{p}}}{4\pi}\frac{1}{2\pi}{\rm Im}\underline{G}^{\rm R}(\varepsilon, \boldsymbol{p}, \boldsymbol{r}),\end{aligned} \tag{A.66}$$

where $\underline{G}^{\rm R}(\varepsilon, \boldsymbol{p}, \boldsymbol{r}) \equiv \underline{G}(\varepsilon_n \to -i\varepsilon + \eta, \boldsymbol{p}, \boldsymbol{r})$ is the retarded Green's functions with η denoting the infinitesimal positive constant, and the normal DOS $N(\epsilon)$ is defined by

$$N(\epsilon) \equiv \int\frac{d^3p}{(2\pi\hbar)^3}\delta(\epsilon - \varepsilon_{\boldsymbol{p}}). \tag{A.67}$$

We here assume that (i) the superconducting DOS approaches the normal one as the single-particle energy increases and (ii) the energy variation of the normal DOS is slowly.

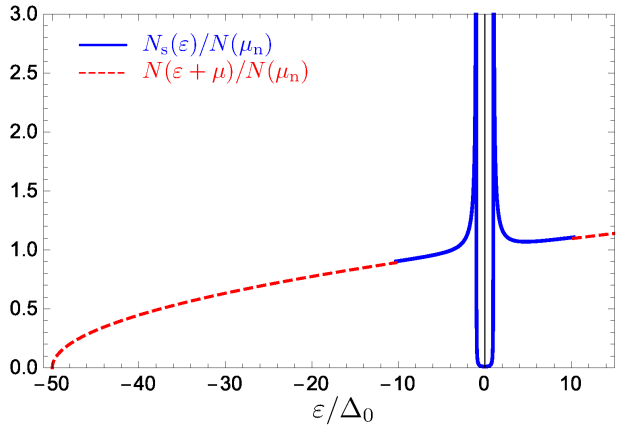

Figure A.3: Superconducting DOS $N_\mathrm{s}(\varepsilon)$ (blue solid line) and normal DOS $N(\varepsilon)$ (red dashed line) in units of $N(\mu_\mathrm{n})$ over $-50\Delta_0 \leq \varepsilon \leq 10\Delta_0$ at $T = 0.1T_\mathrm{c}$ [9].

In this case, superconducting DOS (A.66) may be expressed in terms of $\underline{g}$ and $\underline{g}^{(1)}$. To this end, we expand $N(\epsilon)$ at $\epsilon = \mu - e\Phi(\boldsymbol{r})$ as

$$N(\xi_{\boldsymbol{p}} + \mu - e\Phi(\boldsymbol{r})) \approx N(\mu - e\Phi(\boldsymbol{r})) + N'(\mu - e\Phi(\boldsymbol{r}))\xi_{\boldsymbol{p}}. \tag{A.68}$$

Using $N'(\mu_\mathrm{n})\Delta_0/N(\mu_\mathrm{n}) = O(\delta)$, $\delta\mu/\Delta_0 = O(\delta)$ and $|e|\Phi/\Delta_0 = O(\delta)$, we obtain

$$N(\mu - e\Phi(\boldsymbol{r})) = N(\mu_\mathrm{n})[1 + O(\delta^2)], \tag{A.69}$$

where $\delta\mu \equiv \mu - \mu_\mathrm{n}$ is the chemical potential difference between the normal and superconducting states (μ_n: chemical potential in the normal state). Thus, we rewrite the expansion for $N(\xi_{\boldsymbol{p}} + \mu - e\Phi(\boldsymbol{r}))$ as

$$N(\xi_{\boldsymbol{p}} + \mu - e\Phi(\boldsymbol{r})) \approx N(\mu_\mathrm{n}) + N'(\mu_\mathrm{n})\xi_{\boldsymbol{p}}. \tag{A.70}$$

Substituting it into Eq. (A.66) and using Eqs. (A.58), (A.63) and (A.65), we obtain the superconducting LDOS as

$$\begin{aligned}
N_\mathrm{s}(\varepsilon, \boldsymbol{r}) \approx{}& \frac{N(\mu_\mathrm{n})}{2}\mathrm{Tr}\int\frac{d\Omega_{\boldsymbol{p}}}{4\pi}\left[\mathrm{Re}\underline{g}^\mathrm{R}(\varepsilon, \boldsymbol{p}_\mathrm{F}, \boldsymbol{r}) + \frac{N'(\mu_\mathrm{n})}{N(\mu_\mathrm{n})}\mathrm{Re}\underline{g}^{\mathrm{R}(1)}(\varepsilon, \boldsymbol{p}_\mathrm{F}, \boldsymbol{r})\right]\theta(|\tilde{\varepsilon}_\mathrm{c}| - |\varepsilon|) \\
&+ N(\varepsilon + \mu - e\Phi(\boldsymbol{r}))\theta(|\varepsilon| - |\tilde{\varepsilon}_\mathrm{c}|) \\
\approx{}& \frac{N(\mu_\mathrm{n})}{2}\mathrm{Tr}\int\frac{d\Omega_{\boldsymbol{p}}}{4\pi}\Bigg\{\mathrm{Re}\underline{g}^\mathrm{R}(\varepsilon, \boldsymbol{p}_\mathrm{F}, \boldsymbol{r}) + \frac{N'(\mu_\mathrm{n})}{N(\mu_\mathrm{n})}\varepsilon\mathrm{Re}\underline{g}^\mathrm{R}(\varepsilon, \boldsymbol{p}_\mathrm{F}, \boldsymbol{r}) \\
&+ \frac{1}{2}\frac{N'(\mu_\mathrm{n})}{N(\mu_\mathrm{n})}\mathrm{Im}\left[\underline{\Delta}(\boldsymbol{p}_\mathrm{F}, \boldsymbol{r})\underline{\bar{f}}^\mathrm{R}(\varepsilon, \boldsymbol{p}_\mathrm{F}, \boldsymbol{r}) + \underline{f}^\mathrm{R}(\varepsilon, \boldsymbol{p}_\mathrm{F}, \boldsymbol{r})\underline{\bar{\Delta}}(\boldsymbol{p}_\mathrm{F}, \boldsymbol{r})\right]\Bigg\}\theta(|\tilde{\varepsilon}_\mathrm{c}| - |\varepsilon|) \\
&+ N(\varepsilon + \mu - e\Phi(\boldsymbol{r}))\theta(|\varepsilon| - |\tilde{\varepsilon}_\mathrm{c}|),
\end{aligned} \tag{A.71}$$

where the retarded Green's functions and barred functions in the Keldysh formalism are defined generally by $\underline{g}^\mathrm{R}(\varepsilon, \boldsymbol{p}_\mathrm{F}, \boldsymbol{r}) \equiv \underline{g}(\varepsilon_n \to -i\varepsilon + \eta, \boldsymbol{p}_\mathrm{F}, \boldsymbol{r})$ and $\underline{\bar{g}}^\mathrm{R}(\varepsilon, \boldsymbol{p}_\mathrm{F}, \boldsymbol{r}) \equiv \underline{g}^{\mathrm{R}*}(-\varepsilon, -\boldsymbol{p}_\mathrm{F}, \boldsymbol{r})$,

respectively. The cutoff energy $\tilde{\varepsilon}_{\rm c} > 0$ is determined by

$$\int_{-\tilde{\varepsilon}_{\rm c}}^{\tilde{\varepsilon}_{\rm c}} N_{\rm s}(\varepsilon, \boldsymbol{r}) d\varepsilon = \int_{-\tilde{\varepsilon}_{\rm c}}^{\tilde{\varepsilon}_{\rm c}} N(\varepsilon + \mu - e\Phi) d\varepsilon. \tag{A.72}$$

We note that the notation of the Fermi-surface DOS in the body is used as $N(0)$ but we adopt the notation in Appendix. A as $N(\mu_{\rm n})$. This notation $N(\mu_{\rm n})$ is the same as that in Ref. [9].

Fig. A.3 plots the normal DOS and superconducting DOS at $T = 0.1T_{\rm c}$ for s-wave superconductors with a spherical Fermi surface in the homogeneous system [9]. The superconducting DOS has the particle-hole asymmetry by including SDOS pressure terms and connect approximately with the normal one at a the cutoff energies $\pm\tilde{\varepsilon}_{\rm c}$. These behaviors cannot be described by the standard Eilenberger equations without the slope in the DOS.

A.7 Pair potential

We express the self-consistency equation for the pair potential using the quasiclassical Green's function. First, substituting Eqs. (A.22b), (A.27b), and

$$\mathcal{V}(|\bar{\boldsymbol{r}}_{12}|) = \int \frac{dp^3}{(2\pi\hbar)^3} \mathcal{V}_p {\rm e}^{i\boldsymbol{p}\cdot\bar{\boldsymbol{r}}_{12}/\hbar}, \tag{A.73}$$

into Eq. (A.13), we obtain $\underline{\Delta}(\boldsymbol{p}, \boldsymbol{r}_{12})$ as

$$\underline{\Delta}(\boldsymbol{p}, \boldsymbol{r}_{12}) = \int \frac{dp'^3}{(2\pi\hbar)^3} \mathcal{V}_{|\boldsymbol{p}-\boldsymbol{p}'|} k_{\rm B}T \sum_{n=-\infty}^{\infty} \underline{F}(\varepsilon_n, \boldsymbol{p}', \boldsymbol{r}_{12}). \tag{A.74}$$

Next, we expand the interaction $\mathcal{V}_{|\boldsymbol{p}-\boldsymbol{p}'|}$ with respect to the surface harmonics $Y_{lm}(\hat{\boldsymbol{p}})$ as

$$\mathcal{V}_{|\boldsymbol{p}-\boldsymbol{p}'|} = \sum_{l=0}^{\infty} \mathcal{V}_l(\boldsymbol{p}, \boldsymbol{p}') \sum_{m=-l}^{l} 4\pi Y_{lm}(\hat{\boldsymbol{p}}) Y_{lm}^*(\hat{\boldsymbol{p}}'), \tag{A.75}$$

we also assume that a single l is relevant. Eq. (A.74) then becomes

$$\begin{aligned}
\underline{\Delta}(\boldsymbol{p}, \boldsymbol{r}) &= \int_{-\infty}^{\infty} d\xi_{\boldsymbol{p}'} N(\xi_{\boldsymbol{p}'} + \mu - e\Phi(\boldsymbol{r})) \int \frac{d\Omega_{\boldsymbol{p}'}}{4\pi} \\
&\quad \times \mathcal{V}_l(\boldsymbol{p}, \boldsymbol{p}') \sum_{m=-l}^{l} 4\pi Y_{lm}(\hat{\boldsymbol{p}}) Y_{lm}^*(\hat{\boldsymbol{p}}') k_{\rm B}T \sum_{n=-\infty}^{\infty} \underline{F}(\varepsilon_n, \boldsymbol{p}', \boldsymbol{r}) \\
&= \int_{-\varepsilon_{\rm c}}^{\varepsilon_{\rm c}} d\xi_{\boldsymbol{p}'} N(\xi_{\boldsymbol{p}'} + \mu - e\Phi(\boldsymbol{r})) \int \frac{d\Omega_{\boldsymbol{p}'}}{4\pi} \\
&\quad \times \mathcal{V}_l^{(\rm eff)} \sum_{m=-l}^{l} 4\pi Y_{lm}(\hat{\boldsymbol{p}}) Y_{lm}^*(\hat{\boldsymbol{p}}') k_{\rm B}T \sum_{n=-n_{\rm c}}^{n_{\rm c}} \underline{F}(\varepsilon_n, \boldsymbol{p}', \boldsymbol{r}).
\end{aligned} \tag{A.76}$$

Here, we assumed the constant and weak-coupling interaction, so we rewrote the interaction potential as $\mathcal{V}_l(\boldsymbol{p}, \boldsymbol{p}') = \mathcal{V}_l^{(\rm eff)} \theta(\varepsilon_{\rm c} - |\xi_{\boldsymbol{p}}|) \theta(\varepsilon_{\rm c} - |\xi_{\boldsymbol{p}'}|)$ with the constant potential

$\mathcal{V}_l^{(\mathrm{eff})}$ [13]. Furthermore, using Eqs. (A.58), (A.63), (A.65) and (A.70), we see that only the value at $\boldsymbol{p} = \boldsymbol{p}_\mathrm{F}$ contributes to $\underline{\Delta}(\boldsymbol{p}, \boldsymbol{r})$ as

$$\underline{\Delta}(\boldsymbol{p}_\mathrm{F}, \boldsymbol{r}) \approx -\mathcal{V}_l^{(\mathrm{eff})} N(\mu_\mathrm{n}) \int \frac{d\Omega_{\boldsymbol{p}'}}{4\pi} \sum_{m=-l}^{l} 4\pi Y_{lm}(\hat{\boldsymbol{p}}) Y_{lm}^*(\hat{\boldsymbol{p}}') \times \pi k_\mathrm{B} T \sum_{n=-n_\mathrm{c}}^{n_\mathrm{c}} \left\{ \underline{f}(\varepsilon_n, \boldsymbol{p}_\mathrm{F}', \boldsymbol{r}) - \frac{i}{2} \frac{N'(\mu_\mathrm{n})}{N(\mu_\mathrm{n})} \left[\underline{\Delta}(\boldsymbol{p}_\mathrm{F}', \boldsymbol{r}) \underline{\bar{g}}(\varepsilon_n, \boldsymbol{p}_\mathrm{F}', \boldsymbol{r}) - \underline{g}(\varepsilon_n, \boldsymbol{p}_\mathrm{F}', \boldsymbol{r}) \underline{\Delta}(\boldsymbol{p}_\mathrm{F}', \boldsymbol{r}) \right] \right\}. \tag{A.77}$$

Finally, expanding $\underline{\Delta}(\boldsymbol{p}_\mathrm{F}, \mathbf{r})$ with respect to the surface harmonics as

$$\underline{\Delta}(\boldsymbol{p}_\mathrm{F}, \boldsymbol{r}) = \sum_{m=-l}^{l} \underline{\Delta}_{lm}(\mathbf{r}) \sqrt{4\pi} Y_{lm}(\hat{\boldsymbol{p}}), \tag{A.78}$$

the self-consistency equation for the pair potential is given by

$$\underline{\Delta}_{lm}(\mathbf{r}) = 2\pi \Gamma_0 k_\mathrm{B} T \sum_{n=0}^{n_\mathrm{c}} \int \frac{d\Omega_\mathbf{p}}{4\pi} \sqrt{4\pi} Y_{lm}^*(\hat{\boldsymbol{p}}) \left\{ \underline{f}(\varepsilon_n, \boldsymbol{p}_\mathrm{F}, \boldsymbol{r}) - \frac{i}{2} \frac{N'(\mu_\mathrm{n})}{N(\mu_\mathrm{n})} \left[\underline{\Delta}(\boldsymbol{p}_\mathrm{F}, \boldsymbol{r}) \underline{\bar{g}}(\varepsilon_n, \boldsymbol{p}_\mathrm{F}, \boldsymbol{r}) - \underline{g}(\varepsilon_n, \boldsymbol{p}_\mathrm{F}, \boldsymbol{r}) \underline{\Delta}(\boldsymbol{p}_\mathrm{F}, \boldsymbol{r}) \right] \right\}, \tag{A.79}$$

where $\Gamma_0 \equiv -\mathcal{V}_l^{(\mathrm{eff})} N(\mu_\mathrm{n})$ denotes the coupling constant. Neglecting the spin magnetism as $\underline{g} = g\underline{\sigma}_0$, the gap equation (A.79) becomes the same as that in the standard Eilenberger equations.

A.8 Charge and current densities

We here express the charge density using the quasiclassical Green's function. First, we introduce the electron density $n(\boldsymbol{r})$ by

$$n(\boldsymbol{r}) = k_\mathrm{B} T \mathrm{Tr} \sum_{n=-\infty}^{\infty} \underline{G}(\boldsymbol{r}, \boldsymbol{r}; \varepsilon_n) \mathrm{e}^{-i\varepsilon_n 0_-} = 2 \int_{-\infty}^{\infty} d\varepsilon \frac{N_\mathrm{s}(\varepsilon, \boldsymbol{r})}{\mathrm{e}^{\varepsilon/k_\mathrm{B}T} + 1}. \tag{A.80}$$

Substituting Eq. (A.71) into Eq. (A.80), the electron density is expressible in terms of $\underline{g}^\mathrm{R}$ and $\underline{g}^{\mathrm{R}(1)}$ as

$$n(\boldsymbol{r}) \approx N(\mu_\mathrm{n}) \mathrm{Tr} \int_{-\tilde{\varepsilon}_\mathrm{c}}^{\tilde{\varepsilon}_\mathrm{c}} d\varepsilon \frac{1}{\mathrm{e}^{\varepsilon/k_\mathrm{B}T} + 1} \int \frac{d\Omega_{\boldsymbol{p}}}{4\pi} \left[\mathrm{Re} \underline{g}^\mathrm{R}(\varepsilon, \boldsymbol{p}_\mathrm{F}, \boldsymbol{r}) + \frac{N'(\mu_\mathrm{n})}{N(\mu_\mathrm{n})} \mathrm{Re} \underline{g}^{\mathrm{R}(1)}(\varepsilon, \boldsymbol{p}_\mathrm{F}, \boldsymbol{r}) \right] + 2 \int_{-\infty}^{\infty} d\varepsilon \frac{N(\varepsilon + \mu - e\Phi(\boldsymbol{r}))}{\mathrm{e}^{\varepsilon/k_\mathrm{B}T} + 1} - 2 \int_{-\tilde{\varepsilon}_\mathrm{c}}^{\tilde{\varepsilon}_\mathrm{c}} d\varepsilon \frac{N(\varepsilon + \mu - e\Phi(\boldsymbol{r}))}{\mathrm{e}^{\varepsilon/k_\mathrm{B}T} + 1}. \tag{A.81}$$

We also introduce the electron density at the normal state n_n as

$$n_\mathrm{n} = 2 \int_{-\infty}^{\infty} d\varepsilon \frac{N(\varepsilon + \mu_\mathrm{n})}{\mathrm{e}^{\varepsilon/k_\mathrm{B}T} + 1}. \tag{A.82}$$

Using it, the charge density $\rho(\boldsymbol{r}) = en(\boldsymbol{r}) - en_{\rm n}$ is given as

$$\begin{aligned}\rho(\boldsymbol{r}) \approx{}& eN(\mu_{\rm n}){\rm Tr}\int_{-\tilde{\varepsilon}_{\rm c}}^{\tilde{\varepsilon}_{\rm c}} d\varepsilon \frac{1}{{\rm e}^{\varepsilon/k_{\rm B}T}+1}\int\frac{d\Omega_{\boldsymbol{p}}}{4\pi}\left[{\rm Re}\underline{g}^{\rm R}(\varepsilon,\boldsymbol{p}_{\rm F},\boldsymbol{r}) + \frac{N'(\mu_{\rm n})}{N(\mu_{\rm n})}{\rm Re}\underline{g}^{\rm R(1)}(\varepsilon,\boldsymbol{p}_{\rm F},\boldsymbol{r})\right]\\ &- 2e\int_{-\tilde{\varepsilon}_{\rm c}}^{\tilde{\varepsilon}_{\rm c}} d\varepsilon \frac{N(\varepsilon+\mu-e\Phi(\boldsymbol{r}))}{{\rm e}^{\varepsilon/k_{\rm B}T}+1}\\ &+ 2e\int_{-\infty}^{\infty} d\varepsilon N(\varepsilon)\left[\frac{1}{{\rm e}^{(\varepsilon+e\Phi(\boldsymbol{r})-\delta\mu-\mu_{\rm n})/k_{\rm B}T}+1} - \frac{1}{{\rm e}^{(\varepsilon-\mu_{\rm n})/k_{\rm B}T}+1}\right].\end{aligned} \tag{A.83}$$

Let us carry out a perturbation expansion with respect to the Lorentz and PPG forces as $\underline{g}^{\rm R} = \underline{g}^{\rm R}_0 + \underline{g}^{\rm R}_1\cdots$ and $\underline{g}^{\rm R(1)} = \underline{g}^{\rm R(1)}_0 + \underline{g}^{\rm R(1)}_1\cdots$ [3, 8, 9], and it is performed below up to the first order in the quasiclassical parameter δ. We also use Eq. (A.65), the $\underline{g}^{\rm R}_0$ and gap equations in the standard Eilenberger equations and the following approximation for the distribution function:

$$\frac{1}{{\rm e}^{(\varepsilon+e\Phi(\boldsymbol{r})-\delta\mu-\mu_{\rm n})/k_{\rm B}T}+1} \approx \frac{1}{{\rm e}^{(\varepsilon-\mu_{\rm n})/k_{\rm B}T}+1} + \frac{d}{d\varepsilon}\frac{1}{{\rm e}^{(\varepsilon-\mu_{\rm n})/k_{\rm B}T}+1}[e\Phi(\boldsymbol{r})-\delta\mu]. \tag{A.84}$$

Then, we obtain the formula for the charge density as

$$\begin{aligned}\rho(\boldsymbol{r}) \approx{}& 2\pi k_{\rm B}TeN(\mu_{\rm n}){\rm Tr}\sum_{n=0}^{\tilde{n}_{\rm c}}\int\frac{d\Omega_{\boldsymbol{p}}}{4\pi}{\rm Im}\underline{g}_1(\varepsilon_n,\boldsymbol{p}_{\rm F},\boldsymbol{r})\\ &+ e\frac{N'(\mu_{\rm n})}{N(\mu_{\rm n})}\int_{-\tilde{\varepsilon}_{\rm c}}^{\tilde{\varepsilon}_{\rm c}} d\varepsilon\frac{\varepsilon}{{\rm e}^{\varepsilon/k_{\rm B}T}+1}\left[N_{\rm s0}(\varepsilon,\boldsymbol{r}) - 2N(\mu_{\rm n})\right]\\ &- (-1)^l ceN(\mu_{\rm n})\frac{N'(\mu_{\rm n})}{N(\mu_{\rm n})}{\rm Tr}\sum_{m=-l}^{l}|\underline{\Delta}_{lm}(\boldsymbol{r})|^2 - 2eN(\mu_{\rm n})[e\Phi(\boldsymbol{r})-\delta\mu],\end{aligned} \tag{A.85}$$

where the cutoff $\tilde{n}_{\rm c}$ is obtained from $(2\tilde{n}_{\rm c}+1)\pi k_{\rm B}T = \tilde{\varepsilon}_{\rm c}$, the coefficient c defined by

$$c \equiv \int_{-\tilde{\varepsilon}_{\rm c}}^{\tilde{\varepsilon}_{\rm c}} d\varepsilon \frac{1}{2\varepsilon}\tanh\frac{\varepsilon}{2k_{\rm B}T_{\rm c}}, \tag{A.86}$$

with $N_{\rm s0}(\varepsilon,\boldsymbol{r})$ is the LDOS obtained from the standard Eilenberger equations defined by

$$N_{\rm s0}(\varepsilon,\boldsymbol{r}) \equiv \frac{N(\mu_{\rm n})}{2}{\rm Tr}\int\frac{d\Omega_{\boldsymbol{p}}}{4\pi}{\rm Re}\underline{g}^{\rm R}_0(\varepsilon,\boldsymbol{p}_{\rm F},\boldsymbol{r}). \tag{A.87}$$

Using the Gauss' law $\boldsymbol{\nabla}\cdot\boldsymbol{E} = \rho/\epsilon_0$, we obtain an equation for the electric field as

$$\begin{aligned}&-\lambda_{\rm TF}^2\boldsymbol{\nabla}^2\boldsymbol{E}(\boldsymbol{r}) + \boldsymbol{E}(\boldsymbol{r}) = -\frac{\pi k_{\rm B}T}{e}\boldsymbol{\nabla}{\rm Tr}\sum_{n=0}^{\tilde{n}_{\rm c}}\int\frac{d\Omega_{\boldsymbol{p}}}{4\pi}{\rm Im}\underline{g}_1(\varepsilon_n,\boldsymbol{p}_{\rm F},\boldsymbol{r})\\ &- \frac{1}{e}\frac{N'(\mu_{\rm n})}{N(\mu_{\rm n})}\int_{-\tilde{\varepsilon}_{\rm c}}^{\tilde{\varepsilon}_{\rm c}} d\varepsilon\frac{\varepsilon}{{\rm e}^{\varepsilon/k_{\rm B}T}+1}\boldsymbol{\nabla}\frac{N_{\rm s0}(\varepsilon,\boldsymbol{r})}{N(\mu_{\rm n})} + (-1)^l\frac{c}{2e}\frac{N'(\mu_{\rm n})}{N(\mu_{\rm n})}\boldsymbol{\nabla}{\rm Tr}\sum_{m=-l}^{l}|\underline{\Delta}_{lm}(\boldsymbol{r})|^2,\end{aligned} \tag{A.88}$$

where $\lambda_{\rm TF} \equiv \sqrt{\epsilon_0/2e^2N(\mu_{\rm n})}$ is the Thomas–Fermi screening length. This expression include the same screening effect as that in Refs. [10, 14, 59].

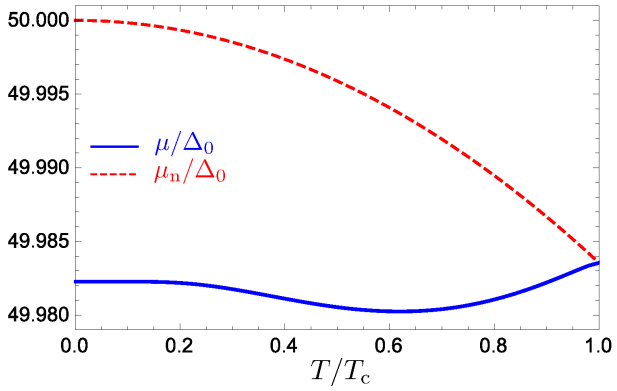

Figure A.4: Superconducting chemical potential μ (blue solid line) and normal chemical potential μ_n (red dashed line) in units of Δ_0 as a function of temperature [9].

On the other hand, using $\langle \boldsymbol{v}_F \rangle_F = \boldsymbol{0}$, we obtain the formula for the current density by the same procedure as

$$\boldsymbol{j}(\boldsymbol{r}) \approx eN(\mu_n)\mathrm{Tr}\int_{-\tilde{\varepsilon}_c}^{\tilde{\varepsilon}_c} d\varepsilon \frac{1}{e^{\varepsilon/k_B T}+1}\int \frac{d\Omega_{\boldsymbol{p}}}{4\pi}\boldsymbol{v}_F\left[\mathrm{Re}\underline{g}_0^R(\varepsilon,\boldsymbol{p}_F,\boldsymbol{r}) + \mathrm{Re}\underline{g}_1^R(\varepsilon,\boldsymbol{p}_F,\boldsymbol{r}) + \frac{N'(\mu_n)}{N(\mu_n)}\mathrm{Re}\underline{g}_0^{R(1)}(\varepsilon,\boldsymbol{p}_F,\boldsymbol{r})\right]. \tag{A.89}$$

The second and third terms in Eq. (A.89) with respect to $\underline{g}_1^R$ and $\underline{g}_0^{R(1)}$ are the correction terms due to the spatial variation of the electron density. Hence, neglecting the second and third terms in the above expression to take the leading-order, we use the formula for the current density as

$$\begin{aligned}\boldsymbol{j}(\boldsymbol{r}) &\approx eN(\mu_n)\mathrm{Tr}\int_{-\tilde{\varepsilon}_c}^{\tilde{\varepsilon}_c} d\varepsilon \frac{1}{e^{\varepsilon/k_B T}+1}\int \frac{d\Omega_{\boldsymbol{p}}}{4\pi}\boldsymbol{v}_F\mathrm{Re}\underline{g}_0^R(\varepsilon,\boldsymbol{p}_F,\boldsymbol{r}) \\ &= 2\pi k_B T eN(\mu_n)\mathrm{Tr}\sum_{n=0}^{\tilde{n}_c}\int \frac{d\Omega_{\boldsymbol{p}}}{4\pi}\boldsymbol{v}_F\mathrm{Im}\underline{g}_0(\varepsilon_n,\boldsymbol{p}_F,\boldsymbol{r}).\end{aligned} \tag{A.90}$$

A.9 Chemical potential

We also obtain the expression for chemical potential μ from Eq. (A.85) and using $\int d^3r\rho(\boldsymbol{r})=0$ as

$$\begin{aligned}\mu = \mu_n &- \pi k_B T\mathrm{Tr}\sum_{n=0}^{\tilde{n}_c}\int \frac{d\Omega_{\boldsymbol{p}}}{4\pi}\frac{1}{V}\int d^3r\mathrm{Im}\underline{g}_1(\varepsilon_n,\boldsymbol{p}_F,\boldsymbol{r}) \\ &- \frac{1}{2}\frac{N'(\mu_n)}{N(\mu_n)}\int_{-\tilde{\varepsilon}_c}^{\tilde{\varepsilon}_c} d\varepsilon \frac{\varepsilon}{e^{\varepsilon/k_B T}+1}\frac{1}{V}\int d^3r\left[\frac{N_{s0}(\varepsilon,\boldsymbol{r})}{N(\mu_n)}-2\right] \\ &+ \frac{(-1)^l}{2}c\frac{N'(\mu_n)}{N(\mu_n)}\mathrm{Tr}\sum_{m=-l}^{l}\frac{1}{V}\int d^3r|\underline{\Delta}_{lm}(\boldsymbol{r})|^2 + e\frac{1}{V}\int d^3r\Phi(\boldsymbol{r}).\end{aligned} \tag{A.91}$$

Note that the expression in (A.91) is different from that proposed by van der Marel [60] and Khomskii and Kusmartsev [4] even the for the homogeneous s-wave pairing case. Fig. A.4 plots the superconducting and normal chemical potentials as a function of temperature. The superconducting chemical potential is smaller than the normal one, and it is consistent with that by van der Marel [60,61] and Khomskii and Kusmartsev [4]. A minimum value near $T = 0.6T_{\mathrm{c}}$ of the superconducting chemical potential arises from difference in temperature dependence between the third and fourth terms in Eq. (A.91) with respect to the slope in the DOS.

B Derivation of Bogoliubov–de Gennes Equations for s-Wave Superconductors

In this chapter, we derive the BdG equations following the procedure in Ref. [62].

B.1 Effective Hamiltonian

As a model for s-wave superconductors, we consider the following Hamiltonian with an attractive contact interaction:

$$\hat{\mathcal{H}} = \hat{\mathcal{H}}_0 + \hat{\mathcal{H}}_1, \tag{B.1a}$$

$$\hat{\mathcal{H}}_0 = \int d^3r \sum_\alpha \hat{\psi}_\alpha^\dagger(\boldsymbol{r}) \left[-\frac{\hbar^2}{2m} \left(\boldsymbol{\nabla} - \frac{ie\boldsymbol{A}(\boldsymbol{r})}{\hbar} \right)^2 + U_0(\boldsymbol{r}) - \mu \right] \hat{\psi}_\alpha(\boldsymbol{r}), \tag{B.1b}$$

$$\hat{\mathcal{H}}_1 = \frac{\Gamma_0}{2} \int d^3r \sum_{\alpha\beta} \hat{\psi}_\alpha^\dagger(\boldsymbol{r}) \hat{\psi}_\beta^\dagger(\boldsymbol{r}) \hat{\psi}_\beta(\boldsymbol{r}) \hat{\psi}_\alpha(\boldsymbol{r}). \tag{B.1c}$$

Here, α denotes the spin coordinate, $U_0(\boldsymbol{r})$ is a one-body potential which captures the effects of impurities and other scalar potentials, $\Gamma_0 < 0$ is the coupling constant for short-range attractive interaction, m is the electron mass. The field operators satisfy the relations

$$\{\hat{\psi}_\alpha(\boldsymbol{r}), \hat{\psi}_\beta^\dagger(\boldsymbol{r}')\} = \delta_{\alpha,\beta}\delta(\boldsymbol{r}-\boldsymbol{r}'), \quad \{\hat{\psi}_\alpha(\boldsymbol{r}), \hat{\psi}_\beta(\boldsymbol{r})\} = \{\hat{\psi}_\alpha^\dagger(\boldsymbol{r}), \hat{\psi}_\beta^\dagger(\boldsymbol{r})\} = 0. \tag{B.2}$$

Using Pauli exclusion principle ($\alpha \neq \beta$) and $\{\hat{\psi}_\alpha(\boldsymbol{r}), \hat{\psi}_\beta(\boldsymbol{r})\} = \{\hat{\psi}_\alpha^\dagger(\boldsymbol{r}), \hat{\psi}_\beta^\dagger(\boldsymbol{r})\} = 0$, $\hat{\mathcal{H}}_1$ becomes

$$\hat{\mathcal{H}}_1 = \Gamma_0 \int d^3r \hat{\psi}_\uparrow^\dagger(\boldsymbol{r}) \hat{\psi}_\downarrow^\dagger(\boldsymbol{r}) \hat{\psi}_\downarrow(\boldsymbol{r}) \hat{\psi}_\uparrow(\boldsymbol{r}). \tag{B.3}$$

Also, since $\hat{\mathcal{H}}_1$ is a two-body interaction term and cannot be calculated exactly, we use the Wick decomposition for the mean-field approximation.

$$\begin{aligned}
&\hat{\psi}_\uparrow^\dagger(\boldsymbol{r}) \hat{\psi}_\downarrow^\dagger(\boldsymbol{r}) \hat{\psi}_\downarrow(\boldsymbol{r}) \hat{\psi}_\uparrow(\boldsymbol{r}) \\
&\approx \langle \hat{\psi}_\uparrow^\dagger \hat{\psi}_\uparrow \rangle \hat{\psi}_\downarrow^\dagger \hat{\psi}_\downarrow + \hat{\psi}_\uparrow^\dagger \hat{\psi}_\uparrow \langle \hat{\psi}_\downarrow^\dagger \hat{\psi}_\downarrow \rangle - \langle \hat{\psi}_\uparrow^\dagger \hat{\psi}_\downarrow \rangle \hat{\psi}_\downarrow^\dagger \hat{\psi}_\uparrow - \hat{\psi}_\uparrow^\dagger \hat{\psi}_\downarrow \langle \hat{\psi}_\downarrow^\dagger \hat{\psi}_\uparrow \rangle \\
&\quad + \langle \hat{\psi}_\uparrow^\dagger \hat{\psi}_\downarrow^\dagger \rangle \hat{\psi}_\downarrow \hat{\psi}_\uparrow + \hat{\psi}_\uparrow^\dagger \hat{\psi}_\downarrow^\dagger \langle \hat{\psi}_\downarrow \hat{\psi}_\uparrow \rangle - \langle \hat{\psi}_\uparrow^\dagger \hat{\psi}_\uparrow \rangle \langle \hat{\psi}_\downarrow^\dagger \hat{\psi}_\downarrow \rangle + \langle \hat{\psi}_\uparrow^\dagger \hat{\psi}_\downarrow \rangle \langle \hat{\psi}_\downarrow^\dagger \hat{\psi}_\uparrow \rangle - \langle \hat{\psi}_\uparrow^\dagger \hat{\psi}_\downarrow^\dagger \rangle \langle \hat{\psi}_\downarrow \hat{\psi}_\uparrow \rangle.
\end{aligned} \tag{B.4}$$

We then define the molecular fields $\tilde{U}(\boldsymbol{r})$ and $\Delta(\boldsymbol{r})$ as follows;

$$\tilde{U}(\boldsymbol{r}) \equiv \Gamma_0 \langle \hat{\psi}_\uparrow^\dagger(\boldsymbol{r}) \hat{\psi}_\uparrow(\boldsymbol{r}) \rangle = \Gamma_0 \langle \hat{\psi}_\downarrow^\dagger(\boldsymbol{r}) \hat{\psi}_\downarrow(\boldsymbol{r}) \rangle, \tag{B.5a}$$

$$\Delta(\boldsymbol{r}) \equiv \Gamma_0 \langle \hat{\psi}_\downarrow(\boldsymbol{r}) \hat{\psi}_\uparrow(\boldsymbol{r}) \rangle, \quad \Delta^*(\boldsymbol{r}) = \Gamma_0 \langle \hat{\psi}_\uparrow^\dagger(\boldsymbol{r}) \hat{\psi}_\downarrow^\dagger(\boldsymbol{r}) \rangle. \tag{B.5b}$$

In Eq. (B.5a), we assumed that the average particle number density of particles with up spin is equal to that with down spin. We also introduce an effective Hamiltonian $\hat{\mathcal{H}}_{\text{eff}}$ that

ignores the constant term and does not take into account external fields or interaction potentials that change the spin direction of the particles. Therefore, the Hamiltonian takes the form

$$\hat{\mathcal{H}}_{\text{eff}} \equiv \hat{\mathcal{H}}_0 + \hat{\mathcal{H}}_1', \tag{B.6a}$$

$$\hat{\mathcal{H}}_1' \equiv \int d^3r \left[\tilde{U}(\boldsymbol{r}) \sum_\alpha \hat{\psi}_\alpha^\dagger(\boldsymbol{r})\hat{\psi}_\alpha(\boldsymbol{r}) + \Delta(\boldsymbol{r})\hat{\psi}_\uparrow^\dagger(\boldsymbol{r})\hat{\psi}_\downarrow^\dagger(\boldsymbol{r}) - \Delta^*(\boldsymbol{r})\hat{\psi}_\downarrow(\boldsymbol{r})\hat{\psi}_\uparrow(\boldsymbol{r}) \right]. \tag{B.6b}$$

B.2 Ground and excited states of the effective Hamiltonian

To determine the excitation field of $\hat{\mathcal{H}}_{\text{eff}}$, we find the fermion operator $\hat{\gamma}_{n,\alpha}$ and $\epsilon_{n,\alpha}$ that satisfy $\left[\hat{\gamma}_{n,\alpha}, \hat{\mathcal{H}_{\text{eff}}}\right] = \epsilon_{n,\alpha}\hat{\gamma}_{n,\alpha}$ and anticommutation relation

$$\left\{\hat{\gamma}_{n,\alpha}, \hat{\gamma}_{n',\alpha'}^\dagger\right\} = \delta_{n,n'}\delta_{\alpha,\alpha'}, \quad \{\hat{\gamma}_{n,\alpha}, \hat{\gamma}_{n',\alpha'}\} = \left\{\hat{\gamma}_{n,\alpha}^\dagger, \hat{\gamma}_{n',\alpha'}^\dagger\right\} = 0. \tag{B.7}$$

As a first step, we find $\left[\hat{\gamma}_{n,\alpha}, \hat{\mathcal{H}_{\text{eff}}}\right] = \epsilon_{n,\alpha}\hat{\gamma}_{n,\alpha}$ by letting $\left[\hat{\gamma}_{n,\alpha}, \hat{\mathcal{H}}\right]$ operates to $\hat{\gamma}_{n_1,\alpha_1}^\dagger\hat{\gamma}_{n_2,\alpha_2}^\dagger \cdots \hat{\gamma}_{n_l,\alpha_l}^\dagger|g\rangle$. $\epsilon_{n,\alpha}$ is the energy eigenvalue of states (n,α), and the excitation energy of excited state $\hat{\gamma}_{n_1,\alpha_1}^\dagger\hat{\gamma}_{n_2,\alpha_2}^\dagger \cdots \hat{\gamma}_{n_l,\alpha_l}^\dagger|g\rangle$ in $\hat{\mathcal{H}}_{\text{eff}}$ is $\sum_{j=1}^l \epsilon_{n_j,\alpha_j}$.

$\hat{\gamma}_{n_k,\alpha_k}(1 \le k \le l)$ operates to excited state $\hat{\gamma}_{n_1,\alpha_1}^\dagger\hat{\gamma}_{n_2,\alpha_2}^\dagger \cdots \hat{\gamma}_{n_l,\alpha_l}^\dagger|g\rangle$

$$\begin{aligned}
&\hat{\gamma}_{n_k,\alpha_k}\hat{\gamma}_{n_1,\alpha_1}^\dagger\hat{\gamma}_{n_2,\alpha_2}^\dagger \cdots \hat{\gamma}_{n_l,\alpha_l}^\dagger|g\rangle \\
&= (-1)^{k-1}\hat{\gamma}_{n_1,\alpha_1}^\dagger\hat{\gamma}_{n_2,\alpha_2}^\dagger \cdots \hat{\gamma}_{n_k,\alpha_k}\hat{\gamma}_{n_k,\alpha_k}^\dagger \cdots \hat{\gamma}_{n_l,\alpha_l}^\dagger|g\rangle \\
&= (-1)^{k-1}\hat{\gamma}_{n_1,\alpha_1}^\dagger\hat{\gamma}_{n_2,\alpha_2}^\dagger \cdots \hat{\gamma}_{n_{k-1},\alpha_{k-1}}^\dagger\hat{\gamma}_{n_{k+1},\alpha_{k+1}}^\dagger \cdots \hat{\gamma}_{n_l,\alpha_l}^\dagger|g\rangle.
\end{aligned} \tag{B.8}$$

Here, we have used the relationship of $\left\{\hat{\gamma}_{n,\alpha}, \hat{\gamma}_{n',\alpha'}^\dagger\right\} = \delta_{n,n'}\delta_{\alpha,\alpha'}$ and $\hat{\gamma}_{n,\alpha}|g\rangle = 0$. It follows that

$$\begin{aligned}
&\left[\hat{\gamma}_{n_k,\alpha_k}, \hat{\mathcal{H}_{\text{eff}}}\right] \hat{\gamma}_{n_1,\alpha_1}^\dagger\hat{\gamma}_{n_2,\alpha_2}^\dagger \cdots \hat{\gamma}_{n_l,\alpha_l}^\dagger|g\rangle \\
&= \hat{\gamma}_{n_k,\alpha_k}\hat{\mathcal{H}_{\text{eff}}}\hat{\gamma}_{n_1,\alpha_1}^\dagger\hat{\gamma}_{n_2,\alpha_2}^\dagger \cdots \hat{\gamma}_{n_l,\alpha_l}^\dagger|g\rangle - \hat{\mathcal{H}_{\text{eff}}}\hat{\gamma}_{n_k,\alpha_k}\hat{\gamma}_{n_1,\alpha_1}^\dagger\hat{\gamma}_{n_2,\alpha_2}^\dagger \cdots \hat{\gamma}_{n_l,\alpha_l}^\dagger|g\rangle \\
&= \sum_{j=1}^l \epsilon_{n_j,\alpha_j}\hat{\gamma}_{n_k,\alpha_k}\hat{\gamma}_{n_1,\alpha_1}^\dagger\hat{\gamma}_{n_2,\alpha_2}^\dagger \cdots \hat{\gamma}_{n_l,\alpha_l}^\dagger|g\rangle - \hat{\mathcal{H}_{\text{eff}}}\hat{\gamma}_{n_k,\alpha_k}\hat{\gamma}_{n_1,\alpha_1}^\dagger\hat{\gamma}_{n_2,\alpha_2}^\dagger \cdots \hat{\gamma}_{n_l,\alpha_l}^\dagger|g\rangle \\
&= \left(\sum_{j=1}^l \epsilon_{n_j,\alpha_j} - \hat{\mathcal{H}_{\text{eff}}}\right)(-1)^{k-1}\hat{\gamma}_{n_1,\alpha_1}^\dagger\hat{\gamma}_{n_2,\alpha_2}^\dagger \cdots \hat{\gamma}_{n_{k-1},\alpha_{k-1}}^\dagger\hat{\gamma}_{n_{k+1},\alpha_{k+1}}^\dagger \cdots \hat{\gamma}_{n_l,\alpha_l}^\dagger|g\rangle \\
&= \left(\sum_{j=1}^l \epsilon_{n_j,\alpha_j} - \sum_{j=1}^{k-1} \epsilon_{n_j,\alpha_j} - \sum_{j=k+1}^l \epsilon_{n_j,\alpha_j}\right) \\
&\qquad \times (-1)^{k-1}\hat{\gamma}_{n_1,\alpha_1}^\dagger\hat{\gamma}_{n_2,\alpha_2}^\dagger \cdots \hat{\gamma}_{n_{k-1},\alpha_{k-1}}^\dagger\hat{\gamma}_{n_{k+1},\alpha_{k+1}}^\dagger \cdots \hat{\gamma}_{n_l,\alpha_l}^\dagger|g\rangle \\
&= \epsilon_{n_k,\alpha_k}\hat{\gamma}_{n_k,\alpha_k}\hat{\gamma}_{n_1,\alpha_1}^\dagger\hat{\gamma}_{n_2,\alpha_2}^\dagger \cdots \hat{\gamma}_{n_l,\alpha_l}^\dagger|g\rangle.
\end{aligned} \tag{B.9}$$

Thus, we showed $\left[\hat{\gamma}_{n,\alpha}, \hat{\mathcal{H}_{\text{eff}}}\right] = \epsilon_{n,\alpha}\hat{\gamma}_{n,\alpha}$.

Next, we show that the following equation

$$\left[\hat{\psi}_\uparrow(\boldsymbol{r}), \hat{\mathcal{H}}_{\text{eff}}\right] = h\hat{\psi}_\uparrow(\boldsymbol{r}) + \Delta(\boldsymbol{r})\hat{\psi}_\downarrow^\dagger(\boldsymbol{r}), \tag{B.10a}$$

$$\left[\hat{\psi}_\downarrow(\boldsymbol{r}), \hat{\mathcal{H}}_{\text{eff}}\right] = h\hat{\psi}_\downarrow(\boldsymbol{r}) - \Delta(\boldsymbol{r})\hat{\psi}_\uparrow^\dagger(\boldsymbol{r}), \tag{B.10b}$$

$$h \equiv -\frac{\hbar^2}{2m}\left(\boldsymbol{\nabla} - \frac{ie\mathbf{A}(\boldsymbol{r})}{\hbar}\right)^2 + U_0(\boldsymbol{r}) + \tilde{U}(\boldsymbol{r}) - \mu. \tag{B.10c}$$

Eq. (B.10a) is obtained as

$$\begin{aligned}
&\hat{\mathcal{H}}_{\text{eff}}\hat{\psi}_\uparrow(\boldsymbol{r}) \\
&= \int d^3r' \left[\sum_\alpha \hat{\psi}_\alpha^\dagger(\boldsymbol{r}')h\hat{\psi}_\alpha(\boldsymbol{r}')\hat{\psi}_\uparrow(\boldsymbol{r}) + \Delta(\boldsymbol{r}')\hat{\psi}_\uparrow^\dagger(\boldsymbol{r}')\hat{\psi}_\downarrow^\dagger(\boldsymbol{r}')\hat{\psi}_\uparrow(\boldsymbol{r}) - \Delta^*(\boldsymbol{r}')\hat{\psi}_\downarrow(\boldsymbol{r}')\hat{\psi}_\uparrow(\boldsymbol{r}')\hat{\psi}_\uparrow(\boldsymbol{r})\right] \\
&= \hat{\psi}_\uparrow(\boldsymbol{r})\hat{\mathcal{H}}_{\text{eff}} - h\hat{\psi}_\uparrow(\boldsymbol{r}) - \Delta(\boldsymbol{r})\hat{\psi}.
\end{aligned} \tag{B.11}$$

Here, each term in the second line was calculated as follows

$$\begin{aligned}
&\int d^3r' \sum_\alpha \hat{\psi}_\alpha^\dagger(\boldsymbol{r}')h\hat{\psi}_\alpha(\boldsymbol{r}')\hat{\psi}_\uparrow(\boldsymbol{r}) \\
&= \hat{\psi}_\uparrow(\boldsymbol{r}) \int d^3r' \sum_\alpha \hat{\psi}_\alpha^\dagger(\boldsymbol{r}')h\hat{\psi}_\alpha(\boldsymbol{r}') - \int d^3r' \sum_\alpha \delta_{\alpha,\uparrow}\delta(\boldsymbol{r}-\boldsymbol{r}')h\hat{\psi}_\alpha(\boldsymbol{r}') \\
&= \hat{\psi}_\uparrow(\boldsymbol{r}) \int d^3r' \sum_\alpha \hat{\psi}_\alpha^\dagger(\boldsymbol{r}')h\hat{\psi}_\alpha(\boldsymbol{r}') - h\hat{\psi}_\uparrow(\boldsymbol{r}),
\end{aligned} \tag{B.12a}$$

$$\begin{aligned}
&\int d^3r' \Delta(\boldsymbol{r}')\hat{\psi}_\uparrow^\dagger(\boldsymbol{r}')\hat{\psi}_\downarrow^\dagger(\boldsymbol{r}')\hat{\psi}_\uparrow(\boldsymbol{r}) \\
&= \hat{\psi}_\uparrow(\boldsymbol{r}) \int d^3r' \Delta(\boldsymbol{r}')\hat{\psi}_\uparrow^\dagger(\boldsymbol{r}')\hat{\psi}_\downarrow^\dagger(\boldsymbol{r}') - \int d^3r' \Delta(\boldsymbol{r}')\delta(\boldsymbol{r}-\boldsymbol{r}')\hat{\psi}_\downarrow^\dagger(\boldsymbol{r}') \\
&= \hat{\psi}_\uparrow(\boldsymbol{r}) \int d^3r' \Delta(\boldsymbol{r}')\hat{\psi}_\uparrow^\dagger(\boldsymbol{r}')\hat{\psi}_\downarrow^\dagger(\boldsymbol{r}') - \Delta(\boldsymbol{r})\hat{\psi}_\downarrow^\dagger(\boldsymbol{r}),
\end{aligned} \tag{B.12b}$$

$$\int d^3r' \Delta^*(\boldsymbol{r}')\hat{\psi}_\downarrow(\boldsymbol{r}')\hat{\psi}_\uparrow(\boldsymbol{r}')\hat{\psi}_\uparrow(\boldsymbol{r}) = \hat{\psi}_\uparrow(\boldsymbol{r}) \int d^3r' \Delta^*(\boldsymbol{r}')\hat{\psi}_\downarrow(\boldsymbol{r}')\hat{\psi}_\uparrow(\boldsymbol{r}'). \tag{B.12c}$$

Similarly, Eq. (B.10b) has obtained by calculating as

$$\begin{aligned}
&\hat{\mathcal{H}}_{\text{eff}}\hat{\psi}_\downarrow(\boldsymbol{r}) \\
&= \int d^3r' \left[\sum_\alpha \hat{\psi}_\alpha^\dagger(\boldsymbol{r}')h\hat{\psi}_\alpha(\boldsymbol{r}')\hat{\psi}_\downarrow(\boldsymbol{r}) + \Delta(\boldsymbol{r}')\hat{\psi}_\uparrow^\dagger(\boldsymbol{r}')\hat{\psi}_\downarrow^\dagger(\boldsymbol{r}')\hat{\psi}_\downarrow(\boldsymbol{r}) - \Delta^*(\boldsymbol{r}')\hat{\psi}_\downarrow(\boldsymbol{r}')\hat{\psi}_\uparrow(\boldsymbol{r}')\hat{\psi}_\downarrow(\boldsymbol{r})\right] \\
&= \hat{\psi}_\downarrow(\boldsymbol{r})\hat{\mathcal{H}}_{\text{eff}} - h\hat{\psi}_\downarrow(\boldsymbol{r}) + \Delta(\boldsymbol{r})\hat{\psi}_\uparrow^\dagger(\boldsymbol{r}).
\end{aligned} \tag{B.13}$$

Here, each term in the second line is

$$\int d^3r' \sum_\alpha \hat{\psi}_\alpha^\dagger(\boldsymbol{r}')h\hat{\psi}_\alpha(\boldsymbol{r}')\hat{\psi}_\downarrow(\boldsymbol{r}) = \hat{\psi}_\downarrow(\boldsymbol{r}) \int d^3r' \sum_\alpha \hat{\psi}_\alpha^\dagger(\boldsymbol{r}')h\hat{\psi}_\alpha(\boldsymbol{r}') - h\hat{\psi}_\downarrow(\boldsymbol{r}), \tag{B.14a}$$

$$\int d^3r'\Delta(\boldsymbol{r}')\hat{\psi}_\uparrow^\dagger(\boldsymbol{r}')\hat{\psi}_\downarrow^\dagger(\boldsymbol{r}')\hat{\psi}_\downarrow(\boldsymbol{r}) = \hat{\psi}_\downarrow(\boldsymbol{r})\int d^3r'\Delta(\boldsymbol{r}')\hat{\psi}_\uparrow^\dagger(\boldsymbol{r}')\hat{\psi}_\downarrow^\dagger(\boldsymbol{r}') + \Delta(\boldsymbol{r})\hat{\psi}_\uparrow^\dagger(\boldsymbol{r}), \quad \text{(B.14b)}$$

$$\int d^3r'\Delta^*(\boldsymbol{r}')\hat{\psi}_\downarrow(\boldsymbol{r}')\hat{\psi}_\uparrow(\boldsymbol{r}')\hat{\psi}_\downarrow(\boldsymbol{r}) = \hat{\psi}_\downarrow(\boldsymbol{r})\int d^3r'\Delta^*(\boldsymbol{r}')\hat{\psi}_\downarrow(\boldsymbol{r}')\hat{\psi}_\uparrow(\boldsymbol{r}'). \quad \text{(B.14c)}$$

For these expressions to be satisfied, we write $\hat{\psi}_\uparrow(\boldsymbol{r})$ as

$$\hat{\psi}_\uparrow(\boldsymbol{r}) = \sum_n \left(u_n(\boldsymbol{r})\hat{\gamma}_{n,\uparrow} + v_n^*(\boldsymbol{r})\hat{\gamma}_{n,\downarrow}^\dagger\right). \quad \text{(B.15)}$$

Substituting Eq. (B.15) for the left side of $\left\{\hat{\psi}_\uparrow(\boldsymbol{r}), \hat{\psi}_\uparrow^\dagger(\boldsymbol{r}')\right\} = \delta(\boldsymbol{r}-\boldsymbol{r}')$,

$$\begin{aligned}
&\left\{\sum_n \left(u_n(\boldsymbol{r})\hat{\gamma}_{n,\uparrow} + v_n^*(\boldsymbol{r})\hat{\gamma}_{n,\downarrow}^\dagger\right), \sum_m \left(u_m^*(\boldsymbol{r}')\hat{\gamma}_{m,\uparrow}^\dagger + v_m(\boldsymbol{r}')\hat{\gamma}_{m,\downarrow}\right)\right\} \\
&= \sum_n\sum_m \left\{\left(u_n(\boldsymbol{r})\hat{\gamma}_{n,\uparrow} + v_n^*(\boldsymbol{r})\hat{\gamma}_{n,\downarrow}^\dagger\right), \left(u_m^*(\boldsymbol{r}')\hat{\gamma}_{m,\uparrow}^\dagger + v_m(\boldsymbol{r}')\hat{\gamma}_{m,\downarrow}\right)\right\} \\
&= \sum_n\sum_m \left(u_n(\boldsymbol{r})u_m^*(\boldsymbol{r}')\left\{\hat{\gamma}_{n,\uparrow}, \hat{\gamma}_{m,\uparrow}^\dagger\right\} + v_n^*(\boldsymbol{r})v_m(\boldsymbol{r}')\left\{\hat{\gamma}_{n,\downarrow}^\dagger, \hat{\gamma}_{m,\downarrow}\right\}\right) \\
&= \sum_n\sum_m \left(u_n(\boldsymbol{r})u_m^*(\boldsymbol{r}')\delta_{n,m} + v_n^*(\boldsymbol{r})v_m(\boldsymbol{r}')\delta_{n,m}\right) \\
&= \sum_n \left(u_n(\boldsymbol{r})u_n^*(\boldsymbol{r}') + v_n^*(\boldsymbol{r})v_n(\boldsymbol{r}')\right). \quad \text{(B.16)}
\end{aligned}$$

We thereby obtain

$$\sum_n \left(u_n(\boldsymbol{r})u_n^*(\boldsymbol{r}') + v_n^*(\boldsymbol{r})v_n(\boldsymbol{r}')\right) = \delta(\boldsymbol{r}-\boldsymbol{r}'). \quad \text{(B.17)}$$

Similarly, we assume that $\hat{\psi}_\downarrow(\boldsymbol{r})$ is

$$\hat{\psi}_\downarrow(\boldsymbol{r}) = \sum_n \left(u_n(\boldsymbol{r})\hat{\gamma}_{n,\downarrow} + {v'}_n^*(\boldsymbol{r})\hat{\gamma}_{n,\uparrow}^\dagger\right). \quad \text{(B.18)}$$

Since it can be written as $\hat{\psi}_\alpha(\boldsymbol{r}) = \sum_n u_n(\boldsymbol{r})\hat{\gamma}_{n,\alpha}$ in the case of $\Delta = 0$, we added $'$ to $v_n(\boldsymbol{r})$ only. $\left\{\hat{\psi}_\uparrow(\boldsymbol{r}), \hat{\psi}_\downarrow(\boldsymbol{r})\right\} = 0$ is expressible as

$$\begin{aligned}
\left\{\hat{\psi}_\uparrow(\boldsymbol{r}), \hat{\psi}_\downarrow(\boldsymbol{r})\right\} &= \left\{\sum_n \left(u_n(\boldsymbol{r})\hat{\gamma}_{n,\uparrow} + v_n^*(\boldsymbol{r})\hat{\gamma}_{n,\downarrow}^\dagger\right), \sum_m \left(u_m(\boldsymbol{r})\hat{\gamma}_{m,\downarrow} + {v'}_n^*(\boldsymbol{r})\hat{\gamma}_{n,\uparrow}^\dagger\right)\right\} \\
&= \sum_n\sum_m \left(u_n(\boldsymbol{r}){v'}_m^*(\boldsymbol{r})\left\{\hat{\gamma}_{n,\uparrow}, \hat{\gamma}_{m,\uparrow}^\dagger\right\} + v_n^*(\boldsymbol{r})u_m(\boldsymbol{r})\left\{\hat{\gamma}_{n,\downarrow}^\dagger, \hat{\gamma}_{m,\downarrow}\right\}\right) \\
&= \sum_n\sum_m \left(u_n(\boldsymbol{r}){v'}_m^*(\boldsymbol{r})\delta_{n,m} + v_n^*(\boldsymbol{r})u_m(\boldsymbol{r})\delta_{n,m}\right) \\
&= \sum_n \left(u_n(\boldsymbol{r}){v'}_n^*(\boldsymbol{r}) + v_n^*(\boldsymbol{r})u_n(\boldsymbol{r})\right) = 0, \quad \text{(B.19)}
\end{aligned}$$

we obtained $v'_n(\boldsymbol{r}) = -v_n(\boldsymbol{r})$ and

$$\hat{\psi}_\downarrow(\boldsymbol{r}) = \sum_n \left(u_n(\boldsymbol{r})\hat{\gamma}_{n,\downarrow} - v_n^*(\boldsymbol{r})\hat{\gamma}_{n,\uparrow}^\dagger \right). \tag{B.20}$$

Substituting Eqs. (B.15) and (B.20) into Eq. (B.10a)

$$\begin{aligned} u_n(\boldsymbol{r}) \left[\hat{\gamma}_{n,\uparrow}, \hat{\mathcal{H}}_{\text{eff}}\right] + v_n^*(\boldsymbol{r}) \left[\hat{\gamma}_{n,\downarrow}^\dagger, \hat{\mathcal{H}}_{\text{eff}}\right] = \\ h u_n(\boldsymbol{r})\hat{\gamma}_{n,\uparrow} + h v_n^*(\boldsymbol{r})\hat{\gamma}_{n,\downarrow}^\dagger + \Delta(\boldsymbol{r}) u_n^*(\boldsymbol{r})\hat{\gamma}_{n,\downarrow}^\dagger - \Delta(\boldsymbol{r}) v_n(\boldsymbol{r})\hat{\gamma}_{n,\uparrow}. \end{aligned} \tag{B.21}$$

Using $\left[\hat{\gamma}_{n,\alpha}, \hat{\mathcal{H}}_{\text{eff}}\right] = \epsilon_{n,\alpha}\hat{\gamma}_{n,\alpha}$ and $\left[\hat{\gamma}_{n,\alpha}, \hat{\mathcal{H}}_{\text{eff}}\right]^\dagger = \left[\hat{\mathcal{H}}_{\text{eff}}, \hat{\gamma}_{n,\alpha}^\dagger\right] = -\left[\hat{\gamma}_{n,\alpha}^\dagger, \hat{\mathcal{H}}_{\text{eff}}\right] = \epsilon_{n,\alpha}\hat{\gamma}_{n,\alpha}^\dagger$, Eq. (B.21) becomes

$$\epsilon_n u_n(\boldsymbol{r})\hat{\gamma}_{n,\uparrow} - \epsilon_n v_n^*(\boldsymbol{r})\hat{\gamma}_{n,\downarrow}^\dagger = \left(h u_n(\boldsymbol{r}) - \Delta(\boldsymbol{r}) v_n(\boldsymbol{r})\right)\hat{\gamma}_{n,\uparrow} + \left(h v_n^*(\boldsymbol{r}) + \Delta(\boldsymbol{r}) u_n^*(\boldsymbol{r})\right)\hat{\gamma}_{n,\downarrow}^\dagger. \tag{B.22}$$

Here, we defined $\epsilon_{n,\uparrow} = \epsilon_{n,\downarrow} \equiv \epsilon_n$. Thus, we obtain the BdG equations (2.16) as

$$\epsilon_n u_n(\boldsymbol{r}) = h u_n(\boldsymbol{r}) - \Delta(\boldsymbol{r}) v_n(\boldsymbol{r}) \tag{B.23}$$

$$-\epsilon_n v_n^*(\boldsymbol{r}) = h v_n^*(\boldsymbol{r}) + \Delta(\boldsymbol{r}) u_n^*(\boldsymbol{r}) \tag{B.24}$$

In this thesis, we consider that $\tilde{U}(\boldsymbol{r})$ includes a constant chemical potential. Moreover, since we restrict our analysis to clean superconductors, we don't consider the potential due to impurities in U_0, and only the effect of scalar potential, $e\Phi$, is taken into account.

B.3 Expectation of the fermion operators

$\langle \hat{\gamma}_{n,\uparrow}^\dagger \hat{\gamma}_{m,\uparrow} \rangle$ can be written in terms of the thermodynamic potential Ω, a quantum number $q_j \equiv (n_j, \alpha_j)$, and an occupancy number $n_{q_j} = 0, 1$, and is expressed as

$$\langle \hat{\gamma}_{n,\uparrow}^\dagger \hat{\gamma}_{m,\uparrow} \rangle = \sum_{n_{q_1}} \sum_{n_{q_2}} \cdots \langle n_{q_1} n_{q_2} \cdots | \mathrm{e}^{\beta\left(\Omega - \hat{\mathcal{H}}_{\text{eff}}\right)} \hat{\gamma}_{n,\uparrow}^\dagger \hat{\gamma}_{m,\uparrow} | n_{q_1} n_{q_2} \cdots \rangle. \tag{B.25}$$

To perform the diagonal sum of the above formula, we calculate

$$\langle n_{q_1} n_{q_2} \cdots | \hat{\gamma}_{n,\uparrow}^\dagger \hat{\gamma}_{m,\uparrow} | n_{q_1} n_{q_2} \cdots \rangle = \langle n_{q_1} n_{q_2} \cdots | \delta_{n,m} \hat{\gamma}_{n,\uparrow}^\dagger \hat{\gamma}_{n,\uparrow} \left(\hat{\gamma}_{q_1}^\dagger\right)^{n_{q_1}} \left(\hat{\gamma}_{q_2}^\dagger\right)^{n_{q_2}} \cdots | g \rangle. \tag{B.26}$$

In the case of $n_{n,\uparrow} = 0$, $\langle n_{q_1} n_{q_2} \cdots | \hat{\gamma}_{n,\uparrow}^\dagger \hat{\gamma}_{m,\uparrow} | n_{q_1} n_{q_2} \cdots \rangle = 0$ due to $\hat{\gamma}_{n,\uparrow} | g \rangle = 0$. On the other hand, in the case of $n_{n,\uparrow} = 1$, Eq. (B.26) becomes

$$\langle n_{q_1} n_{q_2} \cdots | \hat{\gamma}_{n,\uparrow}^\dagger \hat{\gamma}_{m,\uparrow} | n_{q_1} n_{q_2} \cdots \rangle \tag{B.27}$$

$$\begin{aligned} &= \langle n_{q_1} n_{q_2} \cdots | \delta_{n,m} \left(\hat{\gamma}_{q_1}^\dagger\right)^{n_{q_1}} \left(\hat{\gamma}_{q_2}^\dagger\right)^{n_{q_2}} \cdots \hat{\gamma}_{n,\uparrow}^\dagger \hat{\gamma}_{n,\uparrow} \hat{\gamma}_{n,\uparrow}^\dagger \cdots | g \rangle \\ &= \langle n_{q_1} n_{q_2} \cdots | \delta_{n,m} \left(\hat{\gamma}_{q_1}^\dagger\right)^{n_{q_1}} \left(\hat{\gamma}_{q_2}^\dagger\right)^{n_{q_2}} \cdots \hat{\gamma}_{n,\uparrow}^\dagger \cdots | g \rangle \\ &\quad - \langle n_{q_1} n_{q_2} \cdots | \delta_{n,m} \left(\hat{\gamma}_{q_1}^\dagger\right)^{n_{q_1}} \left(\hat{\gamma}_{q_2}^\dagger\right)^{n_{q_2}} \cdots \hat{\gamma}_{n,\uparrow}^\dagger \hat{\gamma}_{n,\uparrow}^\dagger \hat{\gamma}_{n,\uparrow} \cdots | g \rangle \\ &= \delta_{n,m}. \end{aligned} \tag{B.28}$$

Here, we used $\left\{\hat{\gamma}_{n,\uparrow}, \hat{\gamma}_{n,\uparrow}^\dagger\right\} = 1$. Therefore, it can express in a unified way as

$$\langle n_{q_1} n_{q_2} \cdots | \hat{\gamma}_{n,\uparrow}^\dagger \hat{\gamma}_{m,\uparrow} | n_{q_1} n_{q_2} \cdots \rangle = \delta_{n,m} n_{n,\uparrow}. \tag{B.29}$$

Using Eqs. (B.29) and

$$\hat{\mathcal{H}}_{\text{eff}} | n_{q_1} n_{q_2} \cdots \rangle = \sum_{j=1}^{\infty} n_{q_j} \epsilon_{q_j} | n_{q_1} n_{q_2} \cdots \rangle, \tag{B.30}$$

$\langle \hat{\gamma}_{n,\uparrow}^\dagger \hat{\gamma}_{m,\uparrow} \rangle$ can expressed as

$$\begin{aligned}
\langle \hat{\gamma}_{n,\uparrow}^\dagger \hat{\gamma}_{m,\uparrow} \rangle &= \sum_{n_{q_1}} \sum_{n_{q_2}} \cdots \mathrm{e}^{\beta\left(\Omega - \sum_{j=1}^{\infty} n_{q_j} \epsilon_{q_j}\right)} \langle n_{q_1} n_{q_2} \cdots | \hat{\gamma}_{n,\uparrow}^\dagger \hat{\gamma}_{m,\uparrow} | n_{q_1} n_{q_2} \cdots \rangle \\
&= \delta_{n,m} \sum_{n_{q_1}} \sum_{n_{q_2}} \cdots \mathrm{e}^{\beta\left(\Omega - \sum_{j=1}^{\infty} n_{q_j} \epsilon_{q_j}\right)} n_{n,\uparrow} \\
&= \delta_{n,m} \frac{\left(\prod_{j=1}^{\infty} \sum_{n_{q_j}} \mathrm{e}^{-\beta n_{q_j} \epsilon_{q_j}}\right) n_{n,\uparrow}}{\prod_{j=1}^{\infty} \sum_{n_{q_j}} \mathrm{e}^{-\beta n_{q_j} \epsilon_{q_j}}} \\
&= \delta_{n,m} \frac{\sum_{n_{n,\uparrow}=0,1} n_{n,\uparrow} \mathrm{e}^{-\beta n_{n,\uparrow} \epsilon_n}}{\sum_{n_{n,\uparrow}=0,1} \mathrm{e}^{-\beta n_{n,\uparrow} \epsilon_n}} \\
&= \delta_{n,m} \frac{1}{\mathrm{e}^{\beta \epsilon_n} + 1}.
\end{aligned} \tag{B.31}$$

Finally, the expectation of the fermion operators are written as

$$\langle \hat{\gamma}_{n,\uparrow}^\dagger \hat{\gamma}_{m,\uparrow} \rangle = \delta_{n,m} f_{\mathrm{F}}(\epsilon_n), \tag{B.32a}$$

$$\langle \hat{\gamma}_{n,\downarrow} \hat{\gamma}_{m,\downarrow}^\dagger \rangle = \left\langle \left(\delta_{n,m} - \hat{\gamma}_{m,\downarrow}^\dagger \hat{\gamma}_{n,\downarrow} \right) \right\rangle = \delta_{n,m} \left(1 - f_{\mathrm{F}}(\epsilon_n)\right), \tag{B.32b}$$

where $f_{\mathrm{F}}(\epsilon_n) \equiv \left(\mathrm{e}^{\beta \epsilon_n} + 1\right)^{-1}$ is the Fermi distribution function.

B.4 Pair potential, particle number density and current density

The pair potential $\Delta(\boldsymbol{r})$ and the particle number density $n(\boldsymbol{r})$ are rewrite by using Eqs. (B.15), (B.20), and (B.32) as

$$\begin{aligned}
\Delta(\boldsymbol{r}) &= \Gamma_0 \langle \hat{\psi}_\downarrow(\boldsymbol{r}) \hat{\psi}_\uparrow(\boldsymbol{r}) \rangle \\
&= \Gamma_0 \left\langle \sum_n \left(u_n(\boldsymbol{r}) \hat{\gamma}_{n,\downarrow} - v_n^*(\boldsymbol{r}) \hat{\gamma}_{n,\uparrow}^\dagger \right) \sum_m \left(u_m(\boldsymbol{r}) \hat{\gamma}_{m,\uparrow} + v_m^*(\boldsymbol{r}) \hat{\gamma}_{m,\downarrow}^\dagger \right) \right\rangle \\
&= \Gamma_0 \sum_n \sum_m \left(u_n(\boldsymbol{r}) v_m^*(\boldsymbol{r}) \langle \hat{\gamma}_{n,\downarrow} \hat{\gamma}_{n,\downarrow}^\dagger \rangle - v_n^*(\boldsymbol{r}) u_m(\boldsymbol{r}) \langle \hat{\gamma}_{n,\uparrow}^\dagger \hat{\gamma}_{m,\uparrow} \rangle \right) \\
&= \Gamma_0 \sum_n u_n(\boldsymbol{r}) v_n^*(\boldsymbol{r}) \left(1 - 2 f_{\mathrm{F}}(\epsilon_n)\right),
\end{aligned} \tag{B.33}$$

$$
\begin{aligned}
n(\boldsymbol{r}) &= n_\uparrow(\boldsymbol{r}) + n_\downarrow(\boldsymbol{r}) \\
&= \langle \hat{\psi}_\uparrow^\dagger(\boldsymbol{r})\hat{\psi}_\uparrow(\boldsymbol{r})\rangle + \langle \hat{\psi}_\downarrow^\dagger(\boldsymbol{r})\hat{\psi}_\downarrow(\boldsymbol{r})\rangle \\
&= 2\sum_n \sum_m \left(u_n^*(\boldsymbol{r})u_m(\boldsymbol{r})\langle \hat{\gamma}_{n,\uparrow}^\dagger \hat{\gamma}_{m,\uparrow}\rangle + v_n(\boldsymbol{r})v_m^*(\boldsymbol{r})\langle \hat{\gamma}_{n,\downarrow}\hat{\gamma}_{m,\downarrow}^\dagger\rangle \right) \\
&= 2\sum_n \left[|u_n(\boldsymbol{r})|^2 f_{\mathrm{F}}(\epsilon_n) + |v_n(\boldsymbol{r})|^2(1 - f_{\mathrm{F}}(\epsilon_n)) \right]. \qquad \text{(B.34)}
\end{aligned}
$$

Next, to derive the formulation of the current density, we introduce a thermodynamic potential $\Omega[\hat{\rho}]$ with the density operator $\hat{\rho}$ and Hamiltonian in Eq. (B.1) as

$$
\Omega[\hat{\rho}] \equiv \mathrm{Tr}\hat{\rho}\left(\hat{\mathcal{H}} + \frac{1}{\beta}\ln\hat{\rho} \right), \qquad \text{(B.35a)}
$$

$$
\hat{\rho} = \exp\left[\beta \left(\Omega_0 - \sum_{n,\alpha} \epsilon_n \hat{\gamma}_{n,\alpha}^\dagger \hat{\gamma}_{n,\alpha} \right) \right], \quad \Omega_0 \equiv \frac{1}{\beta}\sum_{n,\alpha} \ln(1 + \mathrm{e}^{-\beta\epsilon_n}). \qquad \text{(B.35b)}
$$

The kinetic energy term in Eq. (B.35) contributed by the vector potential $\boldsymbol{A}_1 = \boldsymbol{A}(\boldsymbol{r}_1)$ is expressed as

$$
\begin{aligned}
\Omega_{\mathrm{kin}} &= \int d\xi_1 \hat{\mathcal{K}}_{\mathrm{kin}} \rho^{(1)}(\xi_1, \xi_2)\Big|_{\xi_1=\xi_2} \\
&= \int d^3 r_1 \sum_{\alpha_1} \frac{(-\hat{\boldsymbol{p}}_2 - e\boldsymbol{A}_2)\cdot(\hat{\boldsymbol{p}}_1 - e\boldsymbol{A}_1)}{2m} \rho^{(1)}(\xi_1, \xi_2)\Big|_{\xi_2=\xi_1}, \qquad \text{(B.36)}
\end{aligned}
$$

where $\rho^{(1)}(\xi_1, \xi_2)$ and $\hat{\mathcal{K}}_{\mathrm{kin}}$ are defined by

$$
\rho^{(1)}(\xi_1, \xi_2) \equiv \langle \hat{\psi}(\xi_2)\hat{\psi}(\xi_1)\rangle, \quad \hat{\mathcal{K}}_{\mathrm{kin}} \equiv \frac{(\hat{\boldsymbol{p}}_1 - e\boldsymbol{A}_1)^2}{2m}. \qquad \text{(B.37)}
$$

In addition, we consider the energy of the magnetic field

$$
\mathcal{H}_{\mathrm{mag}} = \int d^3 r \frac{1}{2\mu_0} (\boldsymbol{\nabla} \times \boldsymbol{A}_1)^2, \qquad \text{(B.38)}
$$

where, $\boldsymbol{b} = \nabla \times \boldsymbol{A}$. $\mathcal{H}_{\mathrm{mag}}$ is generally neglected in the normal state. On the other hand, in superconductors, we should consider $\mathcal{H}_{\mathrm{mag}}$ because a supercurrent can produce a large magnetic field.

We require that the magnetic field actually realized in the system minimizes $\Omega_{\mathrm{kin}} + \mathcal{H}_{\mathrm{mag}}$. A necessary condition for this is that $\Omega_{\mathrm{kin}} + \mathcal{H}_{\mathrm{mag}}$ is stationary concerning the variation

$\boldsymbol{A}_1 \to \boldsymbol{A}_1 + \delta\boldsymbol{A}_1$. The first-order variation is expressed as

$$
\begin{aligned}
0 &= \delta\Omega_{\mathrm{kin}} + \delta\mathcal{H}_{\mathrm{mag}} \\
&= -e\int d^3r_1 \sum_{\alpha_1} \frac{\delta\boldsymbol{A}_1\cdot(\hat{\boldsymbol{p}}_1 - e\boldsymbol{A}_1) + (-\hat{\boldsymbol{p}}_2 - e\boldsymbol{A}_2)\cdot\delta\boldsymbol{A}_2}{2m}\rho^{(1)}(\xi_1,\xi_2)\Big|_{\xi_2=\xi_1} \\
&\quad + \int d^3r \frac{1}{\mu_0}(\boldsymbol{\nabla}\times\boldsymbol{A}_1)\cdot(\boldsymbol{\nabla}\times\delta\boldsymbol{A}_1) \\
&= \int d^3r_1 \delta\boldsymbol{A}_1 \cdot \left(-e\sum_{\alpha_1} \frac{(\hat{\boldsymbol{p}}_1 - e\boldsymbol{A}_1) + (-\hat{\boldsymbol{p}}_2 - e\boldsymbol{A}_2)}{2m}\rho^{(1)}(\xi_1,\xi_2)\Big|_{\xi_2=\xi_1} \right. \\
&\quad \left. + \frac{1}{\mu_0}\boldsymbol{\nabla}\times\boldsymbol{\nabla}\times\boldsymbol{A}_1 \right).
\end{aligned} \tag{B.39}
$$

Here, we have applied the mathematical identity $(\boldsymbol{\nabla}\times\delta\boldsymbol{A})\cdot\boldsymbol{b} = \boldsymbol{\nabla}\cdot(\delta\boldsymbol{A}\times\boldsymbol{b}) + \delta\boldsymbol{A}\cdot(\boldsymbol{\nabla}\times\boldsymbol{b})$ to the magnetic energy and subsequently removed $(\boldsymbol{\nabla}\times\delta\boldsymbol{A})\cdot\boldsymbol{b}$ using Gauss' low and condition $\delta\boldsymbol{A} = 0$ on the surface. To satisfy Eq. (B.39) with an arbitrary $\delta\boldsymbol{A}_1$, the coefficient of $\delta\boldsymbol{A}_1$ must be zero. By comparing Eq. (B.39) to Ampère's low $\boldsymbol{\nabla}\times\boldsymbol{b}(\boldsymbol{r}) = \mu_o\boldsymbol{j}(\boldsymbol{r})$, we obtain a microscopic expression for the current density as

$$
\boldsymbol{j}(\boldsymbol{r}_1) = e\sum_{\alpha} \frac{(\hat{\boldsymbol{p}}_1 - e\boldsymbol{A}_1) + (-\hat{\boldsymbol{p}}_2 - e\boldsymbol{A}_2)}{2m}\rho^{(1)}(\xi_1,\xi_2)\Big|_{\xi_2=\xi_1}. \tag{B.40}
$$

We further simply as follows,

$$
\begin{aligned}
&\frac{e}{2m}(\hat{\boldsymbol{p}}_1 - \hat{\boldsymbol{p}}_2)\langle\hat{\psi}^\dagger_\uparrow(\boldsymbol{r}_2)\hat{\psi}_\uparrow(\boldsymbol{r}_1)\rangle \\
&= -\frac{-i\hbar e}{2m}(\boldsymbol{\nabla}_1 - \boldsymbol{\nabla}_2)\left\langle \sum_n \left(u^*_n(\boldsymbol{r})\hat{\gamma}_{n,\uparrow} + v_n(\boldsymbol{r})\hat{\gamma}^\dagger_{n,\downarrow}\right)\sum_m \left(u_m(\boldsymbol{r})\hat{\gamma}_{m,\downarrow} - v^*_m(\boldsymbol{r})\hat{\gamma}^\dagger_{m,\uparrow}\right)\right\rangle \\
&= -\frac{-i\hbar e}{2m}\sum_n\sum_m \left(u^*_n(\boldsymbol{r}_2)u_m(\boldsymbol{r}_1)\langle\hat{\gamma}^\dagger_{n,\uparrow}\hat{\gamma}_{m,\uparrow}\rangle + v_n(\boldsymbol{r}_2)v^*_m(\boldsymbol{r}_1)\langle\hat{\gamma}_{n,\downarrow}\hat{\gamma}^\dagger_{m,\downarrow}\rangle\right).
\end{aligned} \tag{B.41}
$$

Finally, we obtain the current density as

$$
\begin{aligned}
\boldsymbol{j}(\boldsymbol{r}) &= e\,\frac{(\hat{\boldsymbol{p}}_1 - e\boldsymbol{A}_1) + (-\hat{\boldsymbol{p}}_2 - e\boldsymbol{A}_2)}{2m}\left(\langle\hat{\psi}^\dagger_\uparrow(\boldsymbol{r}_2)\hat{\psi}_\uparrow(\boldsymbol{r}_1)\rangle + \langle\hat{\psi}^\dagger_\downarrow(\boldsymbol{r}_2)\hat{\psi}_\downarrow(\boldsymbol{r}_1)\rangle\right)\Big|_{\boldsymbol{r}_2=\boldsymbol{r}_1=\boldsymbol{r}} \\
&= \frac{i\hbar e}{m}\sum_n \big[(u^*_n(\boldsymbol{r})\boldsymbol{\nabla}u_n(\boldsymbol{r}) - u_n(\boldsymbol{r})\boldsymbol{\nabla}u^*_n(\boldsymbol{r}))f_{\mathrm{F}}(\epsilon_n) \\
&\quad + (v_n(\boldsymbol{r})\boldsymbol{\nabla}v^*_n(\boldsymbol{r}) - v^*_n(\boldsymbol{r})\boldsymbol{\nabla}v_n(\boldsymbol{r}))(1 - f_{\mathrm{F}}(\epsilon_n))\big] - \frac{e^2\boldsymbol{A}}{m}n(\boldsymbol{r}).
\end{aligned} \tag{B.42}
$$

References

[1] F. London: *Superfluids* (Dover, New York, 1961), Vol. 1, p. 56.

[2] D. I. Khomskii and A. Freimuth, Phys. Rev. Lett. **75**, 1384 (1995).

[3] T. Kita, Phys. Rev. B **79**, 024521 (2009).

[4] D. I. Khomskii and F. V. Kusmartsev, Phys. Rev. B **46**, 14245 (1992).

[5] J. Goryo, Phys. Rev. B **61**, 4222 (2000).

[6] M. Matsumoto and R. Heeb, Phys. Rev. B **65**, 014504 (2001).

[7] G. Eilenberger, Z. Phys. **214**, 195 (1968).

[8] M. Ohuchi, H. Ueki, and T. Kita, J. Phys. Soc. Jpn. **86**, 073702 (2017).

[9] H. Ueki, M. Ohuchi, and T. Kita, J. Phys. Soc. Jpn. **87**, 044704 (2018).

[10] M. Eschrig, J. A. Sauls, and D. Rainer, Phys. Rev. B **60**, 10447 (1999).

[11] M. Eschrig and J. A. Sauls, New J. Phys. **11**, 075009 (2009).

[12] N. B. Kopnin, J. Low Temp. Phys. **97**, 157 (1994).

[13] T. Kita: *Statistical Mechanics of Superconductivity* (Springer, Tokyo, 2015).

[14] J. W. Serene and D. Rainer, Phys. Rep. **101**, 221 (1983).

[15] A. I. Larkin and Y. N. Ovchinnikov: *Sign change of the flux-flow Hall effect in HTSC* (Elsevier, Amsterdam, 1986), Vol. 12, p. 493.

[16] T. Kita, Phys. Rev. B **64**, 054503 (2001).

[17] H. Ueki, W. Kohno, and T. Kita, J. Phys. Soc. Jpn. **85**, 064702 (2016).

[18] E. Arahata and Y. Kato, J. Low Temp. Phys. **175**, 345 (2014).

[19] L. P. Gor'kov, Sov. Phys. JETP **9**, 1364 (1959). [Zh. Eksp. Teor. Fiz. **36**, 1918 (1959)].

[20] L. P. Gor'kov, Sov. Phys. JETP **10**, 998 (1960). [Zh. Eksp. Teor. Fiz. **37**, 1407 (1959)].

[21] Y. Masaki, Phys. Rev. B **99**, 054512 (2019).

[22] W. Kohno, H. Ueki, and T. Kita, J. Phys. Soc. Jpn. **85**, 083705 (2016).

[23] A. A. Abrikosov, Sov. Phys. JETP **5**, 1174 (1957). [Zh. Eksp. Teor. Fiz. **32**, 1442 (1957)].

[24] W. Kohno, H. Ueki, and T. Kita, J. Phys. Soc. Jpn. **86**, 023702 (2017).

[25] C. Caroli, P. G. de Gennes, and J. Matricon, Phys. Lett. **9**, 307 (1964).

[26] H. F. Hess, R. B. Robinson, R. C. Dynes, J. M. Valles, and J. V. Waszczak, Phys. Rev. Lett. **62**, 214 (1989).

[27] P. G. de Gennes: *Superconductivity of Metals and Alloys* (W. A. Benjamin, 1966).

[28] N. Hayashi, T. Isoshima, M. Ichioka, and K. Machida, Phys. Rev. Lett. **80**, 2921 (1998).

[29] S. Kasahara, T. Watashige, T. Hanaguri, Y. Kohsaka, T. Yamashita, Y. Shimoyama, Y. Mizukami, R. Endo, H. Ikeda, K. Aoyama, T. Terashima, S. Uji, T. Wolf, H. von Löhneysen, T. Shibauchi, and Y. Matsuda, Proc. Natl. Acad. Sci. U.S.A. **111**, 16309 (2014).

[30] N. Schopohl and K. Maki, Phys. Rev. B **52**, 490 (1995).

[31] M. Ohuchi, H. Ueki, and T. Kita, e-print arXiv:cond-mat/2011.04856 , (2020).

[32] E. S. Joshua, H. Ueki, W. Kohno, and T. Kita, J. Phys. Soc. Jpn. **89**, 104702 (2020).

[33] N. Hayashi, M. Ichioka, and K. Machida, J. Phys. Soc. Jpn. **67**, 3368 (1998).

[34] M. Machida and T. Koyama, Phys. Rev. Lett. **90**, 077003 (2003).

[35] P. Sharma, J. Low Temp. Phys. **201**, 73 (2020).

[36] N. B. Kopnin: *Theory of Nonequilibrium Superconductivity* (Oxford University Press, New York, 2001).

[37] S. N. Artemenko and A. F. Volkov, Sov. Phys. Usp. **22**, 295 (1979).

[38] K. Yosida, Phys. Rev. **110**, 769 (1958).

[39] F. Gygi and M. Schlüter, Phys. Rev. B **43**, 7609 (1991).

[40] U. Klein, J. Low Temp. Phys. **69**, 1 (1987).

[41] T. Kita, J. Phys. Soc. Jpn. **67**, 2067 (1998).

[42] M. Ichioka, N. Hayashi, and K. Machida, Phys. Rev. B **55**, 6565 (1997).

[43] Y. Nagato, K. Nagai, and J. Hara, J. Low Temp. Phys. **93**, 33 (1993).

[44] N. Schopohl, e-print arXiv:cond-mat/9804064 , (1998).

[45] E. Helfand and N. R. Werthamer, Phys. Rev. Lett. **13**, 686 (1964).

[46] T. Kita and M. Arai, Phys. Rev. B **70**, 224522 (2004).

[47] K.-I. Kumagai, K. Nozaki, and Y. Matsuda, Phys. Rev. B **63**, 144502 (2001).

[48] H. L. Edwards, J. T. Markert, and A. L. de Lozanne, Phys. Rev. Lett. **69**, 2967 (1992).

[49] M. Kato and K. Maki, Prog. Theor. Phys. **107**, 941 (2002).

[50] H. Ueki, H. Morita, M. Ohuchi, and T. Kita, Phys. Rev. B **101**, 184518 (2020).

[51] E. V. Thuneberg, Phys. Rev. Lett. **56**, 359 (1986).

[52] M. M. Salomaa and G. E. Volovik, Phys. Rev. Lett. **51**, 2040 (1983).

[53] T. Kita, Phys. Rev. Lett. **86**, 834 (2001).

[54] T. Kita, Phys. Rev. B **66**, 224515 (2002).

[55] R. C. Regan, J. J. Wiman, and J. A. Sauls, Phys. Rev. B **101**, 024517 (2020).

[56] A. A. Abrikosov, L. P. Gor'kov, and I. E. Dzyaloshinski: *Methods of Quantum Field Theory in Statistical Physics* (Prentice-Hall, Englewood Cliffs, NJ,, 1963).

[57] E. Wigner, Phys. Rev. **40**, 749 (1932).

[58] T. Kita, Prog. Theor. Phys. **123**, 581 (2010).

[59] G. M. Eliashberg, Zh. Eksp. Teor. Phys. **61**, 1254 (1971) [Sov. Phys. JETP **34**, 668] (1972).

[60] D. Van der Marel, Physica C **165**, 35 (1990).

[61] M. Kato and K. Maki, Progress of Theoretical Physics **103**, 867 (2000).

[62] Y. Kato, Kotai Butsuri **49**, 395 (2014).